Black holes from fluid mechanics

A dissertation presented
by

Subhaneil Lahiri

to
The Department of Physics
in partial fulfillment of the requirements
for the degree of
Doctor of Philosophy
in the subject of

Physics

Harvard University
Cambridge, Massachusetts
May 2009

Thesis advisor
Professor Shiraz Minwalla / Professor Xi Yin

Author
Subhaneil Lahiri

Black holes from fluid mechanics

Abstract

We use the AdS/CFT correspondence in a regime where the field theory is well described by fluid mechanics to study large black holes in asymptotically locally anti de Sitter spaces. In particular, we use the fluid description to study the thermodynamics of the black holes and the existence of exotic horizon topologies in higher dimensions.

First we test this method by comparing large rotating black holes in global AdS_D spaces to stationary solutions of the relativistic Navier-Stokes equations on S^{D-2}. Reading off the equation of state of this fluid from the thermodynamics of non-rotating black holes, we proceed to construct the nonlinear spinning solutions of fluid mechanics that are dual to rotating black holes. In all known examples, the thermodynamics and the local stress tensor of our solutions are in precise agreement with the thermodynamics and boundary stress tensor of the spinning black holes. Our results yield predictions for the thermodynamics of all large black holes in all theories of gravity on AdS spaces, for example, IIB string theory on $AdS_5 \times S^5$ and M theory on $AdS_4 \times S^7$ and $AdS_7 \times S^4$.

We then construct solutions to the relativistic Navier-Stokes equations that describe the long wavelength collective dynamics of the deconfined plasma phase of $\mathcal{N} = 4$ Yang Mills theory compactified down to $d = 3$ on a Scherk-Schwarz circle. Our solutions are stationary, axially symmetric spinning balls and rings of plasma. These solutions, which are dual to (yet to be constructed) rotating black holes and black rings in Scherk-Schwarz compactified AdS_5, and have properties that are qualitatively similar to those of black holes and black rings in flat five dimensional gravity.

We also study the stability of these solutions to small fluctuations, which provides an indirect method for studying Gregory-Laflamme instabilities. We also extend the construction to higher dimensions, allowing one to study the existence of new black hole topologies and their phase diagram.

Contents

Citations to previously published work

Part of Chapter 2 and most of Chapters 3 have appeared in the following paper:

> [1] S. Bhattacharyya, S. Lahiri, R. Loganayagam, and S. Minwalla, "Large rotating AdS black holes from fluid mechanics,"
> *JHEP* **09** (2008) 054, `arXiv:0708.1770 [hep-th]`.

Part of Chapter 2 and most of Chapters 4 and 6 have appeared in the following paper:

> [2] S. Lahiri and S. Minwalla, "Plasmarings as dual black rings,"
> *JHEP* **05** (2008) 001, `arXiv:0705.3404 [hep-th]`.

Large portions of Chapter 2 have appeared in the following paper:

> [3] J. Bhattacharya and S. Lahiri, "Lumps of plasma in arbitrary dimensions,"
> `arXiv:0903.4734 [hep-th]`.

Electronic preprints (shown in `typewriter font`) are available on the Internet at the following URL:

> `http://arXiv.org/abs/`

Acknowledgments

First of all, I would like to thank my advisor, Shiraz Minwalla, for his guidance, encouragement and relentless enthusiasm throughout my PhD. He somehow made plowing through pages of calculations seem fun and has alway encouraged me to be confident in thinking for myself.

I'd also like to thank Kyriakos, Joe, Suvrat, Lars, Sayantani, Jyotirmoy and Loganayagam for many helpful conversations and collaborations over the years, and also Indranil and Davide for collaboration on earlier work.

I've learnt a great deal from conversations with my fellow students, especially Aaron, Andy, Can, Chris/Philip, Cliff, Dan, Devin, Dio, Giorgos, Greg, Itay, Jacob, Jared, Jason, Jesse, Jihye, Jon, Josh, Kirill, Liam, Lisa, Megha, Michelle, Monica, Morten, Natalia, Pasha, Rakhi, Tom, Wei, Xi and everyone involved with GSS and also Anindya, Argha, Arnab, Ashik, Basu, Pallab, Partha, Rahul, Rudra, Sakuntala, Shamik, Suresh, Tridib and everyone else in the theory students room at TIFR. I have also had many interesting and useful discussions with the post-docs at Harvard and TIFR, especially Alessandro, Bobby, Cindy, Christoph, Chris, Costis, Kevin, Leonardo, Mikael, Mboyo, Miranda, Nori, Sean, Seok, Toby and Vincent.

I'd like to thank Andrew Strominger, Cumrun Vafa, Frederik Denef, Lubos Motl and Nima Arkani-Hamed for creating such a stimulating environment to work in the Harvard High Energy Theory group and Atish Dabholkar, Avinash Dhar, Gautam Mandal, Sandip Trivedi, Spenta Wadia and Sunil Mukhi for welcoming me to TIFR. I am indebted to TIFR for their hospitality during my stays there.

I deeply grateful to Nancy, Adriana, Sheila and Raju for all their help over the years with all things administrative that has made my life much simpler.

While working on the papers on which this dissertation is based, I have benefited from discussion with O. Aharony, M. Barma, J. David, R. Emparan, F. Gelis, R. Gopakumar, S. Gupta, S. Lee, H. Liu, H. Reall, and A. Starinets. I would also like to thank the organisers, speakers and participants of the Introductory School on Recent Developments in Supersymmetric Gauge Theories at ICTP in 2004, the Summer School on Strings, Cosmology and Gravity at the UBC in 2004, Strings 2005 and 2006, the 1st Asian Winter School on String theory, Geometry, Holography and Black Holes, TASI 2007, and the ICTS Monsoon Workshop on String Theory in 2008.

The entire way I think about physics was shaped by my college tutors, Michael Bowler and James Binney. I am grateful for all the time they spent guiding my earliest investigations.

Finally, I would like to thank my family and friends for their constant support and keeping me somewhat sane.

Chapter 1

Introduction

In this dissertation we will be using insights originating in string theory, namely the AdS/CFT correspondence [4–7], to simplify the study of classical black holes in higher dimensions. General relativity makes sense in any number of dimensions. As emphasised by Barak Kol and collaborators, the number of dimensions, D, can be thought of as a parameter of the theory (or even an expansion parameter [8–11]). It is common in theoretical physics to think about values for parameters that differ from reality in order to understand the theory better. For example, in quantum field theory and statistical mechanics we often consider asymptotically small or large coupling constants for the purposes of perturbation theory. We also often study gauge theories with gauge groups other than the $SU(3) \times SU(2) \times U(1)$ that underlies the standard model.

The study of the general theory of relativity in higher dimensions than the four that we observe may not be as disconnected from reality as it first appears. Interest in the subject dates back to the work of Kaluza and Klein [12, 13] which proposed unification of gravity and electromagnetism starting from general relativity in five dimensions. The basic idea of higher dimensional gravity remains in string theory, which suggests that a consistent theory of quantum gravity requires extra dimensions. In addition, the large extra dimensions scenario [14–16] proposes that the hierarchy problem of particle physics could have a higher dimensional resolution.

One can ask if higher dimensional gravity is just more of the same, or if there are any new features once we take $D > 4$? It turns out that the answer is the latter. In four dimensions, all stationary black holes must have a horizon with the topology of S^2, a sphere [17, 18]. In higher dimensions, we can have extended black objects: black strings and p-branes with horizon topology $S^{D-p-2} \times \mathbb{R}^p$ [19]. Even if we restrict attention to black objects of finite size, once we go to five dimensions, in addition to the usual black holes with spherical S^3 horizons we have black ring solutions with horizon topology $S^1 \times S^2$ [20, 21]. In higher dimensions, the situation is much more complicated and somewhat mysterious [22, 23]. We will discuss these issues further in §1.1.

In this dissertation, we are going to attack these problems with a new tool. The AdS/CFT correspondence [4–7] relates a theory of gravity in asymptotically anti de Sitter spacetimes to lower dimensional non-gravitational field theories, typically gauge theories with a large number of colours, N. One particularly interesting entry in the dictionary

maps black holes on the gravitational side to the deconfined phase of the dual gauge theory. When we put this together with the general lore that field theories at high densities and long wavelengths compared to the scale of microscopic physics are well described by fluid mechanics, we arrive at the conclusion that there should be a regime where classical black hole physics coincides with fluid mechanics.

In the fluid mechanical description, the theory is described by few properties. First there is the equation of state that relates the density, pressure, temperature etc. Then there are the transport coefficients that describe the response on the fluid to deviations from equilibrium. For the fluids that are dual to theories of gravity, the equation of state can be determined by applying the methods of gravitational thermodynamics to static black holes or black branes and the transport coefficients can be computed from small (linearised) fluctuations about these solutions.

Starting with the work of Policastro, Son and Starinets [24], there have been several fascinating studies over the last few years, that have computed fluid mechanical transport coefficients from gravity (see the review [25] and the references therein). In this dissertation, we will be doing the reverse. We are going to use the properties of the fluid found in this way to construct fully non-linear, non-static solutions of fluid mechanics and use these to study non-static black objects on the gravitational side of the duality indirectly.

There is another context in which black holes can be described by fluid mechanics, the membrane paradigm (see [26] and references therein and [27, 28]), where one replaces the interior of the black hole with a dissipative membrane living at the horizon. This is conceptually different from our approach. For some of the complicated black objects we will discuss, the metric of the space the membrane lives on will be very complicated and need not even have the same topology as the spaces where our fluids will live.

Inspired by the membrane paradigm (but not using it) there has been some recent work using an analogy between black holes and fluid droplets [29–31]. In that approach one replaces the interior of the black hole with a fluid droplet with a surface at the horizon. In our approach the fluid lives in a lower dimensional space than the black hole and the horizon corresponds to all of the fluid, not just the surface. We emphasise that our approach is more than just an analogy, in the context of asymptotically locally AdS black holes we are proposing a precise correspondence with a clear regime of validity.

1.1 Higher dimensional gravity

In four dimensions, Hawking's topology theorem [17, 18] states that all stationary black holes must have horizons with spherical topology and be rotationally invariant. The uniqueness theorem for vacuum black holes (i.e. without any electromagnetic fields or other matter) also tells us that, for a given energy and angular momentum, the rotating Kerr black hole is the only solution.

Once we go to higher dimensions, things become more interesting. The higher dimensional generalisation of the topology theorem [32, 33] states that the horizon must be of positive Yamabe type, i.e. they must admit metrics of positive scalar curvature. It is unclear what the complete list of topologies that satisfy this condition are and it is unlikely that all topologies that satisfy this condition can actually be realised as solutions

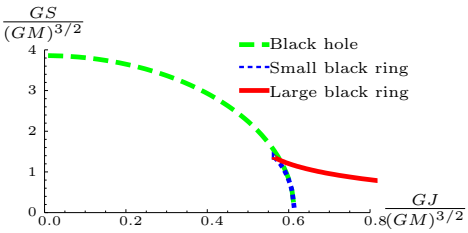

Figure 1.1: Phase diagram of black objects in five dimensions, plotting entropy vs. angular momentum at fixed energy.

to Einstein's equations. One set of topologies that are allowed are products of spheres. The theorem also appears to allow discrete quotients of spheres as well, but these are not expected to exist when we keep the topology of the asymptotic region fixed as a sphere.

In five dimensions there is an explicit example of a new topology – the black ring of Emparan and Reall [20] with horizon topology $S^1 \times S^2$. This solution also demonstrates that the uniqueness theorem does not generalise to higher dimensions – there is a range of energies and angular momenta for which there are three different solutions: the Myers-Perry black hole [34], the small black ring and the large black ring. We have plotted the phase diagram in fig.1.1.

When we go to higher dimensions, the problem becomes much more difficult. In five dimensions, as well as the time-like isometry there are two rotational isometries,so the problem is effectively 2 dimensional. The maximum number of isometries we can expect in D dimensions is 1 time-like and $\left[\frac{D-1}{2}\right]$ rotational (one for each independent plane of rotation),[1] so the problem is effectively $\left[\frac{D}{2}\right]$ dimensional. Once this becomes 3 or larger, the collection of solution generating techniques becomes much weaker.

The only exact solution in 6 or more dimensions is the Myers-Perry rotating black hole. There is also an approximate construction of black rings [22] and other objects [35] that require the size of one of the spherical components to be much larger than the others. In addition, there is a qualitative argument that there must be black holes with wavy horizons [36] but there is not even an approximate construction. Two proposed phase diagrams are presented in fig.1.2, the first of these appeared in [22] and the second appeared in an unpublished earlier draft of that paper [37]. The features of the two proposals that are the same (black holes joining onto wavy black holes joining onto black rings...) are the only features that are robust. The issue of what the correct phase diagram is will be one of the problems that we will begin to address with our fluid mechanical methods.

The instabilities of extended black objects has been one of the most controversial subjects ever since they were proposed by Gregory and Laflamme [38, 39], in particular the question of their endpoint (see [40] for a review). Below a critical dimension, it is thermodynamically favourable for a black string to split into an array of black holes (if we

[1]Here, we use the notation $[x]$ to denote the integer part of the real number x. Note that the theorems only guarantee one rotational isometry. All known solutions have $\left[\frac{D-1}{2}\right]$ of them. It is still an open question whether or not there are any stationary solutions with fewer than this number.

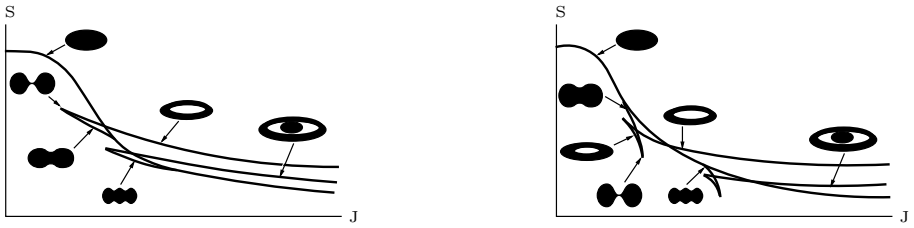

Figure 1.2: Possible phase diagrams of black objects in $D \geq 6$ dimensions.

compactify the extended direction on a circle, this only occurs if the length of the circle is larger than some multiple of the radius of the black string). However, the bifurcation of the horizon cannot take place without naked singularities [18, 41]. It has also been suggested that the pinching process would take an infinite amount of time and that the final state is a wavy black string [42].

The appropriate method to resolve these questions in gravity should be numerical simulations. However, as the pinch is approached the curvatures become large and the simulations break down. If we extrapolate past this breakdown, these suggest that the final state is a black hole, and not an wavy string [43, 44].

The appearance of instabilities when one adjusts a parameter has another interesting consequence. In the stable parameter range the frequency satisfies $\omega^2 > 0$, in the unstable range we have $\omega^2 < 0$. Therefore, at the critical value of the parameter we have $\omega = 0$, i.e. we have a zero mode. If we turn on this zero mode we should move off on a new branch of solutions. In the case of the Gregory-Laflamme instability this new branch of solutions are wavy strings, which have been constructed numerically [45, 46].

Due to the complicated nature of these questions in the gravitational setting, it is worth seeing if we can get any insight into these questions using our holographic fluid mechanics approach.

1.2 Conformal fluids and anti de Sitter space

Before we go on to study fluid mechanical duals of the gravitational physics described above, it is useful to test out our ideas in a setting where we can perform the calculations on both sides of the duality and check that they agree. Such a setting is provided by rotating black hole solutions in global anti de Sitter space.

All theories of gravity on an AdS_D background are expected to admit a dual description as a conformal field theory on $S^{D-2}\times$ time [4, 6]. Putting this together with the fact that quantum field theories at sufficiently high energy density and long wavelengths are expected to admit an effective description in terms of fluid dynamics, we propose that large, rotating black holes in arbitrary global AdS_D spaces admit an accurate dual description as rotating, stationary configurations of a conformal fluid on S^{D-2}. One could regard the agreement between fluid dynamics and gravity described below as a test of the AdS/CFT correspondence, provided we are ready to assume in addition the applicability of fluid

mechanics to quantum field theories at high density.

Assuming our proposal is indeed true, we are able to derive several properties of large rotating AdS black holes in Ch.3 as follows: We first read off the thermodynamic equation of state of the dual fluid from the properties of large, static, non-rotating AdS black holes. Inputting these equations of state into the relativistic Navier-Stokes equations, we are then able to deduce the thermodynamics of large rotating black holes.

Consider a theory of gravity coupled to a gauge field (based on a gauge group of rank c) on AdS_D. In an appropriate limit, the boundary theory is effectively described by conformal fluid dynamics with c simultaneously conserved, mutually commuting $U(1)$ charges R_i $(i = 1 \ldots c)$.

When we input this equation of state into the relativistic Navier-Stokes equations, we are able to construct a set of stationary solutions. These solutions are simply the configurations into which any fluid initial state eventually settles down in equilibrium. These solutions turn out to be universal (i.e. they are independent of the detailed form of the equation of state and the transport coefficients). Their thermodynamics is incredibly simple; it is summarised by the partition function

$$\ln \mathcal{Z}_{\rm gc}(T,\mu,\Omega) = \ln \mathrm{Tr} \exp\left[-\frac{(E-\mu_i R_i - \Omega_a L_a)}{T}\right] = \frac{\ln \mathcal{Z}_{\rm gc}(T,\mu,0)}{\prod_a (1-\Omega_a^2)}\,, \tag{1.1}$$

where E is the energy, R_i and μ_i are the c commuting charges and chemical potentials respectively and L_a and Ω_a represent the angular momenta and the angular velocities of the fluid respectively.

We now turn to the gravitational dual interpretation of the fluid mechanics solutions we have described above. A theory of a rank c gauge field, interacting with gravity on AdS_D, possesses a $c+n+1$ parameter set of black hole solutions, labelled by the energy, angular momentum and electric charges. We propose that these black holes (when large) are dual to our solutions of fluid dynamics. Our proposal yields an immediate prediction for the thermodynamics of large rotating black holes: the grand canonical partition function of these black holes must take the form of (1.1).

We have tested the thermodynamic predictions described above on every class of black hole solutions in AdS_D spaces that we are aware of. In the strict fluid dynamical limit, the thermodynamics of each of these black holes exactly reproduces[2] (1.1). The agreement described in this paragraph occurs only when one would expect it to, as we now explain.

The equations of fluid mechanics assume that the fluid is in local thermodynamic equilibrium at each point in space, even though the energy and the charge densities of the fluid may vary in space. Fluid mechanics applies only when the length scales of variation of thermodynamic variables – and the length scale of curvatures of the manifold on which the fluid propagates – are large compared to the equilibration length scale of the fluid, a distance we shall refer to as the mean free path, $l_{\rm mfp}$, although the terminology of kinetic theory is not really appropriate for these strongly coupled theories.

As we will see, the most stringent bound comes from requiring that $l_{\rm mfp}$ be small compared to the radius of the S^{d-1}. In every case we have studied, it turns out that this

[2]See, however, §3.5.8 for a puzzle regarding the first subleading corrections for a class of black holes in AdS_5.

condition is met whenever the horizon radius (in Boyer-Lindquist coordinates), r_+, of the dual black hole is large compared to the AdS radius , $R_{\rm AdS}$.

It follows that we should expect the Navier-Stokes equations to reproduce the thermodynamics of only large black holes. In all the cases we have studied, this is indeed the case. It is possible to expand the formulae of black hole thermodynamics (and the stress tensor and charge distribution) in a power series in $R_{\rm AdS}/r_+$. While the leading order term in this expansion matches the results of fluid dynamics, we find deviations from the predictions of Navier-Stokes equations at subleading orders.

Since [1] was published the explicit dictionary between solutions of fluid mechanics and solutions of general relativity in a derivative expansion has been established in [47]. Whilst the AdS/CFT correspondence guaranteed that this would work, we now have an explicit demonstration of this fact. This means that we now have a guarantee that this relation between rotating fluids on spheres and rotating AdS black holes was guaranteed to work without relying on the AdS/CFT conjecture. Nevertheless, it is nice to have a simple confirmation of this fact.

1.3 Plasmaballs

When we look at conformal theories, as in the previous section, we cannot create fluid configurations dual to the interesting black objects described in §1.1. We can only talk about fluids that fill the space, so we are always working with horizons with the same topology as the boundary. When we consider fluids in flat space we are always studying black branes, when we consider fluids on spheres we are always studying spherical black holes. We could look at black strings by putting the fluid on $\mathbb{R}\times S^n$, but such black strings do not exhibit the Gregory-Laflamme instability [48]. To study the interesting features of higher dimensional gravity mentioned above, we will have to do something a little different.

Consider a theory of gravity in D dimensions with a negative cosmological constant $\Lambda = -\frac{(D-1)(D-2)}{2R^2_{\rm AdS}}$. Suppose we pick boundary conditions at infinity that tend to Poincaré AdS with one dimension compactified on a circle of radius ${\mathcal{T}_{\rm c}}^{-1}$ with all fermionic fields antiperiodic(a Scherk-Schwarz circle). We will refer to these spaces as SSAdS$_D$. This arises as the near horizon limit of stacks of Scherk-Schwarz compactified D3, M2 and M5 branes. This gravitational theory is dual to the Scherk-Schwarz compactification of a large N, strongly coupled, $D-1$ dimensional conformal theory. Using the gravity side, one can show that the result is a confining theory with a first order confinement/deconfinement transition at temperature $\mathcal{T}=\mathcal{T}_{\rm c}$ [49].

The low temperature confining phase is dual to a gas of supergravitons on the so called AdS soliton background:

$$\mathrm{d}s^2 = \frac{R^2_{\rm AdS}}{z^2}\left(-\mathrm{d}t^2 + F_{\mathcal{T}_{\rm c}}(z)\,\mathrm{d}\theta^2 + \mathrm{d}x_i^2 + \frac{1}{F_{\mathcal{T}_{\rm c}}(z)}\,\mathrm{d}z^2\right), \tag{1.2}$$

where $i=1,\cdots,D-3$, $\theta\sim\theta+{\mathcal{T}_{\rm c}}^{-1}$, and

$$F_a(z) = 1-\left(\frac{4\pi a z}{D-1}\right)^{D-1}. \tag{1.3}$$

Notice that, at small z, $F_x(z) \simeq 1$, so (1.2) reduces to AdS_D in Poincaré-patch coordinates, with z as the radial coordinate and with one of the spatial boundary coordinates, θ, compactified on a circle (the remaining boundary coordinates, x_i and t, remain non-compact). At $z = \frac{D-1}{4\pi \mathcal{T}_c}$, the physical size of the θ circle goes to zero. This happens in the same way as the origin of polar coordinates and space stops here.

The high temperature phase of the same system (at temperature $\mathcal{T}$) is dual to the the black brane

$$\mathrm{d}s^2 = \frac{R_{\mathrm{AdS}}^2}{z^2}\left(-F_{\mathcal{T}}(z)\,\mathrm{d}t^2 + \mathrm{d}\theta^2 + \mathrm{d}x_i^2 + \frac{1}{F_{\mathcal{T}}(z)}\,\mathrm{d}z^2\right). \tag{1.4}$$

The thermodynamics of the high temperature phase are determined in the bulk description by the usual constitutive equations of black brane thermodynamics [50]

$$\mathcal{P} = \frac{\alpha}{\mathcal{T}_c}\left(\mathcal{T}^{D-1} - {\mathcal{T}_c}^{D-1}\right), \quad \text{where} \quad \alpha = \frac{4^{D-3}\pi^{D-2}R_{\mathrm{AdS}}^{D-2}}{(D-1)^{D-1}G_D}. \tag{1.5}$$

For $\mathcal{T} > \mathcal{T}_c$ the free energy density (the negative of the pressure) is negative, and so (in the large N limit) is smaller than the $\mathcal{O}(N^0)$ free energy of the 'confined' gas of gravitons. Consequently, the system undergoes a deconfinement phase transition at temperature $\mathcal{T}_c$.

With this equation of state the pressure can go to zero at finite energy density. This allows the existence of another type of fluid configuration – finite lumps of deconfined fluid separated from the confined phase by a domain wall – the plasmaballs of [50]. At the surface, the density drops rapidly, so fluid mechanics is not valid there. However, there is a standard way to deal with this problem in fluid mechanics – one replaces the domain wall with a delta function localised surface tension.

In order for the surface tension approximation to be valid, it is important that the size of the plasmaball be much larger than the thickness of the surface. When we increase the size of the plasmaball we decrease the curvature of the surface and therefore we decrease the pressure of the fluid. To stay in the regime of fluid mechanics, it is important that the density does not also become small when we do this, so it is essential that we have an equation of state that allows the pressure to vanish at finite energy density. This requires a first order phase transition and cannot happen for the conformal theories discussed in §1.2.

It is worth noting that this demonstrates the power of phrasing the calculation in the language of fluid mechanics. In the case of the conformal theories described in §1.2 we now know how to formulate the derivative expansion of fluid mechanics purely in bulk terms [47]. In some sense, we do not gain very much from the AdS/CFT duality. It saves us from integrating the equations of motion in the radial direction and we knew it was going to work before the calculations of [47], but we don't get a calculating technique that we could not have found any other way. However, once we bring surfaces into the game things change. We have to face situations where gradients are large and a simple derivative expansion won't capture everything. But, once we rephrase it in the language of the dual field theory, we can make use of a couple of hundred years worth of experience in fluid mechanics and realise that we can deal with the problem by using the surface tension approximation. Note that even the zeroth order domain wall solution required some serious numerical relativity, trying to go beyond this flat domain wall on the gravity side would be an extremely difficult task.

We have drawn this setup schematically in fig.1.3. In that diagram Hawking radiation emitted in the vertical direction will see the AdS "boxing" effect and will bounce back, equilibriating with the black hole. On the other hand, Hawking radiation emitted in the horizontal direction will not see this "boxing" effect and will escape to infinity, much like in flat space. In many ways plasmaballs are an intermediate between asymptotically flat and large AdS black holes. They have the large AdS property of having an easily identifiable holographic dual, but they have the asymptotically flat property of negative heat capacity and eventual evaporation. Note that as we increase the number dimensions, the flat-like directions outnumber the AdS-like directions more and more. We might expect plasmaballs to behave less like large AdS black holes and more like asymptotically flat black holes as we increase the number of dimensions.

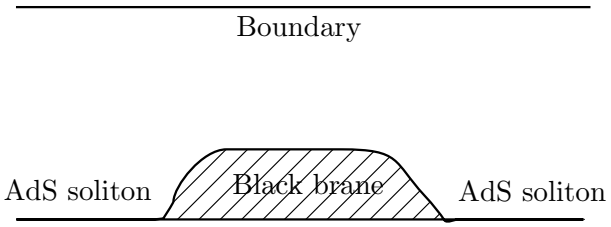

Figure 1.3: Schematic description of the bulk dual of a plasmaball.

In the infinite radius limit the plasma ball reduces to a flat surface separating two half planes of the confined and deconfined phases. In this limit, the authors of [50] constructed the gravity solution numerically and used it to compute the surface tension. We will use this surface tension to construct fluid configuration dual to the exotic black objects discussed in §1.1 and study their properties, in the same spirit that we use the equation of state and transport coefficients computed from gravity as described in §1.2. Unfortunately, we only know the surface tension strictly in the infinite radius limit, corresponding to the temperature $\mathcal{T} = \mathcal{T}_c$. We do not know what its temperature dependence is, so we will be forced to pretend that it is independent of temperature.

At temperatures close to $\mathcal{T}_c$, the microscopic length scale of the fluid is of similar size to the Scherk-Schwarz circle, so it would not be valid to use fluid mechanics in $D-1$ dimensions. We will deal with this by truncating to $d = D-2$ dimensions – we will restrict attention to fluid configurations that have no variation or velocity components in the direction of this circle.

Now by the AdS/CFT correspondence finite energy localized non-dissipative configurations of the plasma fluid in the deconfined phase is dual to stationary black objects in the bulk. Thus, by studying fluid configurations that solve the d dimensional relativistic Navier-Stokes equation we can infer facts about the black objects in SSAdS_{d+2} [2, 51].

The horizon topology can be inferred as follows. Far outside the region corresponding to the plasma, the bulk should look like the AdS-soliton. In this configuration the Scherk-Schwarz circle contracts as one moves away from the boundary, eventually reaching zero size and capping off spacetime smoothly. Deep inside the region corresponding to the

plasma, the bulk should look like the black brane. In this configuration the Scherk-Schwarz circles does not contract, it still has non-zero size when one reaches the horizon. It follows that as one moves along the horizon, the Scherk-Schwarz circle must contract as one approaches the edge of the region corresponding to the plasma. The horizon topology is found by looking at the fibration of a circle over a region the same shape as the plasma configuration, contracting the circle at the edges [2, 50]. We have provided a schematic drawing of this in fig.1.4.

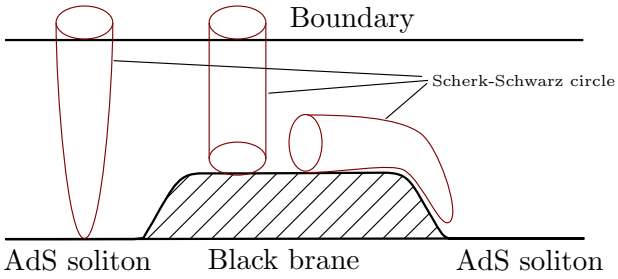

Figure 1.4: Schematic description of circle fibres for a plasmaball.

The simplest example of this is $d = 1 + 1$. The only finite sized fluid configuration we can make is a line interval, B^1. When we fibre a circle over this, we get the sphere, S^2. Not that we cannot give this black hole any angular momentum, to do that we would have to let the fluid move on the Scherk-Schwarz circle, which we cannot do within the regime of validity of our approximations. In general, in D dimensions, when there are $n = \left[\frac{D-1}{2}\right]$ independent angular momenta we will only be able to turn on $n-1$ of them. As we cannot explore the full parameter space, we cannot use this method to rule out the existence of any black hole topologies, we can only rule them in.

In Ch.4 we will look at the case $d = 3, D = 5$ in great detail. We will construct spinning disc solutions dual to black holes an spinning annuli (plasmarings) dual to black rings. The phase diagram that results is shown in fig.1.5. The fact that this has some similarity with fig.1.1 suggests that this method could provide useful suggestions for the phase diagram in higher dimensions. We will also analyse the stability of these solutions to small fluctuations in Ch.5.

In Ch.6 we will turn to the construction of spinning fluid solutions in $d = 4, D = 6$. We again find plasmaball and plasmaring solutions, including wavy ball solutions that could correspond to the wavy black holes mentioned in §1.1. We have plotted the surface of a few examples in fig.1.6. We will not perform an analysis of their thermodynamics – that was performed in [51] including a phase diagram that looks quite similar to the second one in fig.1.2. We see that the methods discussed in this dissertation have led to a strong indication of which is the correct phase diagram for black holes and rings in higher dimensions.

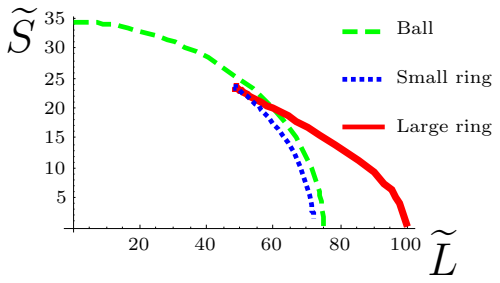

Figure 1.5: Phase diagram for plasmaballs and plasmarings in $d = 3$.

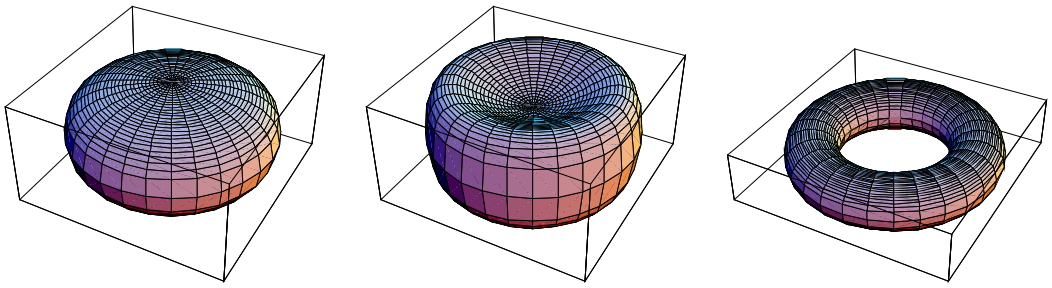

Figure 1.6: Spinning ball and ring solutions.

Chapter 2

Fluid mechanics

In this chapter, we will review the general formalism we will use in the rest of this dissertation: the thermodynamics of fluids, relativistic fluid mechanics and the relativistic treatment of surface tension. In §2.4 we will discuss the construction of equilibrium configurations of fluids and their overall thermodynamics. Our treatment of relativistic fluid mechanics is largely based on [52].

2.1 Thermodynamics

The first law of thermodynamics for a fluid with c conserved (global) charges is

$$\mathrm{d}\mathcal{E} = \mathcal{T}\mathrm{d}\mathcal{S} - \mathcal{P}\mathrm{d}V + \mathfrak{m}_i\,\mathrm{d}\mathcal{R}_i, \tag{2.1}$$

where $\mathcal{E}$ is its energy, $\mathcal{S}$ is its entropy, V is its volume, $\mathcal{R}_i$ is its i^{th} conserved charge, $\mathcal{T}$ is its temperature, $\mathcal{P}$ is its pressure and $\mathfrak{m}_i$ is its i^{th} chemical potential. In a non-relativistic theory particle number could be one of the conserved charges, but in a relativistic theory we have to replace it with something like baryon number, or in this case R-charge. Suppose we rescale the system by a factor $(1+\epsilon)$. Extensivity tells us that $\mathrm{d}\mathcal{E} = \epsilon\mathcal{E}$, $\mathrm{d}\mathcal{S} = \epsilon\mathcal{S}$, $\mathrm{d}V = \epsilon V$ and $\mathrm{d}\mathcal{R}_i = \epsilon\mathcal{R}_i$. Then (2.1) tells us that

$$\mathcal{E} = \mathcal{T}\mathcal{S} - \mathcal{P}V + \mathfrak{m}_i\mathcal{R}_i.$$

Defining intensive quantities $\rho = \mathcal{E}/V$, $s = \mathcal{S}/V$ and $\mathfrak{r}_i = \mathcal{R}/V$, we have

$$\begin{aligned} \rho + \mathcal{P} &= s\mathcal{T} + \mathfrak{m}_i\mathfrak{r}_i, \\ \mathrm{d}\rho &= \mathcal{T}\mathrm{d}s + \mathfrak{m}_i\,\mathrm{d}\mathfrak{r}_i, \\ \mathrm{d}\mathcal{P} &= s\,\mathrm{d}\mathcal{T} + \mathfrak{r}_i\,\mathrm{d}\mathfrak{m}_i. \end{aligned} \tag{2.2}$$

Note that all intensive thermodynamic quantities can be written as functions of $(1+c)$ variables, which we will usually choose to be the temperature and chemical potentials. Once we are given the pressure as a function of temperature and chemical potential, we can use (2.2) to determine the others. In Ch.3 we will consider conformal fluids, which have equations of state of the form (3.3). In Ch.4-6 we will consider uncharged fluids that are dual to Scherk-Schwarz compactifications of AdS that have equations of state of the form (4.7).

2.2 Relativistic fluid mechanics

A fluid static fluid can be described by specifying its rest frame (which can be described by a vector u^μ that takes the form $u^\mu = (1, 0, 0, \dots)$ in that rest frame) and by specifying the the temperature, $\mathcal{T}$, and chemical potentials, $\mathfrak{m}_i$. All other intensive properties of the fluid can be computed using (2.2). It is useful to let $(\mathcal{T}, \mathfrak{m}_i)$ refer to these quantities as measured in the rest frame – this means that they are Lorentz scalars, which is convenient when we construct Lorentz covariant equations of motion.

Now consider a fluid that is disturbed from equilibrium. Provided all length scales of variation are large compared to the thermalisation scale of the fluid (which we call l_{mfp}), each patch of the fluid is well described by equilibrium thermodynamics in its rest frame. The fluid is characterised by the velocity of these patches (described by a vector $u^\mu(x) = \gamma(x)(1, \vec{v}(x))$ where $\gamma = (1 - \vec{v}^2)^{-1/2}$ is a normalisation factor) and the intensive thermodynamic quantities in their rest frames (which can all be computed from the proper temperature, $\mathcal{T}(x)$, and proper chemical potentials, $\mathfrak{m}_i(x)$). We promote the quantities mentioned in the previous paragraph to fields. As long as these quantities vary slowly, we can write equations of motion for them in a derivative expansion. One would expect the length scale associated with this expansion to be the scale of microscopic physics, l_{mfp}.

The equations of fluid dynamics are simply a statement of the conservation of the stress tensor $T^{\mu\nu}$ and the charge currents J_i^μ.

$$\begin{aligned} \nabla_\mu T^{\mu\nu} &= 0\,, \\ \nabla_\mu J_i^\mu &= 0\,. \end{aligned} \tag{2.3}$$

These provide $(d + c)$ equations for the evolution of for the $(d + c)$ quantities $v(\vec{x})$, $\mathcal{T}(x)$ and $\mathfrak{m}_i(x)$ once we write the stress tensor and charge currents in terms of these quantities.

It is also convenient to define an entropy current J_S^μ that describes the density and flux of entropy. This is not an independent object, there are no equations of motion associated to its conservation and the current itself is determined by the stress tensor and charge currents. In fact, its divergence gives the rate of entropy production per unit volume. Demanding that this is positive will impose restrictions on the form of the stress tensor and charge currents.

2.2.1 Perfect fluid stress tensor

The dynamics of a fluid is completely specified once the stress tensor and charge currents are given as functions of $\mathcal{T}$, $\mathfrak{m}_i$ and u^μ. As we have explained in the introduction, fluid mechanics is an effective description at long distances. As a consequence it is natural to expand the stress tensor and charge current in powers of derivatives. In this subsection we briefly review the leading (i.e. zeroth) order terms in this expansion.

It is convenient to define a projection tensor

$$P^{\mu\nu} = g^{\mu\nu} + u^\mu u^\nu. \tag{2.4}$$

This tensor projects vectors onto the $(d - 1)$ dimensional subspace orthogonal to u^μ. In other words, $P^{\mu\nu}$ may be thought of as a projector onto spatial coordinates in the rest frame

of the fluid. In a similar fashion, $-u^\mu u^\nu$ projects vectors onto the time direction in the fluid rest frame.

To zeroth order in the derivative expansion, Lorentz invariance demands that the stress tensor be a linear combination of the two projection tensors mentioned above and that the currents are proportional to the velocity with scalar coefficients. The correct static limit uniquely determine these coefficients in terms of the thermodynamic variables. We have

$$\begin{aligned} T^{\mu\nu}_{\text{perfect}} &= \rho(\mathcal{T},\mathfrak{m})u^\mu u^\nu + \mathcal{P}(\mathcal{T},\mathfrak{m})P^{\mu\nu}, \\ J^\mu_{i,\text{perfect}} &= \mathfrak{r}_i(\mathcal{T},\mathfrak{m})u^\mu, \\ J^\mu_{S,\text{perfect}} &= s(\mathcal{T},\mathfrak{m})u^\mu, \end{aligned} \tag{2.5}$$

where all thermodynamic quantities are measured in the local rest frame of the fluid, so that they are Lorentz scalars. It is not difficult to verify that in this zero-derivative (or perfect fluid) approximation, the entropy current is conserved. Entropy production (associated with dissipation) occurs only at the first subleading order in the derivative expansion, as we will see in the next subsection.

2.2.2 Dissipation and diffusion

Now, we proceed to examine the first subleading order in the derivative expansion. As there is no entropy production when we truncate the derivative expansion to zeroth order, this will be the leading contribution to some questions.

Before we do this, it is useful to think about the physical interpretation of various components of the stress tensor. First of all, consider $u_\mu u_\nu T^{\mu\nu}$. In the rest frame of the fluid this would be T^{tt}. In other words, it is the energy density in the rest frame which we have already defined as ρ, i.e. $\rho = u_\mu u_\nu T^{\mu\nu}$.

Next, consider $q_\mu = -P_{\mu\nu}u_\lambda T^{\lambda\nu}$. In the rest frame of the fluid these are the T^{tx} components, which are physically interpreted as momentum density or energy flux. Energy flow in the rest frame of the fluid will only result from thermal conductivity, and the inertia of flowing heat will lead to some momentum density in the rest frame. So we interpret q^μ as heat flux.

Finally, consider $S_{\mu\nu} = P_{\mu\lambda}P_{\nu\sigma}T^{\lambda\sigma}$. In the rest frame of the fluid these are the T^{xy} components. These have the physical interpretation of force per unit area in the fluid rest frame.

We can write

$$T^{\mu\nu} = \rho u^\mu u^\nu + q^\mu u^\nu + u^\mu q^\nu + S^{\mu\nu}. \tag{2.6}$$

Similarly, we have the charge density, $\mathfrak{r}_i = -u_\mu J^\mu_i$, and the diffusion current, $j^\mu_i = P^\mu_\nu J^\nu_i$, and

$$J^\mu_i = \mathfrak{r}_i u^\mu + j^\mu_i. \tag{2.7}$$

Now, when there is energy flow or charge flow there must also be entropy flow, as given by the second line of (2.2). This tells us that we must have

$$J^\mu_S = su^\mu + \frac{q^\mu - \mathfrak{m}_i j^\mu_i}{\mathcal{T}}\,. \tag{2.8}$$

It is also helpful to separate velocity gradients into the pieces that are orthogonal/parallel to the velocity and into the antisymmetric/symmetric traceless/trace pieces:

$$\nabla_\mu u_\nu = -u_\mu a_\nu + \omega_{\mu\nu} + \sigma_{\mu\nu} + \frac{1}{d-1}\vartheta P_{\mu\nu} \tag{2.9}$$

where

$$\begin{aligned} a^\mu &= u^\nu \nabla_\nu u^\mu, \\ \vartheta &= \nabla_\mu u^\mu, \\ \sigma^{\mu\nu} &= \frac{1}{2}\left(P^{\mu\lambda}\nabla_\lambda u^\nu + P^{\nu\lambda}\nabla_\lambda u^\mu\right) - \frac{1}{d-1}\vartheta P^{\mu\nu}, \\ \omega^{\mu\nu} &= \frac{1}{2}\left(P^{\mu\lambda}\nabla_\lambda u^\nu - P^{\nu\lambda}\nabla_\lambda u^\mu\right), \end{aligned} \tag{2.10}$$

are the acceleration, expansion, shear tensor and rotation tensor respectively.

Using the definitions of q^μ and j_i^μ and (2.2), one can show that

$$\begin{aligned} \nabla_\mu q^\mu &= -u^\mu \partial_\mu \rho - \rho\vartheta - q^\mu a_\mu - S^{\mu\nu}\sigma_{\mu\nu} - \frac{1}{d-1}S^{\mu\nu}P_{\mu\nu}\vartheta, \\ \nabla_\mu j_i^\mu &= -u^\mu \partial_\mu \mathfrak{r}_i - \mathfrak{r}_i \vartheta, \end{aligned}$$

which leads to

$$\mathcal{T}\nabla_\mu J_S^\mu = \vartheta\left(\mathcal{P} - \frac{1}{d-1}P^{\mu\nu}S_{\mu\nu}\right) - \sigma^{\mu\nu}S_{\mu\nu} - \frac{1}{\mathcal{T}}q^\mu\left(\partial_\mu + \mathcal{T}a_\mu\right) - \mathcal{T}j_i^\mu \partial_\mu\left[\frac{\mu_i}{\mathcal{T}}\right]. \tag{2.11}$$

This quantity is the rate of production of entropy per unit volume (times temperature). We demand that this quantity is positive.

Allowing only one terms up to one derivative, this forces us to choose

$$\begin{aligned} q^\mu &= -\kappa P^{\mu\nu}(\partial_\nu \mathcal{T} + a_\nu \mathcal{T}), \\ S^{\mu\nu} &= \mathcal{P}P^{\mu\nu} - \zeta\vartheta P^{\mu\nu} - 2\eta\sigma^{\mu\nu} \\ j_i^\mu &= -D_{ij}P^{\mu\nu}\partial_\nu\left[\frac{\mathfrak{m}_j}{\mathcal{T}}\right], \end{aligned} \tag{2.12}$$

These equations define a set of new fluid dynamical parameters in addition to those of the previous subsection: ζ is the bulk viscosity, η is the shear viscosity, κ is the thermal conductivity and D_{ij} are the diffusion coefficients (they are related to the usual diffusion coefficients by a factor of $\frac{\partial}{\partial \mathfrak{r}_i}\left[\frac{\mathfrak{m}_j}{\mathcal{T}}\right]$). All of these parameters are functions of $(\mathcal{T}, \mathfrak{m}_i)$, the precise dependence will depend on which fluid we are talking about. Fourier's law of heat conduction $\vec{q} = -\kappa\vec{\nabla}\mathcal{T}$ has been relativistically modified with an extra term that is related to the redshifting of the temperature. The diffusive contribution to the charge current is the relativistic generalisation of Fick's law.

To summarise, we have

$$\begin{aligned} T^{\mu\nu}_{\text{dissipative}} &= -\zeta\vartheta P^{\mu\nu} - 2\eta\sigma^{\mu\nu} + q^\mu u^\nu + u^\mu q^\nu, \\ (J_i^\mu)_{\text{dissipative}} &= j_i^\mu, \\ (J_S^\mu)_{\text{dissipative}} &= \frac{q^\mu - \mathfrak{m}_i j_i^\mu}{\mathcal{T}}. \end{aligned} \tag{2.13}$$

where

$$\begin{aligned} q^\mu &= -\kappa P^{\mu\nu}(\partial_\nu \mathcal{T} + a_\nu \mathcal{T})\,, \\ j_i^\mu &= -D_{ij} P^{\mu\nu} \partial_\nu \Big[\frac{\mathfrak{m}_j}{\mathcal{T}}\Big]\,, \end{aligned} \tag{2.14}$$

we also have

$$\mathcal{T}\nabla_\mu J_S^\mu = \zeta\vartheta^2 + 2\eta\sigma_{\mu\nu}\sigma^{\mu\nu} + \frac{q^\mu q_\mu}{\kappa\mathcal{T}} + \mathcal{T}(D^{-1})^{ij} j_i^\mu j_{j\mu}. \tag{2.15}$$

As q^μ, j_i^μ and $\sigma^{\mu\nu}$ are all spacelike vectors and tensors, the RHS of (2.15) is positive provided η, ζ, κ and D are positive parameters, a condition we further assume. This establishes that (even locally) entropy can only be produced but never destroyed. In equilibrium, $\nabla_\mu J_S^\mu$ must vanish. It follows that, q^μ, j_i^μ, ϑ and $\sigma^{\mu\nu}$ each individually vanish in equilibrium.

For fluids with gravity duals, the shear viscosity is given by $\eta = \frac{s}{4\pi}$ [25]. We can estimate the thermalisation length of the fluid by comparing coefficients at different orders in the derivative expansion

$$l_{\text{mfp}} \sim \frac{\eta}{\rho} = \frac{s}{4\pi\rho}. \tag{2.16}$$

This length scale may plausibly be identified with the thermalisation length scale of the fluid. This may be demonstrated within the kinetic theory, where l_{mfp} is simply the mean free path of colliding molecules, but is expected to apply to more generally to any fluid with short range interactions.

When studying fluids on curved manifolds (as we will proceed to do in Ch.3), one could add generally covariant terms, built out of curvatures, to the stress tensor. For instance, we could add a term proportional to $R^{\mu\nu}$ to the expression for $T^{\mu\nu}$. We will ignore all such terms in this dissertation for a reason we now explain. In all the solutions of fluid mechanics that we will study, the length scale over which fluid quantities vary is at least as large as the length scale of curvatures of the manifold. Any expression built out of a curvature contains at least two spacetime derivatives of the metric; it follows that any contribution to the stress tensor proportional to a curvature is effectively at least two orders subleading in the derivative expansion, and so is negligible compared to all the other terms we have retained.

2.2.3 Definitions of velocity

So far, we have been vague regarding precisely what we mean by the velocity, u^μ. We stated that it was the velocity of the rest frame of the fluid without specifying the rest frame. In this section we will discuss various definitions of velocity. Changes in the definition of velocity will change the transport coefficients. Note that this is not a gauge invariance – there is no ambiguity in the evolution of the velocity, these field redefinitions change the equations of motion.

If one views fluid mechanics as a phenomenological theory, designed to describe the results of experiments where one can measure properties of the fluid directly, the velocity *should not* be defined abstractly. The velocity can be measured directly, e.g. by inserting probe particles and watching them or putting small turbines in the fluid. The method of measuring the velocity provides the definition. One determines the transport coefficients

by performing a few experiments and uses these to make predictions for other situations. In writing down the equations of fluid mechanics, one should leave the precise definition of velocity ambiguous, as the measurements of transport coefficients will fix this.

However, when one tries to derive the equations of fluid mechanics, with expressions for the transport coefficients, from a microscopic theory (or a gravity dual!) *one needs* an abstract definition of velocity so that one has a microscopic notion of rest frame. Two popular definitions are due to Landau [53] – the velocity of energy flow – and Eckart [54] – the velocity of charge flow.

The Landau definition boils down to

$$\begin{aligned} q^\mu_{\text{Landau}} &= -u^\lambda P^{\mu\nu} T_{\lambda\nu} = 0, \\ \implies u^\mu_{\text{Landau}} &= u^\mu + \frac{q^\mu}{\rho + \mathcal{P}}\,, \\ j^\mu_{i,\text{Landau}} &= j^\mu_i - \frac{\mathfrak{r}_i}{\rho + \mathcal{P}} q^\mu\,, \end{aligned} \tag{2.17}$$

with the correction to $S^{\mu\nu}$ being second order in derivatives. Essentially, one reabsorbs thermal conductivity into a redefinition of velocity.

In contrast, the Eckart definition boils down to

$$\begin{aligned} j^\mu_{i,\text{Eckart}} &= P^{\mu\nu} J_{i\nu} = 0, \\ \implies u^\mu_{\text{Eckart}} &= u^\mu + \frac{j^\mu_i}{\mathfrak{r}_i}\,, \\ q^\mu_{\text{Eckart}} &= q^\mu - \frac{\rho + \mathcal{P}}{\mathfrak{r}_i} j^\mu_i\,, \end{aligned} \tag{2.18}$$

with the correction to $S^{\mu\nu}$ being second order in derivatives, again. Here one reabsorbs diffusion into a redefinition of velocity.

We emphasise that these two abstract definitions need not agree with the velocity that one would measure in an actual experiment. In fact, the Landau definition will disagree when thermal conduction takes place and the Eckart definition will disagree when there is diffusion.

In this dissertation, we are not in either of these situations. We are not trying to describe the results of experiments and we are not trying to derive transport coefficients from some more fundamental theory. Instead, we wish to use solutions of the equations of fluid mechanics to make predictions for gravity. We do not have any means to measure the velocity, but the actual value of the velocity is not important so long as the equations are consistent. We are free to pursue either approach – use an abstract definition of velocity or leave it ambiguous.

We will choose to leave the velocity ambiguous for the following reason. As mentioned in the introduction, we wish to make as much use as possible of our physical intuition for fluids. Thermal conductivity and diffusion are both physically intuitive effects and we don't want to spoil our intuition by removing thesm with a funny choice of variables.

One can imagine situations where either of the two abstract definitions of velocity would lead to unintuitive descriptions of the physics. For example, consider two parallel infinite plates held at different temperatures with the region between them filled with water.

Clearly there will be heat flow from the hotter plate to the colder one. If we used the Landau definition of velocity, we would have to say that water is flowing from one plate to the other. For this to make sense, water would have to be created at one plate and destroyed at the other. This is clearly an unphysical description of this situation.

2.3 Surfaces

The plasmaball configurations we will consider in Ch.4-6 have a domain wall separating a bubble of the deconfined phase from the confined phase. As the density, pressure, etc. of the deconfined phase are a factor of N^2 larger than the confined phase, we can treat the confined phase as the vacuum and the domain wall as a surface bounding the deconfined fluid.

At surfaces, the density of the fluid changes too rapidly to be described by fluid mechanics. However, provided that we look at length scales much larger than the thickness of the surface, we can replace this region by a delta function localised piece of the stress tensor. At these length scales, this stress tensor will depend on the direction of the surface, with dependance on its curvature being suppressed.

In general, introducing a surface energy density σ_E, a surface entropy density σ_S and a surface tension σ, surface R-charge densities σ_{R_i}, considerations similar to those leading to (2.2) lead to

$$\begin{aligned}\sigma_E &= \sigma + \mathcal{T}\sigma_S + \mathfrak{m}_i\,\sigma_{R_i},\\ \mathrm{d}\sigma_E &= \mathcal{T}\,\mathrm{d}\sigma_S + \mathfrak{m}_i \mathrm{d}\sigma_{R_i}.\\ \mathrm{d}\sigma &= -\sigma_S\,\mathrm{d}\mathcal{T} - \sigma_{R_i}\mathrm{d}\mathfrak{m}_i.\end{aligned}$$

However, the surface tension was only computed at the phase transition $\mathcal{T} = \mathcal{T}_{\rm c}$, $\mathfrak{m}_i = 0$ in [50], so we will have to ignore its temperature and chemical potential dependence. As we can see above, this is equivalent to setting $\sigma_S = \sigma_{R_i} = 0$ and $\sigma_E = \sigma$.

Let's describe the location of the surface by a function $f(x)$ that is positive inside the fluid and has a first order zero on the surface.

$$T^{\mu\nu} = \theta(f)T^{\mu\nu}_{\rm fluid} + \delta(f)T^{\mu\nu}_{\rm surface}. \tag{2.19}$$

At large length scales, as mentioned above, $T^{\mu\nu}_{\rm surface}$ will only depend on the first derivative of f and no higher derivatives.

If we demand invariance under reparameterisations of the function $f(x)$, which can be expressed as $f(x) \to g(x)f(x)$ with $g(x) > 0$, and that the surface moves at the velocity of the fluid

$$u^\mu \partial_\mu f\big|_{f=0} = 0, \tag{2.20}$$

the most general surface stress tensor we can have is (see §2.3 of [2])

$$T^{\mu\nu}_{\rm surface} = \left[An^\mu n^\nu + Bu^\mu u^\nu + C\left(u^\mu n^\nu + n^\mu u^\nu\right) + Dg^{\mu\nu}\right]\sqrt{\partial f\cdot\partial f}\,\delta(f)\,.$$

where $n_\mu = -\partial_\mu f/\sqrt{\partial f\cdot\partial f}$ is the outward pointing unit normal to the surface.

We can fix A, B, C, D by looking at a fluid at rest, $u^\mu = (1, 0, 0, \ldots)$, with a surface $f(x) = x$

$$T^{\mu\nu}_{\text{surface}} = \begin{pmatrix} B-D & -C & 0 \\ -C & A+D & 0 \\ 0 & 0 & D \end{pmatrix} \delta(x) = \begin{pmatrix} \sigma_E & 0 & 0 \\ 0 & 0 & 0 \\ 0 & 0 & -\sigma \end{pmatrix} \delta(x).$$

This gives

$$T^{\mu\nu}_{\text{surface}} = \sqrt{\partial f \cdot \partial f}\left[\sigma_E u^\mu u^\nu - \sigma(g^{\mu\nu} - n^\mu n^\nu + u^\mu u^\nu)\right], \tag{2.21}$$

Note that $(\partial_\mu f) T^{\mu\nu}_{\text{surface}} = 0$.

If we take the surface tension to be constant, as discussed above, we get

$$T^{\mu\nu}_{\text{surface}} = -\sigma h^{\mu\nu}\sqrt{\partial f \cdot \partial f}, \tag{2.22}$$

where $h_{\mu\nu} = g_{\mu\nu} - n_\mu n_\nu$ is the induced metric of the surface.

The factor of $\sqrt{\partial f \cdot \partial f}$ also has a simple interpretation: suppose we use a coordinate system where f is one of the coordinates. Then

$$\sqrt{\partial f \cdot \partial f} = \sqrt{g^{ff}} = \sqrt{\frac{\det h}{\det g}}, \tag{2.23}$$

which provides the correct change of integration measure for localisation to the surface. If we used some other coordinates, there'd be an extra Jacobian factor.

We have

$$\nabla_\mu T^{\mu\nu} = \theta(f)\nabla_\mu T^{\mu\nu}_{\text{fluid}} + \delta(f)(\partial_\mu f) T^{\mu\nu}_{\text{fluid}} + \delta(f)\nabla_\mu T^{\mu\nu}_{\text{surface}}. \tag{2.24}$$

So, in addition to the equation of motion (2.3), we also have the boundary conditions

$$(\partial_\mu f) T^{\mu\nu}_{\text{fluid}} + \nabla_\mu T^{\mu\nu}_{\text{surface}}\Big|_{f=0} = 0. \tag{2.25}$$

Also, when we take the surface tension to be constant:

$$\nabla_\mu T^{\mu\nu}_{\text{surface}} = \sigma\left[\frac{\Box f}{(\partial f \cdot \partial f)^{1/2}} - \frac{(\partial^\mu f)(\partial^\lambda f)\nabla_\mu \partial_\lambda f}{(\partial f \cdot \partial f)^{3/2}}\right]\partial^\nu f = -\sigma\,\Theta\,\partial^\nu f, \tag{2.26}$$

where Θ is the trace of the extrinsic curvature of the surface, as seen from outside the fluid (see §2.A).

If we have several disconnected surfaces, it is convenient to make the separation $f = \prod_i f_i$. As the surfaces are disconnected, the zero sets of the f_i do not intersect. Also, the f_i are all positive inside the fluid. Therefore, whenever one of the f_i is negative or zero, all the others are positive. Luckily, (2.24) splits nicely

$$\nabla_\mu T^{\mu\nu} = \prod_i \theta(f_i)\,\nabla_\mu T^{\mu\nu}_{\text{fluid}} + \sum_i \delta(f_i)\left[(\partial_\mu f_i) T^{\mu\nu}_{\text{fluid}} + \nabla_\mu T^{\mu\nu}_{\text{surface}}(f_i)\right].$$

From the form of the gravity solution fig.1.3, we would expect σ_E/ρ to be similar to the thickness of the surface. We can estimate it using

$$\xi = \frac{\sigma}{\rho_{\text{c}}}. \tag{2.27}$$

Where ρ_{c} is the density at the phase transition.

2.4 Rigid rotation

In this section we will show how to use the general formalism of the previous sections to construct equilibrium configurations of fluids. We will also derive a simple approach to studying the overall thermodynamic properties of these configurations.

2.4.1 Solutions for the interior

We want to find solutions of (2.3) that are independent of time. For this to happen, it is essential that entropy is not being produced, which means we need to set (2.15) to zero. This means we need velocity configurations that have zero expansion and shear. In general, this would be a combination of a uniform boost and rigid rotation (when we consider fluids on spheres in chapter 3 it will just be rigid rotation). We can always boost to a frame where the centre of rotation is static and the rotation lies in the Cartan directions of the rotation group. This gives

$$u = \gamma(\partial_t + \Omega_a \partial_{\phi_a}), \tag{2.28}$$

where Ω_a are the angular velocities and ∂_{ϕ_a} are a set of commuting rotational Killing vectors. The important feature is that the velocity is a normalisation factor times a Killing vector:

$$u^\mu = \gamma K^\mu, \qquad \gamma^2 K^\mu K_\mu = -1, \qquad \nabla_{(\mu} K_{\nu)} = 0. \tag{2.29}$$

One can deduce that

$$\vartheta = \sigma^{\mu\nu} = 0, \qquad u^\mu \partial_\mu \gamma = 0, \qquad a_\mu = -\frac{\partial_\mu \gamma}{\gamma}\,.$$

Which leads to

$$q^\mu = -\kappa\gamma P^{\mu\nu}\partial_\nu\left[\frac{\mathcal{T}}{\gamma}\right], \qquad j_i^\mu = -D_{ij}P^{\mu\nu}\partial_\nu\left[\frac{\mathfrak{m}_j}{\mathcal{T}}\right].$$

One can also show that

$$\begin{aligned}
\nabla_\mu T^{\mu\nu}_{\text{perfect}} =& \gamma\left(sP^{\nu\mu} + \left\{\mathcal{T}\left(\frac{\partial s}{\partial \mathcal{T}}\right) + \mathfrak{m}_i\left(\frac{\partial \mathfrak{r}_i}{\partial \mathcal{T}}\right)\right\}u^\nu u^\mu\right)\partial_\mu\left[\frac{\mathcal{T}}{\gamma}\right] \\
&+ \gamma\left(\mathfrak{r}_i P^{\nu\mu} + \left\{\mathcal{T}\left(\frac{\partial s}{\partial \mathfrak{m}_i}\right) + \mathfrak{m}_j\left(\frac{\partial \mathfrak{r}_j}{\partial \mathfrak{m}_i}\right)\right\}u^\nu u^\mu\right)\partial_\mu\left[\frac{\mathfrak{m}_i}{\gamma}\right], \\
\nabla_\mu J^\mu_{i,\text{perfect}} =& \gamma\left(\frac{\partial \mathfrak{r}_i}{\partial \mathcal{T}}\right)u^\mu\partial_\mu\left[\frac{\mathcal{T}}{\gamma}\right] + \gamma\left(\frac{\partial \mathfrak{r}_i}{\partial \mathfrak{m}_j}\right)u^\mu\partial_\mu\left[\frac{\mathfrak{m}_j}{\gamma}\right]
\end{aligned}$$

So the velocity configuration (2.28) will be an equilibrium solution to the equations of motion provided that

$$\frac{\mathcal{T}}{\gamma} = T = \text{constant}, \qquad \frac{\mathfrak{m}_i}{\gamma} = \mu_i = \text{constant}, \qquad \frac{\mathfrak{m}_i}{\mathcal{T}} = \nu_i = \frac{\mu_i}{T} = \text{constant}. \tag{2.30}$$

Using the equation of state and (2.2), this determines all of the intensive thermodynamic quantities in the fluid.

2.4.2 Solutions for surfaces

The fluid configurations described in the previous subsection have $T^{\mu\nu}_{\text{dissipative}} = 0$. Therefore

$$(\partial_\mu f) T^{\mu\nu}_{\text{fluid}} = (\partial_\mu f) T^{\mu\nu}_{\text{perfect}} = \mathcal{P}\partial^\nu f.$$

This means that (2.25) and (2.26) reduce to

$$\mathcal{P}|_{f=0} = \sigma\Theta. \tag{2.31}$$

As the pressure is determined by (2.30), this provides a differential equation that determines allowed positions of surfaces. Demanding that the surface has no conical singularities turns out to provide enough boundary conditions to determine the position of the surface completely (up to discrete choices) in terms of the parameters Ω_a, T and μ_i.

2.4.3 Thermodynamics of solutions

We compute the extensive thermodynamic properties of these solutions by integrating the time components of the corresponding currents (noting that the current associated with a Killing vector ζ^μ is $J^\mu_\zeta = T^{\mu\nu}\zeta_\nu$):

$$Q_X = \int \mathrm{d}V J^0_X. \tag{2.32}$$

In particular, also noting that for equilibrium configurations $\partial^0 f = 0$,

$$Q_\zeta = \int \mathrm{d}V \theta(f) \left[(\rho + \mathcal{P})\gamma^2 K^0 K\cdot\zeta + \mathcal{P}\zeta^0\right] - \int \mathrm{d}V \delta(f)\sqrt{\partial f\cdot\partial f}\sigma\zeta^0. \tag{2.33}$$

Noting that $K^0 = (\partial_t)^0 = 1$ and $(\partial_{\phi_a})^0 = 0$, this gives

$$\begin{aligned}
E = -Q_{\partial_t} &= -\int \mathrm{d}V \theta(f) \left[(\rho + \mathcal{P})\gamma^2 K\cdot\partial_t + \mathcal{P}\right] + \int \mathrm{d}V \delta(f)\sqrt{\partial f\cdot\partial f}\sigma, \\
L_a = Q_{\partial_{\phi_a}} &= \int \mathrm{d}V \theta(f) \left[(\rho + \mathcal{P})\gamma^2 K\cdot\partial_{\phi_a}\right], \\
S = Q_S &= \int \mathrm{d}V \theta(f) \left[\gamma s\right], \\
R_i = Q_{R_i} &= \int \mathrm{d}V \theta(f) \left[\gamma \mathfrak{r}_i\right].
\end{aligned} \tag{2.34}$$

From these quantities, we can compute overall angular velocities Ω_a, temperature T and chemical potentials μ_i thermodynamically

$$\mathrm{d}E = \Omega_a \,\mathrm{d}L_a + T\,\mathrm{d}S + \mu_i\,\mathrm{d}R_i. \tag{2.35}$$

Note that these quantities are different from the local thermodynamic properties of the fluid in its rest frame. The quantities $(\mathcal{T}, \mathfrak{m}_i)$ are properties of each patch of fluid, in contrast to (T, μ_i), which are properties of the entire configuration. In particular, the local temperature,

$\mathcal{T}$, only knows about the thermal energy of the plasma, whereas the overall temperature, T, also knows about its kinetic energy.

A priori, it may not seems that these quantities have to be the same as Ω_a, T and μ_i from (2.28) and (2.30). However, we can show that they are the same by checking that the quantities taken from (2.28) and (2.30) satisfy (2.35). In practice, it is easier to verify the equivalent statement

$$\mathrm{d}(E - \Omega_a L_a - TS - \mu_i R_i) = -L_a \,\mathrm{d}\Omega_a - S\,\mathrm{d}T - R_i\,\mathrm{d}\mu_i. \tag{2.36}$$

First, making use of (2.2), we see that

$$E - \Omega_a L_a - TS - \mu_i R_i = -Q_K - TQ_S - \mu_i Q_{R_i} = -\int \mathrm{d}V \theta(f)\mathcal{P} + \int \mathrm{d}V \delta(f)\sqrt{\partial f \cdot \partial f}\sigma. \tag{2.37}$$

Note that the second integral is simply σ times the surface area: as we saw in (2.23) the factor of $\sqrt{\partial f \cdot \partial f}$ provides the correct change of measure for the delta function to localise the integral to the surface.

Consider an infinitesimal change of Ω_a, T and μ_i. We have

$$\mathrm{d}\mathcal{P} = s\,\mathrm{d}(\gamma T) + r_i\,\mathrm{d}(\gamma\mu_i) = \frac{\rho + \mathcal{P}}{\gamma}\,\mathrm{d}\gamma + \gamma s\,\mathrm{d}T + \gamma \mathfrak{r}_i\,\mathrm{d}\mu_i,$$
$$\gamma^{-3}\,\mathrm{d}\gamma = K \cdot \mathrm{d}K = K \cdot l_a\,\mathrm{d}\Omega_a.$$

From this, we see that (2.36) is satisfied by the contributions from the interior. As the right hand side of (2.36) has no contributions from the surface, we need to check that the surface contributions of the variation of (2.37) cancel.

The change in the surface area can be written as

$$\mathrm{d}\mathcal{A} = \oint \mathrm{d}A\, \vec{n} \cdot \vec{w},$$

where the integral is performed over the union of the initial and final surfaces, $\vec{n}$ is a unit normal vector pointing into the initial fluid and out of the final fluid and $\vec{w}$ is some vector field that is equal to the outward pointing normal at both the initial and final surfaces. By Gauss' theorem, this can be written as

$$\mathrm{d}\mathcal{A} = \int \mathrm{d}V\, \nabla \cdot \vec{w},$$

with the integral performed over the region between the two surfaces. The volume element can be written as $\int \mathrm{d}V = \int \mathrm{d}A\,(\vec{n} \cdot \Delta x)$, with $\vec{n}$ pointing outwards. As the volume element is already infinitesimal, we can replace $\vec{w}$ with the vector field described in (2.45), as the difference would be infinitesimal, i.e. $\nabla \cdot \vec{w} \to \Theta$. Also, as $f = 0$ on the initial surface, and $f + \mathrm{d}f = 0$ on the final surface ($\mathrm{d}f$ refers to the change in f due to the change in Ω_a, T and μ_i), we have

$$\partial_\mu f \Delta x^\mu + \frac{\partial f}{\partial \Omega_a}\mathrm{d}\Omega_a + \frac{\partial f}{\partial T}\mathrm{d}T + \frac{\partial f}{\partial \mu_i}\mathrm{d}\mu_i = 0,$$
$$\implies \vec{n} \cdot \Delta x = \frac{\mathrm{d}f}{\sqrt{\partial f \cdot \partial f}}.$$

Therefore

$$\mathrm{d}\mathcal{A} = \int \mathrm{d}V \delta(f) \Theta \, \mathrm{d}f.$$

So, we can write the surface contribution to the variation of (2.37) as

$$\mathrm{d}(E - \Omega_a L_a - TS - \mu_i R_i)_{\text{surface}} = -\int \mathrm{d}V \delta(f)\, \mathcal{P}\, \mathrm{d}f + \int \mathrm{d}V \delta(f)\, \sigma \Theta \, \mathrm{d}f,$$

which vanishes due to (2.31).

The thermodynamics of the solution can be summarised by defining a grand partition function

$$\mathcal{Z}_{\text{gc}} = \mathrm{Tr} \exp\left(-\frac{E - \Omega_a L_a - \mu_i R_i}{T}\right). \tag{2.38}$$

In the thermodynamic limit,

$$\begin{aligned} -T \ln \mathcal{Z}_{\text{gc}} &= E - \Omega_a L_a - TS - \mu_i R_i, \\ \mathrm{d}(T \ln \mathcal{Z}_{\text{gc}}) &= L_a \, \mathrm{d}\Omega_a + S \, \mathrm{d}T + R_i \, \mathrm{d}\mu_i. \end{aligned} \tag{2.39}$$

We have seen that

$$T \ln \mathcal{Z}_{\text{gc}} = \int_{f>0} \mathrm{d}V \, \mathcal{P} - \int_{f=0} \mathrm{d}A \, \sigma \tag{2.40}$$

and the Ω_a, T and μ_i are the same as those given by (2.28) and (2.30).

Appendices

2.A Extrinsic curvature

Suppose we have a timelike surface with unit normal vector n pointing toward us (spacelike surfaces will require some sign differences). The induced metric on the surface is

$$h_{\mu\nu} = g_{\mu\nu} - n_\mu n_\nu. \tag{2.41}$$

The extrinsic curvature is given by [55]

$$\Theta_{\mu\nu} = \frac{1}{2}\mathcal{L}_n h_{\mu\nu} = \nabla_\mu n_\nu. \tag{2.42}$$

We have to be a little careful with the last expression. It agrees with the first expression when projected tangent to the surface. The first expression has vanishing components normal to the surface. The normal components of the second expression depend on how we extend n off the surface.

The conventional choice for extending n is as follows: at each point on the surface, construct the geodesic that passes through that point tangent to n and parallel transport n along it. In other words

$$n^\mu \nabla_\mu n^\nu = 0. \tag{2.43}$$

This ensures that the second expression in (2.42) has vanishing components normal to the surface. The other normal component, $n^\nu \nabla_\mu n_\nu$, vanishes due to the normalisation of n.

For the surfaces given by $f(x) = 0$, considered in §2.3, the unit normal on the surface is given by

$$n_\mu = -\frac{\partial_\mu f}{\sqrt{\partial f \cdot \partial f}}. \tag{2.44}$$

However, if we used this vector away from the surface, it would not satisfy (2.43). We could still use either expression in (2.42) with this vector — we would just have to project the second one tangent to the surface. Alternatively, we can use

$$n_\mu = -\frac{\partial_\mu f}{(\partial f \cdot \partial f)^{1/2}} + \left[\frac{\partial^\nu f \, \nabla_\nu \partial_\mu f}{(\partial f \cdot \partial f)^{3/2}} - \frac{\partial_\mu f \, \partial^\lambda f \, \partial^\nu f \, \nabla_\lambda \partial_\nu f}{(\partial f \cdot \partial f)^{5/2}}\right] f + \mathcal{O}(f^2). \tag{2.45}$$

The $\mathcal{O}(f^2)$ terms don't contribute to (2.42) or (2.43) on the surface. The contribution of the $\mathcal{O}(f)$ terms on the surface to (2.42) are normal to the surface and ensure that n satisfies (2.43).

Either way, on the surface, we get

$$\Theta_{\mu\nu} = -\frac{\nabla_\mu \partial_\nu f}{(\partial f \cdot \partial f)^{1/2}} + \frac{\partial_\mu f \, \partial^\lambda f \, \nabla_\lambda \partial_\nu f + \partial_\nu f \, \partial^\lambda f \, \nabla_\lambda \partial_\mu f}{(\partial f \cdot \partial f)^{3/2}} - \frac{\partial_\mu f \, \partial_\nu f \, \partial^\lambda f \, \partial^\sigma f \, \nabla_\lambda \partial_\sigma f}{(\partial f \cdot \partial f)^{5/2}}. \tag{2.46}$$

As this is perpendicular to n, it doesn't matter if we contract its indices with the full metric $g_{\mu\nu}$ or the induced metric $h_{\mu\nu}$. We get

$$\Theta = \Theta^\mu_\mu = -\frac{\Box f}{(\partial f \cdot \partial f)^{1/2}} + \frac{\partial^\mu f \, \partial^\nu f \, \nabla_\mu \partial_\nu f}{(\partial f \cdot \partial f)^{3/2}}. \tag{2.47}$$

Chapter 3

Large rotating AdS black holes from fluid mechanics

In this chapter, we predict certain universal features in the thermodynamics and other classical properties of large rotating black holes in global AdS_D spaces for arbitrary D. Our analysis applies to black holes in any consistent theory of gravity that admits an AdS_D background; for example, IIB theory on $AdS_5 \times S^5$ or M theory on $AdS_7 \times S^4$ or $AdS_4 \times S^7$.

When we combine the statement that all theories of gravity on an AdS_D background are expected to admit a dual description as a conformal field theory on $S^{D-2}\times$ time [4, 6] with the statement that quantum field theories at sufficiently high energy density admit an effective description in terms of fluid dynamics, we are led to the proposal that large, rotating black holes in arbitrary global AdS_D spaces admit an accurate dual description as rotating, stationary configurations of a conformal fluid on S^{D-2}.

As discussed in §1.2, we are able to derive several properties of large rotating AdS black holes by reading off the thermodynamic equation of state of the dual 'fluid' from the properties of large, static, non-rotating AdS black holes and inputting these equations of state into the Navier-Stokes equations. We are then able to deduce the thermodynamics of rotating black holes. In the rest of this introduction, we will describe our proposal and its consequences, including the tests it successfully passes, in more detail.

Consider a theory of gravity coupled to a gauge field (based on a gauge group of rank c) on AdS_D. In an appropriate limit, the boundary theory is effectively described by conformal fluid dynamics with c simultaneously conserved, mutually commuting $U(1)$ charges R_i $(i = 1 \dots c)$. Conformal invariance and extensivity force the grand canonical partition function of this fluid to take the form

$$\ln \mathcal{Z}_{\mathrm{gc}}(T, \mu) = V T^{d-1}\ h(\mu/T)\,, \tag{3.1}$$

where μ represents the set of the c chemical potentials conjugate to the $U(1)$ charges of the fluid, V and T represent the volume and the overall temperature of the fluid respectively and $d = D - 1$ is the spacetime dimensions of the boundary. As we have explained above, the as yet unknown function $h(\mu/T)$ may be read off from the thermodynamics of large, charged, static black holes in AdS.

The thermodynamic equation of state described above forms an input into the relativistic Navier-Stokes equations that govern the effective dynamics of the boundary conformal fluid. The full equations of fluid dynamics require more data than just the equation of state; for example we need to input dissipative parameters like viscosity. However, fluid dynamics on S^{d-1} admits a distinguished $c+n+1$ parameter set of stationary solutions (the parameters are their energy E, c commuting charges R_i and $n = \text{rank}(SO(d)) = \left[\frac{d}{2}\right]$ commuting angular momenta[1] on S^{d-1}). These solutions are simply the configurations into which any fluid initial state eventually settles down in equilibrium. They have the feature that their form and properties are independent of the values of dissipative parameters.

Although these solutions are nonlinear (i.e. they cannot be thought of as a small fluctuation about a uniform fluid configuration), it turns out that they are simple enough to be determined explicitly. These solutions turn out to be universal (i.e. they are independent of the detailed form of the function $h(\mu/T)$). Their thermodynamics is incredibly simple; it is summarised by the partition function

$$\begin{aligned}\ln \mathcal{Z}_{\rm gc}(T,\mu,\Omega) =& \ln \text{Tr} \exp\left[-\frac{(E-\mu_i R_i - \Omega_a L_a)}{T}\right] \\ =& \frac{VT^{d-1}h(\mu/T)}{\prod_{a=1}^{n}(1-\Omega_a^2)} = \frac{\ln \mathcal{Z}_{\rm gc}(T,\mu,0)}{\prod_{a=1}^{n}(1-\Omega_a^2)}\,,\end{aligned} \tag{3.2}$$

where E,L_a and Ω_a represent the energy, angular momenta and the angular velocities of the fluid respectively.

On the gravitational side of the duality, these fluid solutions correspond to stationary black holes. A theory of a rank c gauge field, interacting with gravity on AdS_D, possesses a $c+n+1$ parameter set of black hole solutions, labelled by the conserved charges described above. We propose that these black holes (when large) are dual to the solutions of fluid dynamics described in the previous paragraph. Our proposal yields an immediate prediction about the thermodynamics of large rotating black holes: the grand canonical partition function of these black holes must take the form of (3.2).

Notice that while the dependence of the partition function (3.2) on μ/T is arbitrary, its dependence on Ω_a is completely fixed. Thus, while our approach cannot predict thermodynamic properties of the static black holes, it does allow us to predict the thermodynamics of large rotating black holes in terms of the thermodynamics of their static counterparts. Further, our solution of fluid dynamics yields a detailed prediction for the boundary stress tensor and the local charge distribution of the corresponding black hole solution, which may be compared with the boundary stress tensor and currents calculated from black hole solutions (read off from the black hole solutions using the AdS/CFT dictionary [56–63]).

We have tested the thermodynamic predictions described above on every class of black hole solutions in AdS_D spaces that we are aware of. These solutions include the most general uncharged rotating black holes in arbitrary AdS_D space [64–66], various classes of charged rotating black holes in $AdS_5 \times S^5$ [67–70], in $AdS_7 \times S^4$ and in $AdS_4 \times S^7$ [71–73]. In the strict fluid dynamical limit, the thermodynamics of each of these black holes exactly

[1]Here, we use the notation $[x]$ to denote the integer part of the real number x.

reproduces[2] (3.2). In all the cases we have checked, the boundary stress tensor and the charge densities of these black holes are also in perfect agreement with our fluid dynamical solutions. The agreement described in this paragraph occurs only when one would expect it to, as we now explain in detail.

Recall that the equations of fluid mechanics describe the evolution of local energy densities, charge densities and fluid velocities as functions of spatial position. These equations are applicable only under certain conditions. First, the fluctuations about mean values (of variables like the local energy density) must be negligible. In the situations under study in this dissertation, the neglect of fluctuations is well justified by the 'large N' limit of the field theory, dual to the classical limit of the gravitational bulk.

Second, the equations of fluid mechanics assume that the fluid is in local thermodynamic equilibrium at each point in space, even though the energy and the charge densities of the fluid may vary in space. Fluid mechanics applies only when the length scales of variation of thermodynamic variables - and the length scale of curvatures of the manifold on which the fluid propagates - are large compared to the equilibration length scale of the fluid, a distance we shall refer to as the mean free path, $l_{\rm mfp}$.

The mean free path for any fluid may be estimated as [25] $l_{\rm mfp} \sim \frac{\eta}{\rho}$ where η is the shear viscosity and ρ is the energy density of the fluid. For fluids described by a gravitational dual, $\eta = \frac{s}{4\pi}$ where s is the entropy density [25]. Consequently, for the fluids under study in this paper, $l_{\rm mfp} \sim \frac{s}{4\pi\rho}$. As we will see in §3.2.5, the most stringent bound on $l_{\rm mfp}$, for the solutions presented in this chapter, comes from requiring that $l_{\rm mfp}$ be small compared to the radius of the S^{d-1}, which we set to unity. Consequently, fluid dynamics should be an accurate description for our solutions whenever $\frac{s}{4\pi\rho} \ll 1$. In every case we have studied, it turns out that this condition is met whenever the horizon radius, r_+, of the dual black hole is large compared to the AdS radius , $R_{\rm AdS}$. Black holes that obey this condition include all black holes whose temperature is large compared to unity, but also includes large radius extremal black holes in $AdS_5 \times S^5$, $AdS_7 \times S^4$ and $AdS_4 \times S^7$. It, however, never includes supersymmetric black holes in the same backgrounds, whose horizon radii always turn out to be of the same order as the AdS radius.

It follows that we should expect the Navier-Stokes equations to reproduce the thermodynamics of only large black holes. In all the cases we have studied, this is indeed the case. It is possible to expand the formulae of black hole thermodynamics (and the stress tensor and charge distribution) in a power series in $R_{\rm AdS}/r_+$. While the leading order term in this expansion matches the results of fluid dynamics, we find deviations from the predictions of Navier-Stokes equations at subleading orders.

While in this chapter we have used fluid dynamics to make predictions for black hole physics, the reverse view point may also prove useful. Existing black hole solutions in AdS spaces provide exact equilibrium solutions to the equations of fluid dynamics to all orders in $l_{\rm mfp}$. A study of the higher order corrections of these solutions (away from the $l_{\rm mfp} \to 0$ limit) might yield useful information about the nature of the fluid dynamical approximation of quantum field theories.

The plan of this chapter is as follows - In §3.1, we describe the general features of

[2]See, however, §3.5.8 for a puzzle regarding the first subleading corrections for a class of black holes in AdS_5.

fluid mechanics in conformal theories that are necessary for our work. It is followed by §3.2 in which we consider in detail a specific example of rigidly rotating fluid - a conformal fluid in $S^3 \times \mathbb{R}$. A straightforward generalisation gives us a succinct way of formulating fluid mechanics in spheres of arbitrary dimensions in §3.3.

We proceed then to compare the fluid mechanical predictions with various types of black holes in arbitrary dimensions. First, we consider uncharged rotating black holes in arbitrary dimensions in §3.4. Their thermodynamics, stress tensors and charge distributions are computed and are shown to exactly match the fluid mechanical predictions. In §3.5, we turn to the large class of rotating black hole solutions in $AdS_5 \times S^5$. Many different black holes with different sets of charges and angular momenta are considered in the large horizon radius limit and all of them are shown to fit exactly into our proposal in the strict fluid dynamical limit. However we also find deviations from the predictions of the Navier-Stokes equations at first subleading order in $l_{\rm mfp}$ for black holes with all SO(6) Cartan charges nonzero (these deviations vanish when the angular velocities, or one of the SO(6) charges is set to zero). This finding is at odds with naive expectations from fluid dynamics, which predict the first deviations from the Navier-Stokes equations to occur at $\mathcal{O}(l_{\rm mfp}^2)$ and is an as yet unresolved puzzle (a resolution was proposed in [74, 75], we will discuss this crtically in §3.7).

This is followed by §3.6, dealing with large rotating black holes in $AdS_4 \times S^7$ and $AdS_7 \times S^4$ backgrounds which are dual to field theories on M2 and M5 branes respectively. The thermodynamics of the rotating black hole solutions in these spaces are derived from their static counterparts using the duality to fluid mechanics and it is shown how the known rotating black hole solutions agree with the fluid mechanical predictions in the large horizon radius limit. In each of these cases, the formulae of black hole thermodynamics deviate from the predictions of the Navier-Stokes equations only at $\mathcal{O}(l_{\rm mfp}^2)$ in accord with general expectations. In the final section, we conclude our work and discuss further directions.

In Appendix 3.A, we discuss the constraints imposed by conformal invariance on the equations of fluid mechanics. In Appendix 3.B, we discuss the thermodynamics of free theories on spheres.

3.1 Fluid mechanics of conformal theories

In this section, we will discuss how our general treatment of fluid mechanics in §2.2 applies to a conformal fluid – the fluid of the 'stuff' of a conformal field theory in d dimensions. Conformal invariance imposes restrictions on both the thermodynamics of the fluid and the derivative expansion of the stress tensor.

3.1.1 Conformal thermodynamics

In this subsection, we review the thermodynamics of the conformal fluids we discuss in this chapter. The notation set up in this subsection will be used through the rest of this chapter.

Recall from §2.1 that the thermodynamics of a fluid is completely specified once we express the pressure, $\mathcal{P}$, in terms of the temperature $\mathcal{T}$ and chemical potentials $\mathfrak{m}_i$. Let

us define the dimensionless quantity $\nu_i = \mathfrak{m}_i/\mathcal{T}$. As a conformal theory has no dimensionful parameters, it follows from dimensional analysis that the most general equation of state we can have is

$$\mathcal{P} = \mathcal{T}^d h(\nu)\,, \tag{3.3}$$

where $h(\nu)$ is an arbitrary function, defined by this expression. All remaining thermodynamic expressions are easily determined in terms of the function $h(\nu)$ using (2.2):

$$\begin{aligned} \rho &= (d-1)\mathcal{P} = (d-1)\mathcal{T}^d h(\nu)\,, \\ \mathfrak{r}_i &= \mathcal{T}^{d-1} h_i(\nu)\,, \\ s &= \mathcal{T}^{d-1}(dh(\nu) - \nu_i h_i(\nu))\,, \end{aligned} \tag{3.4}$$

where $h_i(\nu) = \frac{\partial h(\nu)}{\partial \nu_i}$ denotes the derivative of $h(\nu)$ with respect to its i^{th} argument.

3.1.2 Conformal fluids

We will now discuss the restrictions imposed on the derivative expansion of the stress tensor by conformal invariance.

To start with, conformal invariance requires that the stress tensor be traceless.[3] This requirement relates the pressure of a conformal fluid to its density as $\mathcal{P} = \frac{\rho}{d-1}$ (this requirement may also be deduced from conformal thermodynamics, as seen in the previous subsection) where d is the dimension of the spacetime in which the fluid lives. Further, the tracelessness of the stress tensor also forces the bulk viscosity, ζ, to be zero.

It is easy to verify that these constraints are sufficient to guarantee the conformal invariance of the fluid dynamical equations listed above. Consider a conformal transformation $g_{\mu\nu} = \mathrm{e}^{2\phi}\tilde{g}_{\mu\nu}$ under which fluid velocity, temperature, rest energy density, pressure, entropy density and the charge densities transform as

$$\begin{aligned} u^\mu &= \mathrm{e}^{-\phi}\tilde{u}^\mu, \\ \mathcal{T} &= \mathrm{e}^{-\phi}\widetilde{\mathcal{T}}\,, \\ \rho &= \mathrm{e}^{-d\phi}\tilde{\rho}\,, \quad \mathcal{P} = \mathrm{e}^{-d\phi}\widetilde{\mathcal{P}}\,, \\ s &= \mathrm{e}^{-(d-1)\phi}\tilde{s}\,, \\ r_i &= \mathrm{e}^{-(d-1)\phi}\tilde{r}_i\,. \end{aligned}$$

It is easy to verify that these transformations induce the following transformations on the stress tensors and currents listed §2.2.2 (noting that under such a scaling, the viscosity, conductivity etc. scale as $\kappa = \mathrm{e}^{-(d-2)\phi}\tilde{\kappa}$, $\eta = \mathrm{e}^{-(d-1)\phi}\tilde{\eta}$, $\mu_i = \mathrm{e}^{-\phi}\tilde{\mu}_i$ and

[3] More accurately, conformal invariance relates the nonzero trace of the stress tensor to certain curvature forms; for example, in two dimensions $T^\mu_\mu = \frac{c}{12}R$ where R is the scalar curvature. However, as we have described above, curvatures are effectively zero in the one derivative expansion studied in this chapter. All formulae through the rest of this chapter and in the appendices apply only upon neglecting curvatures. We thank R. Gopakumar for a discussion of this point.

$D_{ij} = \mathrm{e}^{-(d-2)\phi}\widetilde{D}_{ij}$),

$$\begin{aligned} T^{\mu\nu} &= \mathrm{e}^{-(d+2)\phi}\widetilde{T}^{\mu\nu}, \\ J_i^\mu &= \mathrm{e}^{-d\phi}\widetilde{J}_i^\mu, \\ J_S^\mu &= \mathrm{e}^{-d\phi}\widetilde{J}_S^\mu. \end{aligned} \tag{3.5}$$

These are precisely the transformation properties that ensure the conformal invariance of the conservation equations (2.3). See Appendix 3.A for more details.

3.2 Equilibrium configurations of rotating conformal fluids on S^3

In this section and in the next, we will determine the equilibrium solutions of fluid dynamics equations for conformal fluids on spheres of arbitrary dimension. In this section, we work out the fluid dynamics on S^3 plus a time dimension in detail.[4] In the next section, we generalise the results of this section to spheres of arbitrary dimension.

3.2.1 Coordinates and isometries

Consider a unit S^3 embedded in $\mathbb{R}^4$ as

$$\begin{aligned} x^1 &= \sin\theta\cos\phi_1 \\ x^2 &= \sin\theta\sin\phi_1 \\ x^3 &= \cos\theta\cos\phi_2 \\ x^4 &= \cos\theta\sin\phi_2 \end{aligned} \tag{3.6}$$

with $\theta \in [0, \frac{\pi}{2}]$, $\phi_a \in [0, 2\pi)$. The metric of the spacetime $S^3 \times \mathbb{R}$ is

$$\mathrm{d}s^2 = -\mathrm{d}t^2 + \mathrm{d}\theta^2 + \sin^2\theta\,\mathrm{d}\phi_1^2 + \cos^2\theta\,\mathrm{d}\phi_2^2\,. \tag{3.7}$$

The Killing vectors of interest are ∂_t (Energy) and ∂_{ϕ_a} (SO(4) Cartan angular momenta).

3.2.2 Equilibrium solutions

In this subsection, we will discuss the construction of an equilibrium configurations of a conformal fluid on S^3 along the lines of §2.4. In this case, we are considering fluids without surfaces, so we can ignore the considerations of §2.4.2 and surface terms in §2.4.3.

As we have explained in the §2.4.1, an equilibrium configuration can be specified by a time-like Killing vector that describes the fluid flow. This has a unique solution – the fluid motion should be just a rigid rotation. By an $SO(4)$ rotation we can choose the two

[4] In this case, the dimensions of the spacetime in which the fluid lives is $d = 3 + 1 = 4$. The number of mutually commuting angular momenta is $n = 2$. The black hole dual lives in AdS space of dimensions $D = d + 1 = 5$.

orthogonal two planes of this rotation as the (1-2) and (3-4) planes (see (3.6)). This implies that

$$u = \gamma(\partial_1 + \Omega_1 \partial_{\phi_1} + \Omega_2 \partial_{\phi_2}), \quad \text{where} \quad \gamma = \left(1 - v^2\right)^{-1/2} \quad \text{and} \quad v^2 = \Omega_1^2 \sin^2\theta + \Omega_2^2 \cos^2\theta \,. \tag{3.8}$$

for some constants Ω_1 and Ω_2.

As discussed in §2.4.1, we are also forced to set

$$\mathcal{T} = T\gamma \,, \qquad \mathfrak{m}_i = \gamma \mu_i = \mathcal{T} \nu_i \,, \tag{3.9}$$

for constant T, μ_i and ν_i. These conditions completely determine all the thermodynamic quantities as a function of the coordinates on the sphere.

In summary the $3 + c$ parameter set of stationary solutions to fluid mechanics listed in this subsection (the parameters are T, Ω_a and ν_i where $i = 1 \ldots c$) constitute the most general stationary solutions of fluid mechanics on S^3.

3.2.3 Stress tensor and currents

Using the equations of state (3.4), we find that

$$\begin{aligned} \rho = 3\mathcal{P} &= 3T^4 \gamma^4 h(\nu), \\ s &= T^3 \gamma^3 [4h(\nu) - \nu_i h_i(\nu)], \\ r_i &= T^3 \gamma^3 h_i(\nu). \end{aligned} \tag{3.10}$$

The stress tensor is

$$T^{\mu\nu} = \mathcal{T}_{\rm c}{}^4 A \gamma^6 \times \begin{pmatrix} 3 + v^2 & 0 & 4\Omega_1 & 4\Omega_2 \\ 0 & 1 - v^2 & 0 & 0 \\ 4\Omega_1 & 0 & 3\Omega_1^2 + \csc^2\theta - \Omega_2^2 \cot^2\theta & 4\Omega_1\Omega_2 \\ 4\Omega_2 & 0 & 4\Omega_1\Omega_2 & 3\Omega_2^2 + \sec^2\theta - \Omega_1^2 \tan^2\theta \end{pmatrix} . \tag{3.11}$$

Charge and entropy currents are given by

$$\begin{aligned} J_i^\mu &= \mathcal{T}_{\rm c}{}^3 \gamma^4 C_i(1, 0, \Omega_1, \Omega_2) \,, \\ J_S^\mu &= \mathcal{T}_{\rm c}{}^3 \gamma^4 B(1, 0, \Omega_1, \Omega_2) \,, \end{aligned} \tag{3.12}$$

where we have defined

$$\begin{aligned} A &= h(\nu) \,, \\ B &= 4h(\nu) - \nu_i h_i(\nu) \,, \\ C_i &= h_i(\nu) = \frac{\partial h}{\partial \nu_i} \,. \end{aligned} \tag{3.13}$$

3.2.4 Overall thermodynamics

As discussed in §2.4.3, the quantities T, Ω_a and μ_i can be interpreted as the overall temperature, angular velocities and chemical potentials of the configuration. Note that these are distinct from the local rest frame temperature and chemical potentials of the fluid, $\mathcal{T}$ and $\mathfrak{m}_i$. The latter are related to the thermal internal energy of the fluid in its rest frame, the former are related to the total energy of the whole configuration, which includes contributions from the kinetic energy.

One can compute the all the other thermodynamic properties using (2.40), which in this case gives

$$T \ln \mathcal{Z}_{\rm gc} = \int \mathrm{d}V \mathcal{P} = T^4 h(\nu) \int \mathrm{d}V \gamma^4 = \frac{V_4 T^4 h(\nu)}{(1-\Omega_1^2)(1-\Omega_2^2)} \,. \tag{3.14}$$

where $V_4 = \mathrm{Vol}(S^3) = 2\pi^2$ is the volume of S^3. In other words

$$\ln \mathcal{Z}_{\rm gc}(T, \mu_i, \Omega_a) = \frac{\ln \mathcal{Z}_{\rm gc}(T, \mu_i, 0)}{(1-\Omega_1^2)(1-\Omega_2^2)} \,.$$

The energy, angular momentum, entropy and R-charges may now easily be evaluated by differentiation: we find

$$\begin{aligned}
E &= \frac{V_4 T^4 A}{(1-\Omega_1^2)(1-\Omega_2^2)} \left[\frac{2\Omega_1^2}{1-\Omega_1^2} + \frac{2\Omega_2^2}{1-\Omega_2^2} + 3 \right] , \\
L_1 &= \frac{V_4 T^4 A}{(1-\Omega_1^2)(1-\Omega_2^2)} \left[\frac{2\Omega_1}{1-\Omega_1^2} \right] , \\
L_2 &= \frac{V_4 T^4 A}{(1-\Omega_1^2)(1-\Omega_2^2)} \left[\frac{2\Omega_2}{1-\Omega_2^2} \right] , \\
S &= \frac{V_4 T^3 B}{(1-\Omega_1^2)(1-\Omega_2^2)} \,, \\
R_i &= \frac{V_4 T^3 C_i}{(1-\Omega_1^2)(1-\Omega_2^2)} \,,
\end{aligned} \tag{3.15}$$

These formulae constitute a complete specification of the thermodynamics of stationary rotating conformal fluids on S^3.

3.2.5 Validity of fluid mechanics

A systematic way to estimate the domain of validity of the Navier-Stokes equations would be to list all possible higher order corrections to these equations, and to check under what circumstances the contributions of these correction terms to the stress tensor and currents are small compared to the terms we have retained. Rather than carrying out such a detailed (and worthwhile) exercise, we present in this section a heuristic physical estimate of the domain of validity of fluid dynamics.

Consider a fluid composed of a collection of interacting 'quasiparticles', that move at an average speed v_p and whose collisions are separated (on the average) by the distance

$l_{\rm mfp}$ in the fluid rest frame. Consider a particular quasiparticle that undergoes two successive collisions: the first at the coordinate location x_1 and subsequently at x_2. In order for the fluid approximation to hold, it must be that

1. The fractional changes in thermodynamic quantities between the two collision points (e.g. $[\mathcal{T}(x_1) - \mathcal{T}(x_2)]/\mathcal{T}(x_1)$) are small. This condition is necessary in order for us to assume local thermal equilibrium.

2. The distance between the two successive collisions is small compared to the curvature/compactification scales of the manifold on which the fluid propagates. This approximation is necessary, for example, in order to justify the neglect of curvature corrections to the Navier-Stokes equations.

Let us now see when these two conditions are obeyed on our solutions. Recall that the local temperatures in our solutions take the form $\mathcal{T} = T\gamma$ where T is the overall temperature of the solution. If we treat the free path $l_{\rm mfp}$ as a function of temperature and chemical potentials, conformal invariance implies that

$$l_{\rm mfp}(\mathcal{T}, \nu_i) = \frac{1}{\gamma} l_{\rm mfp}(T, \nu_i)\,.$$

Hence, the first condition listed above is satisfied when the fractional variation in (say) the temperature is small over the rest frame mean free path $l_{\rm mfp}(\mathcal{T}, \nu_i)$, i.e. provided

$$\frac{l_{\rm mfp}(T, \nu_i)}{\gamma} \ll \gamma \left(\frac{\partial \gamma}{\partial \theta}\right)^{-1}, \tag{3.16}$$

which must hold for all points of the sphere.[5] The strictest condition one obtains from this is

$$l_{\rm mfp}(T, \nu_i) \ll \frac{1}{\left|\sqrt{1-\Omega_1^2} - \sqrt{1-\Omega_2^2}\right|}\,. \tag{3.17}$$

It turns out that the second condition listed above is always more stringent, especially when applied to fluid quasiparticles whose rest frame motion between two collisions is in the same direction as the local fluid velocity. It follows from the formulae of Lorentz transformations that the distance on the sphere between two such collisions is $l_{\rm mfp}(\mathcal{T}, \nu_i)\gamma(1 + v/v_p) = l_{\rm mfp}(T, \nu_i)(1 + v/v_p)$, where v_p is the quasiparticle's velocity in the rest frame of the fluid and v the fluid velocity. As the factor $(1 + v/v_p)$ is bounded between 1 and 2, we conclude that the successive collisions happen at distances small compared to the radius of the sphere provided

$$l_{\rm mfp}(T, \nu_i) \ll 1\,. \tag{3.18}$$

Hence, we conclude that the condition (3.18) (which is always more stringent than (3.17)) is the condition for the applicability of the equations of fluid mechanics.

[5] Recall that all variations in the temperature are perpendicular to fluid velocities, so that the typical scale of variation in both the rest frame and the lab frame coincide.

Of course the model (of interacting quasiparticles) that we have used to obtain (3.18) need not apply to the situations of our interest. However the arguments that led to (3.18) were essentially kinematical which leads us to believe that the result will be universal. Nonetheless, it would be useful to verify this result by performing the detailed analysis alluded to at the beginning of this subsection.

3.3 Rotating fluids on spheres of arbitrary dimension

We now generalise the discussion of the previous section to the study of conformal fluids on spheres of arbitrary dimension.

Let us embed S^{2n} in $\mathbb{R}^{2n+1}$ as

$$\begin{aligned} x^{2a-1} &= \left(\prod_{b=1}^{a-1}\cos\theta_b\right)\sin\theta_a\cos\phi_a\,, \\ x^{2a} &= \left(\prod_{b=1}^{a-1}\cos\theta_b\right)\sin\theta_a\sin\phi_a\,, \\ x^{2n+1} &= \left(\prod_{b=1}^{n}\cos\theta_b\right), \end{aligned} \tag{3.19}$$

Where $\theta_n \in [0,\pi]$, all other $\theta_a \in [0,\frac{\pi}{2}]$ and $\phi_a \in [0,2\pi)$. Any products with the upper limit smaller than the lower limit should be set to one. Although we appear to have specialised to even dimensional spheres above, we can obtain all odd dimensional sphere, S^{2n-1}, simply by setting $\theta_n = \pi/2$ in all the formulae of this section.

The metric on $S^{2n}\times$ time is given by

$$\mathrm{d}s^2 = -\mathrm{d}t^2 + \sum_{a=1}^{n}\left(\prod_{b=1}^{a-1}\cos^2\theta_b\right)\mathrm{d}\theta_a^2 + \sum_{a=1}^{n}\left(\prod_{b=1}^{a-1}\cos^2\theta_b\right)\sin^2\theta_a\mathrm{d}\phi_a^2\,. \tag{3.20}$$

We choose a rigidly rotating velocity

$$\begin{gathered} u^t = \gamma \qquad u^{\theta_a} = 0 \qquad u^{\phi_a} = \gamma\Omega_a \\ \gamma = (1-v^2)^{-1/2} \qquad v^2 = \sum_{a=1}^{n}\left(\prod_{b=1}^{a-1}\cos^2\theta_b\right)\sin^2\theta_a\Omega_a^2 \end{gathered} \tag{3.21}$$

As in §3.2.2, the equations of motion are solved, without dissipation, by setting

$$\frac{\mathcal{T}}{\gamma} = T = \text{constant}, \qquad \frac{\mu_i}{\mathcal{T}} = \nu_i = \text{constant}, \tag{3.22}$$

This gives a stress tensor

$$\begin{gathered} T^{tt} = T^d A(d\gamma^{d+2} - \gamma^d) \qquad T^{t\phi_a} = T^{\phi_a t} = T^d A d\gamma^{d+2}\Omega_a \\ T^{\theta_a\theta_a} = T^d A\gamma^d \left(\prod_{b=1}^{a-1} \sec^2\theta_b\right) \\ T^{\phi_a\phi_a} = T^d A\left[d\gamma^{d+2}\Omega_a^2 + \gamma^d\left(\prod_{b=1}^{a-1}\sec^2\theta_b\right)\csc^2\theta_a\right] \qquad T^{\phi_a\phi_b} = T^d A d\gamma^{d+2}\Omega_a\Omega_b \end{gathered} \tag{3.23}$$

and currents

$$\begin{aligned} J_S^t &= T^{d-1}B\gamma^d \quad J_S^{\theta_a} = 0 \quad J_S^{\phi_a} = T^{d-1}B\gamma^d\Omega_a\,, \\ J_i^t &= T^{d-1}C_i\gamma^d \quad J_i^{\theta_a} = 0 \quad J_i^{\phi_a} = T^{d-1}C_i\gamma^d\Omega_a\,, \end{aligned} \tag{3.24}$$

where

$$\begin{aligned} A &= h(\nu)\,, \\ B &= dh(\nu) - \nu_i h_i(\nu)\,, \\ C_i &= h_i(\nu)\,. \end{aligned} \tag{3.25}$$

The grand partition function is given by[6]

$$\ln \mathcal{Z}_{\rm gc} = \frac{V_d\, T^{d-1}\, h(\mu/T)}{\prod_b(1-\Omega_b^2)}\,, \tag{3.26}$$

where

$$V_d = \mathrm{Vol}(S^{d-1}) = \frac{2\cdot\pi^{d/2}}{\Gamma(d/2)}\,.$$

Differentiating this gives

$$\begin{aligned} E &= \frac{V_d\, T^d\, h(\nu)}{\prod_b(1-\Omega_b^2)}\left[2\sum_a \frac{\Omega_a^2}{1-\Omega_a^2} + d - 1\right]\,, \\ S &= \frac{V_d\, T^{d-1}[dh(\nu) - \nu_i h_i(\nu)]}{\prod_b(1-\Omega_b^2)}\,, \\ L_a &= \frac{V_d\, T^d\, h(\nu)}{\prod_b(1-\Omega_b^2)}\left[\frac{2\Omega_a}{1-\Omega_a^2}\right]\,, \\ R_i &= \frac{V_d\, T^{d-1}\, h_i(\nu)}{\prod_b(1-\Omega_b^2)}\,, \end{aligned} \tag{3.27}$$

As in the previous subsection, the fluid dynamical approximation is expected to be valid provided $l_{\rm mfp}(T,\nu_i) \ll 1$.

In Appendix 3.B, we have computed the thermodynamics of a free charged scalar field on a sphere, and compared with the general results of this section.

[6]In deriving this formula we have 'conjectured' that $\int_{S^{d-1}}\gamma^d = \frac{V_d}{\prod_{b=1}^{[d/2]}(1-\Omega_b^2)}$. It is easy to derive this formula for odd spheres. We have also analytically checked this formula for S^2 and S^4. We are ashamed, however, to admit that we have not yet found an analytic derivation of this integral for general even spheres.

3.4 Comparison with uncharged black holes in arbitrary dimensions

In the rest of this chapter, we will compare the predictions from fluid dynamics derived above with the thermodynamics, stress tensors and charge distributions of various classes of large rotating black hole solutions in AdS spaces. We start with uncharged rotating black holes on D dimensional AdS spaces (where D is arbitrary), which are dual to rotating configurations of uncharged fluids on spheres of dimension $(D-2)$.

3.4.1 Thermodynamics and stress tensor from fluid mechanics

In case of uncharged fluids the function $h(\nu)$ in the above section is a constant $h(\nu) = h$ and the $h_i(\nu) = \frac{\partial h(\nu)}{\partial \nu_i}$ are all equal to zero. It follows from (3.26) that the partition function is given by

$$\ln \mathcal{Z}_{\rm gc} = \frac{V_d\, T^{d-1}\, h}{\prod_b (1-\Omega_b^2)}\,, \tag{3.28}$$

and the analogue of equations (3.27) are

$$\begin{aligned} E &= \frac{V_d\, T^d\, h}{\prod_b (1-\Omega_b^2)} \left[\sum_a \frac{2\Omega_a^2}{1-\Omega_a^2} + d - 1 \right], \\ S &= \frac{V_d\, T^{d-1} h d}{\prod_b (1-\Omega_b^2)}\,, \\ L_a &= \frac{V_d\, T^d\, h}{\prod_b (1-\Omega_b^2)} \left[\frac{2\Omega_a}{1-\Omega_a^2} \right], \\ R_i &= 0\,. \end{aligned} \tag{3.29}$$

The stress tensor becomes

$$\begin{gathered} T^{tt} = hT^d(d\gamma^{d+2} - \gamma^d) \qquad T^{t\phi_a} = T^{\phi_a t} = hT^d d\gamma^{d+2}\Omega_a \\ T^{\theta_a\theta_a} = hT^d\gamma^d \left(\prod_{b=1}^{a-1} \sec^2\theta_b \right) \\ T^{\phi_a\phi_a} = hT^d \left[d\gamma^{d+2}\Omega_a^2 + \gamma^d \left(\prod_{b=1}^{a-1} \sec^2\theta_b \right) \csc^2\theta_a \right] \qquad T^{\phi_a\phi_b} = hT^d d\gamma^{d+2}\Omega_a\Omega_b\,. \end{gathered} \tag{3.30}$$

The mean free path in fluid dynamics can be estimated by taking the ratio of shear viscosity to energy density. As mentioned in the introduction, for fluids with gravity duals we can equivalently estimate $l_{\rm mfp}$ by taking the ratio of entropy to 4π times the energy (because of the universal relation $s = 4\pi\eta$).

$$l_{\rm mfp}(T,\nu)|_{\Omega=0} \sim \left[\frac{S}{4\pi E} \right]_{\Omega=0} = \frac{d}{4\pi T(d-1)}. \tag{3.31}$$

Consequently the expansion in $l_{\rm mfp}$ translates simply to an expansion in inverse powers of the temperature of our solutions.

3.4.2 Thermodynamics from black holes

The most general solution for uncharged rotating black holes in AdS_D was obtained in [65, 66]. These solutions are labelled by the $n+1$ parameters[7] a_i and r_+ (these are related to the n angular velocities and the horizon radius (or equivalently the mass parameter) of the black holes). The surface gravity κ and the horizon area A of these black holes are given by[8]

$$\kappa = \begin{cases} r_+(1+r_+^2)\displaystyle\sum_{i=1}^{n}\frac{1}{r_+^2+a_i^2} - \frac{1}{r_+} & \text{when } D=2n+1\,, \\ r_+(1+r_+^2)\displaystyle\sum_{i=1}^{n}\frac{1}{r_+^2+a_i^2} - \frac{1-r_+^2}{2r_+} & \text{when } D=2n+2\,, \end{cases}$$
$$A = \begin{cases} \dfrac{V_d}{r_+}\displaystyle\prod_{i=1}^{n}\frac{r_+^2+a_i^2}{1-a_i^2} & \text{when } D=2n+1\,, \\ V_d\displaystyle\prod_{i=1}^{n}\frac{r_+^2+a_i^2}{1-a_i^2} & \text{when } D=2n+2\,. \end{cases} \tag{3.32}$$

We will be interested in these formulae in the limit of large r_+. In this limit the parameter m (which appears in the formulae of [65, 66]) and the temperature $T=\kappa/2\pi$ are given as functions of r_+ by

$$\begin{aligned} T &= \left[\frac{(D-1)r_+}{4\pi}\right]\left(1+\mathcal{O}(1/r_+^2)\right), \\ 2m &= r_+^{D-1}\left(1+\mathcal{O}(1/r_+^2)\right). \end{aligned} \tag{3.33}$$

From these equations, it follows that the parameter m is related to the temperature T as

$$2m = T^{D-1}\left[\frac{4\pi}{D-1}\right]^{D-1}\left(1+\mathcal{O}(1/T^2)\right). \tag{3.34}$$

To leading order in r_+, the thermodynamic formulae take the form

$$\begin{aligned} \Omega_i &= a_i\,, \\ E &= \frac{V_{D-1}T^{D-1}}{16\pi G_D\prod_{j=1}^{n}(1-a_j^2)}\left[\frac{4\pi}{D-1}\right]^{D-1}\left[\sum_{i=1}^{n}\frac{2a_i^2}{1-a_i^2}+D-2\right], \\ L_i &= \frac{V_{D-1}T^{D-1}}{16\pi G_D\prod_{j=1}^{n}(1-a_j^2)}\left[\frac{4\pi}{D-1}\right]^{D-1}\left[\frac{2a_i}{1-a_i^2}\right], \\ S &= \frac{V_{D-1}T^{D-2}(D-1)}{16\pi G_D\prod_{j=1}^{n}(1-a_j^2)}\left[\frac{4\pi}{D-1}\right]^{D-1}, \\ R_i &= 0\,, \end{aligned} \tag{3.35}$$

[7] Recall that n denotes the number of commuting angular momenta and is given by the expression $n = \mathrm{rank}\,[SO(D-1)]$ on AdS_D.

[8] In the expression of κ for even dimension, the sign inside the second term in equation (4.7) of [66] is different form the sign given in equation (4.18) of [65]; we believe the latter sign is the correct one.

where V_{D-1} is the volume of S^{D-2} and G_D is Newton's constant in D dimensions. The corrections to each of these expressions are suppressed by factors of $\mathcal{O}(1/r_+^2) = \mathcal{O}(1/T^2)$ relative to the leading order results presented above (i.e. there are no next to leading order corrections).

These thermodynamic formulae listed in (3.35) are in perfect agreement with the fluid mechanics expressions in (3.29) upon making the following identifications: the space-time dimensions of the boundary theory $d = D-1$, the black hole angular velocities a_i are identified with Ω_a and the constant h is identified as

$$h = \frac{1}{16\pi G_D}\left[\frac{4\pi}{D-1}\right]^{D-1}. \tag{3.36}$$

In the next subsection, we will see that this agreement goes beyond the global thermodynamic quantities. Local conserved currents are also in perfect agreement with the black hole physics.

3.4.3 Stress tensor from rotating black holes in $\mathbf{AdS}_D$

The uncharged rotating black holes both in odd dimensions ($D = 2n+1$) and even dimensions ($D = 2n+2$) are presented in detail in [65], equation (E-3) and [66], equation (4.2). After performing some coordinate transformations that take the metric of that paper to the standard form of AdS_D at the boundary, we have computed the stress tensor of this solution.

Our calculation uses the standard AdS/CFT dictionary (the details are presented in an appendix of [1] but we do not reproduce them here). In more detail, we foliate the solution in boundary spheres, compute the extrinsic curvature Θ^μ_ν of these foliations near the boundary, subtract off the appropriate counter terms contributions [56–63], and finally multiply the answer by the r^{D-1} to obtain the stress tensor on a unit sphere.

We find that the stress tensor so calculated takes the form

$$\begin{aligned}
\Pi^{tt} &= \frac{2m}{16\pi G_D}[(D-1)\gamma^{D+1} - \gamma^{D-1}] \\
\Pi^{\phi_a\phi_a} &= \frac{2m}{16\pi G_D}[(D-1)\gamma^{D+1}\Omega_a^2 + \gamma^{D-1}\mu_a^{-2}] \\
\Pi^{t\phi_a} &= \Pi^{\phi_a t} = \frac{2m}{16\pi G_D}(D-1)\gamma^{D+1}\Omega_a \\
\Pi^{\phi_a\phi_b} &= \Pi^{\phi_b\phi_a} = \frac{2m}{16\pi G_D}\gamma^{D+1}\Omega_a\Omega_b \\
\Pi^{\theta_a\theta_a} &= \frac{2m}{16\pi G_D}\gamma^{D-1}\left(\prod_{b=1}^{a-1}\sec^2\theta_b\right).
\end{aligned} \tag{3.37}$$

Here $\gamma^{-2} = 1 - \sum_{a=1}^n \Omega_a^2\mu_a^2$ where $\mu_a = \left(\prod_{b=1}^{a-1}\cos\theta_b\right)\sin\theta_a$.

Note that the functional form of these expressions (i.e. dependence of various components of the stress tensor on the coordinates of the sphere) agrees exactly with the

predictions of fluid dynamics even at finite values of r_+. In the large r_+ limit (using (3.34) and (3.36)), we further have

$$D-1=d\,,$$
$$\frac{2m}{16\pi G_D}=T^d h\,.$$

With these identifications, (3.37) coming from gravity agrees precisely with (3.30) from fluid mechanics.

We proceed now to estimate the limits of validity of our analysis above. From the black hole side, since we have expanded the formulae of black hole thermodynamics in $1/r_+$ to match them with fluid mechanics, this analysis is valid if r_+ is large. From the fluid mechanics side, we expect corrections of the order of $l_{\rm mfp}$. To estimate $l_{\rm mfp}$ in this case, we substitute (3.33) into (3.31) to get

$$l_{\rm mfp}\sim\frac{1}{r_+(d-1)}\ll 1\,.$$

Hence, we see that the condition from fluid mechanics is exactly the same as taking large horizon radius limit: the expansion of black hole thermodynamics in a power series in $\frac{1}{r_+}$ appears to be exactly dual to the fluid mechanical expansion as a power series in $l_{\rm mfp}$.

3.5 Comparison with black holes in $AdS_5\times S^5$

Large N, $\mathcal{N}=4$ Yang-Mills, at strong 't Hooft coupling on $S^3\times\mathbb{R}$, is dual to classical gravity on $AdS_5\times S^5$. Hence, we can specialise the general fluid dynamical analysis presented above to the study of equilibrium configurations of the rotating $\mathcal{N}=4$ plasma on S^3 and then compare the results with the physics of classical black holes in $AdS_5\times S^5$.

Large black holes in $AdS_5\times S^5$ are expected to appear in a six parameter family, labelled by three SO(6) Cartan charges ($c=3$), two $SO(4)$ rotations ($n=2$) and the mass. While the most general black hole in $AdS_5\times S^5$ has not yet been constructed, several sub-families of these black holes have been determined.

In this section, we will compare the thermodynamic predictions of fluid mechanics with all black hole solutions that we are aware of and demonstrate that the two descriptions agree in the large horizon radius limit. For one class of black holes we will also compare black hole stress tensor and charge distributions with that of the fluid mechanics and once again find perfect agreement (in the appropriate limit).

We begin this section with a review of the predictions of fluid mechanics for strongly coupled $\mathcal{N}=4$ Yang-Mills on S^3. Note that this is a special case of the conformal fluid dynamics of previous sections with $d=D-1=4$.

3.5.1 The strongly coupled $\mathcal{N}=4$ Yang-Mills Plasma

The gravity solution for SO(6) charged black branes (or, equivalently, large SO(6) charged but non-rotating black holes in $AdS_5\times S^5$) has been used to extract the equation

of state of $\mathcal{N}=4$ Yang-Mills (see [76, §2] for the thermodynamic expressions in the infinite radius limit).

Rather than listing all the thermodynamic variables, we use the earlier parametrisation of (3.4) to state our results. The thermodynamics of the $\mathcal{N}=4$ Yang-Mills is described by the following equations[9]

$$\begin{aligned} h(\nu) = \frac{\mathcal{P}}{\mathcal{T}^4} &= 2\pi^2 N^2 \frac{\prod_j (1+\kappa_j)^3}{(2+\sum_j \kappa_j - \prod_j \kappa_j)^4}\,, \\ \nu_i = \frac{\mu_i}{\mathcal{T}} &= \frac{2\pi \prod_j (1+\kappa_j)}{\left(2+\sum_j \kappa_j - \prod_j \kappa_j\right)} \frac{\sqrt{\kappa_i}}{1+\kappa_i}\,, \\ h_i(\nu) = \frac{r_i}{\mathcal{T}^3} &= \frac{2\pi N^2 \prod_j (1+\kappa_j)^2}{\left(2+\sum_j \kappa_j - \prod_j \kappa_j\right)^3} \sqrt{\kappa_i}\,. \end{aligned} \tag{3.38}$$

where the κ_i are auxiliary parameters. They can be directly related to the entropy and charge densities:

$$\kappa_i = \left(\frac{2\pi \mathfrak{r}_i}{s}\right)^2, \tag{3.39}$$

and they are constrained by the conditions

$$\begin{gathered} \kappa_i \geq 0, \\ \frac{2+\sum_j \kappa_j - \prod_j \kappa_j}{\prod_j (1+\kappa_j)} = \left[\sum_j \frac{1}{1+\kappa_j} - 1\right] \geq 0, \end{gathered}$$

which are obtained by requiring that the temperature $\mathcal{T} \geq 0$. It follows from (3.39) that κ_i is finite for configurations with finite charge and non-zero entropy. The configurations with $\kappa_i \to \infty$ (for any i) are thermodynamically singular, since in this limit, the i^{th} charge density is much larger than the entropy density. Hence, in the following, we shall demand that κ_i be finite.

The general analysis presented before now allows us to construct the most general stationary solution of the $\mathcal{N}=4$ fluid rotating on a 3-sphere. The thermodynamic formulae and currents of these solutions follow from (3.12), (3.11) and (3.15) upon setting

$$\begin{aligned} A = h(\nu) &= 2\pi^2 N^2 \frac{\prod_j (1+\kappa_j)^3}{(2+\sum_j \kappa_j - \prod_j \kappa_j)^4}\,, \\ B = 4h(\nu) - \nu_i h_i(\nu) &= 4\pi^2 N^2 \frac{\prod_j (1+\kappa_j)^2}{(2+\sum_j \kappa_j - \prod_j \kappa_j)^3}\,, \\ C_i = h_i(\nu) &= 2\pi N^2 \sqrt{\kappa_i} \frac{\prod_j (1+\kappa_j)^2}{(2+\sum_j \kappa_j - \prod_j \kappa_j)^3}\,, \end{aligned} \tag{3.40}$$

[9] Note that our convention for the gauge field differs from [76, §2] by a factor of $\sqrt{2}$.

which leads to

$$\mu_i = \frac{2\pi T \prod_j (1+\kappa_j)}{\left(2+\sum_j \kappa_j - \prod_j \kappa_j\right)} \frac{\sqrt{\kappa_i}}{1+\kappa_i}\,, \tag{3.41}$$

and

$$\ln \mathcal{Z}_{\rm gc} = \frac{2\pi^2 N^2 V_4 T^3 \prod_j (1+\kappa_j)^3}{(1-\Omega_1^2)(1-\Omega_2^2)\left(2+\sum_j \kappa_j - \prod_j \kappa_j\right)^4}\,, \tag{3.42}$$

where we have used the notation $V_4 = \mathrm{Vol}(S^3) = 2\pi^2$ as before.

As before, the mean free path in fluid mechanics can be estimated as

$$\begin{aligned} l_{\rm mfp} \sim \left[\frac{S}{4\pi E}\right]_{\Omega=0} &= \frac{B}{(d-1)4\pi T A} = \frac{\left(2+\sum_j \kappa_j - \prod_j \kappa_j\right)}{6\pi T \prod_j (1+\kappa_j)} \\ &= \frac{1}{6\pi T}\left[\sum_j \frac{1}{1+\kappa_j} - 1\right]. \end{aligned} \tag{3.43}$$

3.5.2 The extremal limit

The strongly coupled $\mathcal{N}=4$ Yang-Mills plasma has an interesting feature: it has interesting and nontrivial thermodynamics even at zero temperature. In this subsection, we investigate this feature and point out that it implies the existence of interesting zero temperature solutions of fluid dynamics which will turn out to be dual to large, extremal black holes.

Thermodynamics

In the above section, we presented the thermodynamics of strongly coupled $\mathcal{N}=4$ Yang-Mills plasma in terms of the parameters κ_i. These parameters are constrained by the conditions $\kappa_i \geq 0$ and $\sum_i \frac{1}{1+\kappa_i} \geq 1$ with κ_i finite. In order to visualise the allowed range over which the variables κ_i's can vary, it is convenient to define a new set of variables

$$\begin{aligned} X_i &= \frac{1}{1+\kappa_i}\,, \\ \chi &= \frac{T}{X_1+X_2+X_3-1}\,. \end{aligned} \tag{3.44}$$

The constraints $\kappa_i \geq 0$ and $\sum_i \frac{1}{1+\kappa_i} \geq 1$ with κ_i finite translate into the constraints $0 < X_i \leq 1$ and $X_1+X_2+X_3 \geq 1$. Geometrically, this is just the statement that X_i's can lie anywhere inside the cube shown in fig.3.1, away from the planes $X_i = 0$ and on or above the plane $X_1+X_2+X_3 = 1$.

The energy density, the entropy density and the charge densities of the Yang-Mills plasma may be rewritten as a function of X_1, X_2, X_3 and χ as

$$\begin{aligned} &\rho = 6\pi^2 N^2 X_1 X_2 X_3 \chi^4, \qquad s = 4\pi^2 N^2 X_1 X_2 X_3 \chi^3, \\ &\mathfrak{r}_i = 2\pi N^2 X_1 X_2 X_3 \chi^3 \sqrt{\frac{1-X_i}{X_i}}. \end{aligned} \tag{3.45}$$

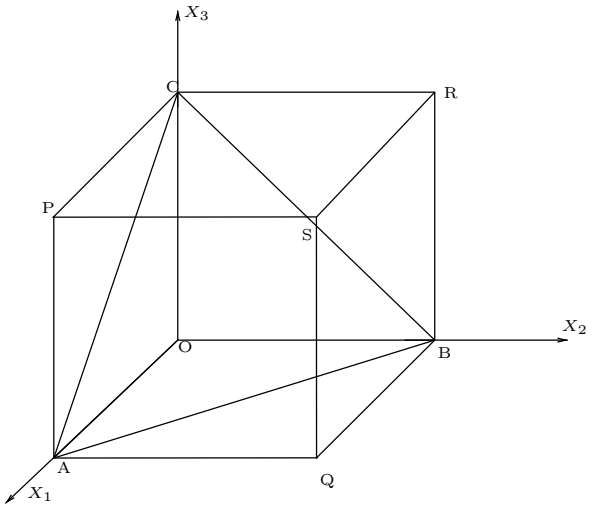

Figure 3.1: The space of allowed κ_i's. The axes correspond to $X_i = \frac{1}{1+\kappa_i}$. The X_i's can lie anywhere in the cube outside the "extremal" plane $X_1 + X_2 + X_3 = 1$.

The condition for the validity of fluid mechanics becomes

$$l_{\rm mfp} \sim \frac{1}{6\pi\chi} \ll 1 \qquad \text{or} \qquad \chi \gg 1\,. \tag{3.46}$$

Consider now the case in which χ is large, but finite and X_1, X_2, X_3 take values close to the interior of the triangle ABC in fig.3.1. From (3.44) and (3.45), it is evident that this is equivalent to taking an extremal limit $T \to 0$ with appropriate chemical potentials. All thermodynamic quantities listed above are smooth in this limit and the fluid mechanics continues to be valid.

The $\mathcal{N} = 4$ Yang-Mills plasma with three nonzero R-charges always has a nonsingular extremal limit. In the case that one of the charges say r_3 is zero, then we are constrained to move on the $X_3 = 1$ plane in the space of X_i's. Hence, we can never approach the 'extremal triangle' $X_1 + X_2 + X_3 = 1$.[10] Thus, we have no nonsingular extremal limit if any one of the three R-charges is zero. By a similar argument, no nonsingular extremal limit exists if two of the R-charges were zero.

We note that Gubser and Mitra have previously observed that charged black branes near extremality are sometimes thermodynamically unstable [77]. Although we have not performed a careful analysis of the thermodynamic stability of the charged fluids we study in this chapter (see however [76]), we suspect that these fluids all have Gubser-Mitra type thermodynamic instabilities near extremality. If this is the case, the near extremal fluid solutions we study in this section and the next – and the black holes that these are dual to – are presumably unstable to small fluctuations. Whether stable or not, these configurations

[10]Remember that we have already excluded, on physical grounds, the point $X_1 = X_2 = 0,\ X_3 = 1$ which lies in the intersection of $X_3 = 1$ plane and the extremal plane $X_1 + X_2 + X_3 = 1$.

are valid solutions of fluid dynamics. We postpone a serious discussion of stability to future work.[11]

Fluid mechanics

The thermodynamic expressions for the charges of a rotating Yang-Mills plasma take the form

$$\begin{aligned}
E &= \frac{2\pi^2 N^2 X_1 X_2 X_3 V_4}{(1-\Omega_1^2)(1-\Omega_2^2)}\left[\frac{2\Omega_1^2}{1-\Omega_1^2}+\frac{2\Omega_2^2}{1-\Omega_2^2}+3\right]\left[\frac{T}{X_1+X_2+X_3-1}\right]^4,\\
L_1 &= \frac{2\pi^2 N^2 X_1 X_2 X_3 V_4}{(1-\Omega_1^2)(1-\Omega_2^2)}\left[\frac{2\Omega_1}{1-\Omega_1^2}\right]\left[\frac{T}{X_1+X_2+X_3-1}\right]^4,\\
L_2 &= \frac{2\pi^2 N^2 X_1 X_2 X_3 V_4}{(1-\Omega_1^2)(1-\Omega_2^2)}\left[\frac{2\Omega_2}{1-\Omega_2^2}\right]\left[\frac{T}{X_1+X_2+X_3-1}\right]^4,\\
S &= \frac{4\pi^2 N^2 X_1 X_2 X_3 V_4}{(1-\Omega_1^2)(1-\Omega_2^2)}\left[\frac{T}{X_1+X_2+X_3-1}\right]^3,\\
R_i &= \frac{2\pi N^2 X_1 X_2 X_3 V_4}{(1-\Omega_1^2)(1-\Omega_2^2)}\left[\frac{T}{X_1+X_2+X_3-1}\right]^3\sqrt{\frac{1-X_i}{X_i}},
\end{aligned} \tag{3.47}$$

and the mean free path

$$l_{\rm mfp} \sim \frac{X_1+X_2+X_3-1}{6\pi T} \ll 1\,. \tag{3.48}$$

We see that all thermodynamical charges of our rotating fluid configurations are nonsingular, and that fluid mechanics is a valid approximation for these solutions, in the extremal limit described in the previous subsection, provided only that $\chi \gg 1$.[12]

The solution so obtained describes a rotating fluid whose local temperature vanishes everywhere, but whose rest frame charge density is a function of location on the S^3 (it scales like γ^3). As we will see below these extremal configurations of rotating fluid on S^3 are exactly dual to large, rotating, extremal black holes in AdS_5.

3.5.3 Black holes with all R-charges equal

Having derived the fluid mechanics predictions for various different black holes, we now proceed to examine the black hole solutions. First, we will focus on the case of black holes with arbitrary angular momenta in AdS_5 but equal SO(6) charges. The relevant solution has been presented in [68].

---

[11] We thank Sangmin Lee for discussion of these issues.

[12] In greater generality, in order for fluid mechanics to be a valid approximation for our solutions it is necessary that either $T \gg 1$ (which is by itself sufficient) or that $X+Y+Z-1 \to 0$ (under which condition the ratio χ of the previous section must be large and (conservatively) none of X, Y or Z be very small).

Thermodynamics

The black holes presented in [68] are labelled by two angular velocities a, b, and three more parameters q, m and r_+. These five parameters are not all independent; they are constrained by one equation relating horizon radius to the parameter m ($\Delta_r = 0$ in that paper). We thus have a four parameter set of black holes.[13]

The relatively complicated black hole thermodynamic formulae of [68] simplify if the parameter r_+ (which may be interpreted as the horizon radius) is taken to be large. In particular, consider the limit

$$r_+ \gg 1 \qquad \text{and} \quad k = q/r_+^3 \quad \text{fixed.} \tag{3.49}$$

In this limit, to leading order,we have

$$\begin{aligned} T &= \frac{r_+}{2\pi}(2-k^2)\,, \\ 2m &= r_+^4(1+k^2)\,. \end{aligned} \tag{3.50}$$

From the positivity of T and r_+ it follows immediately that $0 \leq k^2 \leq 2$.

Multiplying all thermodynamic integrals in [68] by $\frac{R^3_{\rm AdS}}{G_5} = \frac{2N^2}{\pi}$ and noting that our charge R is equal to their $Q/\sqrt{3}$, the black hole thermodynamic formulae reduce to (to leading order in r_+)

$$\begin{aligned} \Omega_1 &= a\,, \\ \Omega_2 &= b\,, \\ \mu_i &= \frac{2\pi k T}{(2-k^2)}\,, \\ \ln \mathcal{Z}_{\rm gc} &= \frac{2\pi^2 N^2(1+y^2)}{(2-y^2)^4}\left[\frac{V_4 T^3}{(1-\Omega_1^2)(1-\Omega_2^2)}\right]. \end{aligned} \tag{3.51}$$

Once we identify the black hole parameter k^2 with the fluid parameter $\kappa \equiv \kappa_1 = \kappa_2 = \kappa_3$, these formula take precisely the form of fluid mechanics formulae (3.41) and (3.42).

We can now compute the fluid mechanical mean free path $l_{\rm mfp}$ as a function of bulk black hole parameters. From equations (3.50) and (3.43), we find (assuming that r_+ is large)

$$l_{\rm mfp} \sim \frac{1}{3r_+(1+\kappa)}\,.$$

As $1+\kappa = 1+k^2$ is bounded between 1 and 2, it appears from this equation that the expansion in powers of $1/r_+$ is simply identical to the fluid dynamical expansion in powers of $l_{\rm mfp}$. This explains why black hole thermodynamics agrees with the predictions of the Navier-Stokes equations when (and only when) r_+ is large.

[13] We work in conventions in which the AdS radius and hence the parameter g of [68] is set to unity.

Stress tensor and charge currents

Just as in §3.4.3, we have computed the boundary stress tensor corresponding to this black hole solution (by foliating the space into S^3 's at infinity, computing the extrinsic curvature of these sections, and subtracting the appropriate counterterms). At leading order in $\frac{1}{r_+}$

$$\begin{aligned}
\Pi^{tt} &= \frac{m}{8\pi G_5}\gamma^4(4\gamma^2-1), & \Pi^{\theta\theta} &= \frac{m}{8\pi G_5}\gamma^4,\\
\Pi^{\phi\phi} &= \frac{m}{8\pi G_5}\gamma^4(4\gamma^2a^2+\csc^2\theta), & \Pi^{\psi\psi} &= \frac{m}{8\pi G_5}\gamma^4(4\gamma^2a^2+\sec^2\theta),\\
\Pi^{t\phi} &= \Pi^{\phi t} = \frac{4m}{8\pi G_5}a\gamma^6, & \Pi^{t\psi} &= \Pi^{\psi t} = \frac{4m}{8\pi G_5}b\gamma^6,\\
\Pi^{\phi\psi} &= \Pi^{\psi\phi} = \frac{4m}{8\pi G_5}ab\gamma^6.
\end{aligned} \tag{3.52}$$

In a similar fashion, the charge currents on S^3 may be computed from the AdS/CFT dictionary entry $J_i^\mu = -r^4 g^{\mu\nu}A_\nu|_{r\to\infty}$ where the indices μ,ν are tangent to the $S^3\times$ time foliations and and the bulk gauge field A_ν is given in the equation (2) of [68]. We find

$$\begin{aligned}
J_1^t = J_2^t = J_3^t &= \frac{q}{8\pi G_5}\gamma^4 \qquad J_1^\theta = J_2^\theta = J_3^\theta = 0\\
J_1^\phi = J_2^\phi = J_3^\phi &= \frac{q}{8\pi G_5}\gamma^4 a \quad J_1^\psi = J_2^\psi = J_3^\psi = \frac{q}{8\pi G_5}\gamma^4 b\,.
\end{aligned} \tag{3.53}$$

Noting that the bulk parameters are related to the function $h(\nu)$ and its derivatives by

$$h(\nu) = \frac{2N^2}{\pi}\left[\frac{2m}{16\pi T^4}\right] = \frac{m}{8\pi G_5 T^4}\,, \quad h_i(\nu) = \frac{2N^2}{\pi}\frac{q}{8\pi T^3} = \frac{q}{8\pi G_5 T^3}\,, \tag{3.54}$$

it is evident that the expressions in (3.52) and (3.53) are in precise agreement with the predictions (3.24) of fluid dynamics.

3.5.4 Black holes with independent SO(6) charges and two equal rotations

The most general (five parameter) black hole solutions with the two angular velocities set equal can be found in [67]. The thermodynamics of these black holes was computed in [73].

The black hole solutions depend on the parameters $\delta_1,\delta_2,\delta_3,a,m,r_+$ that are related by the equation $Y(r)=0$. The thermodynamics of these black holes simplify in the limit

$$r_+ \gg 1\,, \qquad \frac{2ms_i^2}{r_+^2} = H_i - 1 \quad \text{fixed.}$$

Then solving the equation $Y=0$ in this limit, one can express m as

$$2m = \frac{(H_1H_2H_3)r_+^4}{(1-a^2)}\,.$$

The various thermodynamic quantities in this limit[14] (after multiplying integrals by $\frac{R^3_{\rm AdS}}{G_5} = \frac{2N^2}{\pi}$) can be summarised by

$$\begin{aligned}
&\Omega_1 = \Omega_2 = a\,, \qquad T = \frac{r_+\sqrt{1-a^2}}{2\pi}\left(\sum_j H_j^{-1} - 1\right)\prod_j \sqrt{H_j}\,,\\
&\mu_i = r_+\sqrt{1-a^2}\left(\frac{\sqrt{H_i-1}}{H_i}\right)\prod_j \sqrt{H_j} = \frac{2\pi T}{\sum_j H_j^{-1}-1}\left(\frac{\sqrt{H_i-1}}{H_i}\right)\,,\\
&\ln \mathcal{Z}_{\rm gc} = \frac{\pi N^2 r_+^3}{2\sqrt{1-a^2}}\left(\frac{\prod_j \sqrt{H_j}}{\sum_j H_j^{-1}-1}\right) = \frac{4\pi^4 N^2 T^3}{(1-\Omega^2)^2\left(\prod_j H_j\right)\left(\sum_j H_j^{-1}-1\right)^4}
\end{aligned} \tag{3.55}$$

These expressions match with (3.41) and (3.42) if κ_i is identified with $H_i - 1$ and we set $\Omega_1 = \Omega_2 = a$, demonstrating perfect agreement between black hole and fluid dynamical thermodynamics.

Translating the estimate for the mean free path into the black hole variables, we find

$$l_{\rm mfp} \sim \frac{1}{3r_+\prod_j \sqrt{H_j}} \ll 1\,,$$

(an equation that is valid only in the large r_+ limit). Notice that $l_{\rm mfp}$ is automatically small in the large r_+ limit, explaining why black hole thermodynamics agrees with the predictions of the Navier-Stokes equations in this limit.

Notice that the fluid mechanical expansion parameter $l_{\rm mfp}$ appears to differ from the expansion parameter of black hole thermodynamics used above, $1/r_+$, by a factor of $1/\sqrt{\prod_i H_i}$. When the three charges of the black hole are in any fixed ratio $a : b : c$, with none of a, b or c either zero or infinity, it may easily be verified that this additional factor is bounded between a nonzero number (which depends on a, b, c) and unity. In this case the two expansion parameters - $l_{\rm mfp}$ and $1/r_+$ - are essentially the same.

However when one of the black hole charges (say R_1) vanishes H_2 and/or H_3 can formally take arbitrarily large values. In this extreme limit $l_{\rm mfp}$ appears to differ significantly from the bulk expansion parameter $1/r_+$. However large H_i implies large κ_i, a limit that we have argued above to be thermodynamically singular. Keeping away from the suspicious large κ_i limit, it is always true that $l_{\rm mfp}$ is essentially identical $1/r_+$, the parameter in which we have expanded the formulas of black hole thermodynamics.

3.5.5 Black holes with two equal large R-charges and third R-charge small

Chong et al. [69] have determined a class of black hole solutions with two SO(6) charges held equal, while the third charge is a function of these two equal charges. In the large radius limit, it turns out that this third charge is negligible compared to the first two, so for our purposes these solutions can be thought of as black holes with two equal SO(6)

[14] We believe that [73] has a typo: (3.10) should read $\Phi_i = \frac{2m}{r^2 H_i}(s_i c_i + \frac{1}{2}a\Omega(c_i s_j s_k - s_i c_j c_k))$. Note that they also use coordinates $\psi = \phi_1 + \phi_2$ and $\varphi = \phi_1 - \phi_2$ so that $\Omega\partial_\psi = \frac{\Omega}{2}\partial_{\phi_1} + \frac{\Omega}{2}\partial_{\phi_2}$ so that $\Omega_a = \frac{\Omega}{2}$.

charges, with arbitrary rotations and the third SO(6) charge set to zero. The parameters of this black hole solution are a, b, m, r_+, s, which are related by the equation $X(r_+) = 0$.

Black hole formulae simplify in the limit

$$r_+ \gg 1 \quad \text{and} \quad k = \frac{2ms^2}{r_+^2} \quad \text{fixed},$$

in units where the inverse AdS radius $g = 1$, which leads to

$$2m = r_+^4(1+k)^2 \,.$$

Multiplying all thermodynamic integrals in [69] by $\frac{R^3_{\rm AdS}}{G_5} = \frac{2N^2}{\pi}$, in this limit, the thermodynamics can be summarised by

$$\begin{aligned} \Omega_1 = a\,, \quad \Omega_2 = b\,, \quad T = \frac{r_+}{\pi}\,, \\ \mu_1 = \mu_2 = \pi T\sqrt{k}\,, \qquad \mu_3 \sim \mathcal{O}\left(\frac{1}{r_+^2}\right)\,, \\ \ln \mathcal{Z}_{\rm gc} = \frac{\pi^2 N^2 V_4 T^3 (1+k)^2}{8(1-a^2)(1-b^2)}\,. \end{aligned} \tag{3.56}$$

Note that μ_3 and R_3 are subleading in r_+. These formulae are in perfect agreement with (3.41) and (3.42) if we identify $\kappa \equiv \kappa_1 = \kappa_2 = k$, $\kappa_3 = 0$.

Translating the estimate for the fluid dynamical mean free path into the black hole variables we find (assuming $r_+ \gg 0$)

$$l_{\rm mfp} \sim \frac{1}{3r_+(1+\kappa)}\,.$$

It follows that the fluid dynamical expansion parameter is essentially the same as $1/r_+$, provided we stay away from the thermodynamically suspect parameter regime of large κ .

3.5.6 Black holes with two R-charges zero

The solution for the most general black hole with two R-charges set to zero relevant solution has was presented in [70]. The parameters of this black hole are x_0, m, δ, a, b related by $X(x_0) = 0$.

The thermodynamics of these black holes simplifies in the limit

$$x_0 \gg 1\,, \qquad k = \sqrt{x_0}\delta \quad \text{fixed},$$

in units where $g = 1$, which leads to

$$2m = \frac{x_0^2}{(1-k^2)}\,.$$

This gives an upper bound on k: $k \leq 1$.

Multiplying all thermodynamic integrals in [70] by $\frac{R^3_{\rm AdS}}{G_5} = \frac{2N^2}{\pi}$, in this limit, the thermodynamic formulae can be summarised by

$$\begin{aligned} \Omega_1 &= a\,, \qquad \Omega_2 = b\,, \\ T &= \frac{\sqrt{x_0}(2-k^2)}{2\pi\sqrt{1-k^2}}\,, \quad \mu = \sqrt{x_0}k = \frac{2\pi T k\sqrt{1-k^2}}{2-k^2}\,, \\ \ln \mathcal{Z}_{\rm gc} &= \frac{x_0^{3/2}\pi N^2}{2\sqrt{1-k^2}(2-k^2)(1-a^2)(1-b^2)} = \frac{4\pi^4 N^2 T^3(1-k^2)}{(1-\Omega_1^2)(1-\Omega_2^2)(2-k^2)^4} \end{aligned} \tag{3.57}$$

Upon identifying $\kappa_1 = \frac{k^2}{1-k^2}$, $\kappa_2 = \kappa_3 = 0$, we find perfect agreement with (3.41) and (3.42).

The fluid dynamical mean free path may be evaluated as a function of bulk parameters as

$$l_{\rm mfp} \sim \frac{1}{3\sqrt{x_0(1+\kappa_1)}}\,.$$

Note that $l_{\rm mfp}$ is small whenever $\sqrt{x_0} = r_+$ is large, an observation that explains the agreement of black hole thermodynamics in the large r_+ limit with the Navier-Stokes equations. In more generality we see that $l_{\rm mfp}$ is essentially the same as $1/r_+$, provided we keep away from the thermodynamically suspicious parameter regime of κ_1 large.

3.5.7 BPS bound and supersymmetric black holes

All solutions of IIB supergravity on $AdS_5 \times S^5$, and all configurations of $\mathcal{N} = 4$ Yang-Mills on S^3 obey the BPS bound

$$E \geq L_1 + L_2 + \sum_i R_i\,. \tag{3.58}$$

Within the validity of the fluid dynamical approximation, described in this chapter,

$$E - L_1 - L_2 = \frac{2\pi^2 T^4 A}{(1-\Omega_1^2)(1-\Omega_2^2)} \frac{3+\Omega_1+\Omega_2-\Omega_1\Omega_2}{(1+\Omega_1)(1+\Omega_2)}\,; \tag{3.59}$$

notice that the RHS of this equation is positive definite. The BPS bound is obeyed provided

$$TA\frac{3+\Omega_1+\Omega_2-\Omega_1\Omega_2}{(1+\Omega_1)(1+\Omega_2)} \geq \sum_i C_i\,. \tag{3.60}$$

Plugging in the explicit expressions for A and C_i from (3.40) for the case with all charges equal, we find this condition is satisfied provided

$$r_+ = \frac{2\pi T}{2-\kappa} \geq \frac{6\sqrt{\kappa}(1+\Omega_1)(1+\Omega_2)}{(1+\kappa)(3+\Omega_1+\Omega_2-\Omega_1\Omega_2)}\,. \tag{3.61}$$

The RHS of (3.61) is of order unity. It follows that (3.58) is saturated only when r_+ is of unit order. When $r_+ \gg 1$ (so that fluid dynamics is a valid approximation) the BPS bound is always obeyed as a strict inequality. Supersymmetric black holes are never reliably

described within fluid mechanics.[15] The extremal black holes with large horizon radius, that are well described by fluid mechanics (see §3.5.2) are always far from supersymmetry.

We have noted above that a large class of extremal configurations in strongly interacting Yang-Mills – all those that admit a fluid dynamic description – are not BPS. This is in sharp contrast with the results of computations in free Yang-Mills theory, in which all extremal configurations are supersymmetric [78]. This difference is related to the fact, noted previously, the divergent mean free path prevents a fluid mechanical description from applying to free theories. A practical manifestation of this fact is that the function $h(\nu)$, which appears in the analysis of free Yang-Mills in equation (5.2) of [78], and plays the role of r_+ in our discussion here, is always of order unity for all allowed values of the chemical potential, and so can never become large.

3.5.8 Fluid dynamics versus black hole physics at next to leading order

As we have explained above, the formulae for all thermodynamic charges and potentials of black holes of temperature T and chemical potentials ν_i, in $AdS_5 \times S^5$, may be expanded as a Taylor series in $1/r_+ \sim l_{\rm mfp}(T, \nu_i)$. As we have verified above, for every known family of large AdS black holes, the leading order results in this expansion perfectly match the predictions of the Navier-Stokes equations. Higher order terms in this expansion represent corrections to Navier-Stokes equations. In this subsection we investigate the structure of these corrections.

Let us first investigate the case of black holes with at least one SO(6) charge set equal to zero (the black holes studied in §3.5.5 and §3.5.6). It is not difficult to verify that the first deviations from the large radius thermodynamics of these black holes occur at $\mathcal{O}(1/r_+^2) \sim l_{\rm mfp}^2$. This result is in perfect accord with naive expectations from fluid mechanics. As we have explained above, the fluid dynamical configurations presented in this chapter are exact solutions to the equations of fluid mechanics with all one derivative terms, i.e. to the first order in $l_{\rm mfp}$. In general we would expect our solutions (and their thermodynamics) to be modified at $\mathcal{O}(l_{\rm mfp}^2)$, exactly as we find from the black hole formulae.

However when we turn our attention to black holes with all three SO(6) charges nonzero we run into a bit of a surprise. It appears that the thermodynamics (and stress tensor and charge currents) of these black holes receives corrections at order $\mathcal{O}(1/r_+) \sim l_{\rm mfp}$. This result is a surprise because, for the reason we have explained in the previous paragraph, we would have expected the first corrections to our fluid mechanical configuration to occur at $\mathcal{O}(l_{\rm mfp}^2)$.

We do not have a satisfactory resolution to this puzzle. In this subsection we will simply present the expressions for the first order corrections to black hole thermodynamics

[15] Although it is possible to make the energy of supersymmetric black holes parametrically larger than their entropy, this is achieved by scaling either Ω_1 or Ω_2 to unity with r_+ kept at unit order. It is easy to verify that in this limit the local, rest frame mean free path of the fluid is of unit order in regions of the S^3 and so fluid mechanics may not be used to describe these configurations. Note that the 'physical' radius $\sim$ (Area)$^{1/3}$ of the black hole is distinct from the parameter r_+ which determines the validity of fluid dynamics. The physical radius can be made arbitrarily large for supersymmetric black holes. Nevertheless fluid mechanics is only valid if r_+ is large, which never happens for supersymmetric black holes.

in a particular case (the case of black holes with all SO(6) charges equal), and leave the explanation of these formulae to future work.

As we have mentioned above, the thermodynamics of a charged rotating black hole in $AdS_5 \times S^5$ with three equal charges and two different angular momenta can be found in [68]. To calculate next to leading order (NLO) corrections to the thermodynamics of large black holes, we systematically expand the thermodynamic quantities.

We find it convenient to shift to a new parametrisation in which there are no NLO corrections to the intensive quantities. This allows us to cast the NLO corrections entirely in terms of the extensive quantities. The parameters we choose are related to the parameters in [68] in the following way

$$\begin{aligned} a &= \omega_a - \frac{\sqrt{\kappa}(1-\omega_a^2)\omega_b}{\ell}\,, \\ b &= \omega_b - \frac{\sqrt{\kappa}(1-\omega_b^2)\omega_a}{\ell}\,, \\ r_+ &= \ell \ + \sqrt{\kappa}\omega_a\omega_b\,, \\ q &= \sqrt{\kappa}\ell^3 + 3\kappa\ell^2\omega_a\omega_b\,. \end{aligned} \tag{3.62}$$

In terms of these parameters, the intensive quantities can be written as

$$\begin{aligned} \Omega_a &= \omega_a + \mathcal{O}\left[\frac{1}{\ell^2}\right], \\ \Omega_b &= \omega_b + \mathcal{O}\left[\frac{1}{\ell^2}\right], \\ T &= \left[\frac{2-\kappa}{2\pi}\right]\ell + O\left[\frac{1}{\ell}\right], \\ \nu &= \frac{2\pi\sqrt{\kappa}}{2-\kappa} + \mathcal{O}\left[\frac{1}{\ell^2}\right], \end{aligned} \tag{3.63}$$

where we have calculated up to NLO and confirmed that the intensive quantities do not get corrected in this order.

This in turn means that the new parameters can be directly interpreted in terms of the intensive quantities.

$$\omega_a = \Omega_a + \mathcal{O}\big[l_{\rm mfp}^2\big]\,, \qquad \omega_b = \Omega_b + \mathcal{O}\big[l_{\rm mfp}^2\big]\,,$$

where $l_{\rm mfp} \sim \frac{2-\kappa}{T}$.

$$\ell = T\left[\frac{\sqrt{\pi^2+2\nu^2}+\pi}{2}\right] + \mathcal{O}\left[\frac{1}{T^2}\right], \qquad \sqrt{\kappa} = \frac{\sqrt{\pi^2+2\nu^2}-\pi}{\nu} + \mathcal{O}\left[\frac{1}{T^2}\right].$$

Now, we calculate NLO corrections to the extensive quantities in terms of the new

parameters.

$$
\begin{aligned}
2m &= (1+\kappa)\ell^4 + 4\sqrt{\kappa}(1+\kappa)\Omega_a\Omega_b\ell^3 + \mathcal{O}[\ell^2]\,,\\
S &= \frac{T^3}{G_5(1-\Omega_a^2)(1-\Omega_b^2)}\left[\frac{4\pi^5}{(2-\kappa)^3} + \mathcal{O}\left[\frac{1}{T^2}\right]\right],\\
L_a &= \frac{T^4}{G_5(1-\Omega_a^2)(1-\Omega_b^2)}\left[\frac{2\Omega_a}{1-\Omega_a^2}\left[\frac{2\pi^5(1+\kappa)}{(2-\kappa)^4}\right] - \frac{\pi\nu^3\Omega_b}{4T}\left[\frac{1+\Omega_a^2}{1-\Omega_a^2}\right] + \mathcal{O}\left[\frac{1}{T^2}\right]\right],\\
L_b &= \frac{T^4}{G_5(1-\Omega_a^2)(1-\Omega_b^2)}\left[\frac{2\Omega_b}{1-\Omega_b^2}\left[\frac{2\pi^5(1+\kappa)}{(2-\kappa)^4}\right] - \frac{\pi\nu^3\Omega_a}{4T}\left[\frac{1+\Omega_b^2}{1-\Omega_b^2}\right] + \mathcal{O}\left[\frac{1}{T^2}\right]\right],\\
R &= \frac{T^3}{G_5(1-\Omega_a^2)(1-\Omega_b^2)}\left[\frac{2\pi^4\sqrt{\kappa}}{(2-\kappa)^3} - \frac{\pi\nu^2}{4T}\Omega_a\Omega_b + \mathcal{O}\left[\frac{1}{T^2}\right]\right],\\
E &= \frac{T^4}{G_5(1-\Omega_a^2)(1-\Omega_b^2)}\left[\frac{2\pi^5(1+\kappa)}{(2-\kappa)^4}\left[\frac{2}{1-\Omega_a^2} + \frac{2}{1-\Omega_b^2} - 1\right]\right.\\
&\quad \left. - \frac{\pi\nu^3\Omega_a\Omega_b}{4T}\left[\frac{2}{1-\Omega_a^2} + \frac{2}{1-\Omega_b^2}\right] + \mathcal{O}\left[\frac{1}{T^2}\right]\right],
\end{aligned}
\tag{3.64}
$$

where $G_5 = \pi R_{\rm AdS}^3/(2N^2)$ is the Newton's constant in AdS_5.

In particular, the subleading terms can be isolated and written as

$$
\begin{aligned}
\Delta S &= 0\,,\\
\Delta E &= -\frac{\pi\mu^3\Omega_a\Omega_b}{4G_5(1-\Omega_a^2)(1-\Omega_b^2)}\left[\frac{2}{1-\Omega_a^2} + \frac{2}{1-\Omega_b^2}\right],\\
\Delta L_a &= -\frac{\pi\mu^3\Omega_b(1+\Omega_a^2)}{4G_5(1-\Omega_a^2)^2(1-\Omega_b^2)}\,,\\
\Delta L_b &= -\frac{\pi\mu^3\Omega_a(1+\Omega_b^2)}{4G_5(1-\Omega_a^2)(1-\Omega_b^2)^2}\,,\\
\Delta R &= -\frac{\pi\mu^2\Omega_a\Omega_b}{4G_5(1-\Omega_a^2)(1-\Omega_b^2)}\,,\\
\Delta \ln \mathcal{Z}_{\rm gc} &= \frac{\pi\mu^3\Omega_a\Omega_b}{4G_5T(1-\Omega_a^2)(1-\Omega_b^2)}\,.
\end{aligned}
\tag{3.65}
$$

3.6 Comparison with black holes in $AdS_4 \times S^7$ and $AdS_7 \times S^4$

In this section we compare solutions of rotating fluids of the M5 or M2 brane conformal field theory on S^2 or S^5 to the classical physics of black holes in M theory on $AdS_4 \times S^7$ and $AdS_7 \times S^5$ respectively. Our results turn out to be qualitatively similar to those of the previous section with one difference: the puzzle regarding the next to leading order agreement between fluid dynamics and black hole physics seems to be absent in this case.

3.6.1 Predictions from fluid mechanics

The equations of state of the strongly coupled M2 and M5 brane fluids were computed from spinning brane solutions in [79]. Our parameters are related to theirs by $\kappa_i = l_i^2/r_H^2$.

M2 branes

We define our R-charges to be half of the angular momenta of [79] to agree with gauged supergravity conventions. The equation of state is

$$\begin{aligned} h(\nu) &= \frac{4\pi^2(2N)^{3/2}\prod_j(1+\kappa_j)^{5/2}}{3(3+2\sum_j\kappa_j+\sum_{j<k}\kappa_j\kappa_k-\prod_j\kappa_j)^3}\,, \\ \nu_i &= \frac{4\pi\prod_j(1+\kappa_j)}{(3+2\sum_j\kappa_j+\sum_{j<k}\kappa_j\kappa_k-\prod_j\kappa_j)}\left(\frac{\sqrt{\kappa_i}}{1+\kappa_i}\right)\,, \\ h_i(\nu) &= \frac{\pi(2N)^{3/2}\prod_j(1+\kappa_j)^{3/2}}{3(3+2\sum_j\kappa_j+\sum_{j<k}\kappa_j\kappa_k-\prod_j\kappa_j)^2}\sqrt{\kappa_i}\,, \end{aligned} \tag{3.66}$$

where $i,j,k=1\ldots4$.

The stress tensor and currents are given by (3.23) and (3.24) with

$$\begin{aligned} A &= \frac{4\pi^2(2N)^{3/2}\prod_j(1+\kappa_j)^{5/2}}{3(3+2\sum_j\kappa_j+\sum_{j<k}\kappa_j\kappa_k-\prod_j\kappa_j)^3}\,, \\ B &= \frac{4\pi^2(2N)^{3/2}\prod_j(1+\kappa_j)^{3/2}}{3(3+2\sum_j\kappa_j+\sum_{j<k}\kappa_j\kappa_k-\prod_j\kappa_j)^2}\,, \\ C_i &= \frac{\pi(2N)^{3/2}\prod_j(1+\kappa_j)^{3/2}}{3(3+2\sum_j\kappa_j+\sum_{j<k}\kappa_j\kappa_k-\prod_j\kappa_j)^2}\sqrt{\kappa_i}\,. \end{aligned} \tag{3.67}$$

The thermodynamics can be summarised by

$$\begin{aligned} \mu_i &= \frac{4\pi T\prod_j(1+\kappa_j)}{(3+2\sum_j\kappa_j+\sum_{j<k}\kappa_j\kappa_k-\prod_j\kappa_j)}\left(\frac{\sqrt{\kappa_i}}{1+\kappa_i}\right)\,, \\ \ln\mathcal{Z}_{\rm gc} &= \frac{16\pi^3(2N)^{3/2}T^2\prod_j(1+\kappa_j)^{5/2}}{3(1-\Omega^2)(3+2\sum_j\kappa_j+\sum_{j<k}\kappa_j\kappa_k-\prod_j\kappa_j)^3}\,. \end{aligned} \tag{3.68}$$

The mean free path in fluid dynamics is given by

$$\begin{aligned} l_{\rm mfp}\sim\left[\frac{S}{4\pi E}\right]_{\Omega=0} &= \frac{B}{(d-1)4\pi TA} = \frac{\left(3+2\sum_j\kappa_j+\sum_{j<k}\kappa_j\kappa_k-\prod_j\kappa_j\right)}{8\pi T\prod_j(1+\kappa_j)} \\ &= \frac{1}{8\pi T}\left[\sum_j\frac{1}{1+\kappa_j}-1\right]. \end{aligned} \tag{3.69}$$

It is evident that the thermodynamic equations of state listed above allow a set of extremal fluid configurations very similar to those discussed in §3.5.2. The analysis of §3.5.2 can be easily extended to fluids on S^2.

M5 branes

We define our R-charges to be twice the angular momenta of [79] to agree with gauged supergravity conventions. The equation of state is

$$\begin{aligned} h(\nu) &= \frac{64\pi^3 N^3 \prod_j (1+\kappa_j)^4}{3(3+\sum_j \kappa_j - \prod_j \kappa_j)^6}\,, \\ \nu_i &= \frac{2\pi \prod_j (1+\kappa_j)}{(3+\sum_j \kappa_j - \prod_j \kappa_j)} \left(\frac{\sqrt{\kappa_i}}{1+\kappa_i}\right)\,, \\ h_i(\nu) &= \frac{128\pi^2 N^3 \prod_j (1+\kappa_j)^3}{3(3+\sum_j \kappa_j - \prod_j \kappa_j)^5} \sqrt{\kappa_i}\,, \end{aligned} \tag{3.70}$$

where $i = 1, 2$.

The stress tensor and currents are given by (3.23) and (3.24) with

$$\begin{aligned} A &= \frac{64\pi^3 N^3 \prod_j (1+\kappa_j)^4}{3(3+\sum_j \kappa_j - \prod_j \kappa_j)^6}\,, \\ B &= \frac{128\pi^3 N^3 \prod_j (1+\kappa_j)^3}{3(3+\sum_j \kappa_j - \prod_j \kappa_j)^5} \\ C_i &= \frac{128\pi^2 N^3 \prod_j (1+\kappa_j)^3}{3(3+\sum_j \kappa_j - \prod_j \kappa_j)^5} \sqrt{\kappa_i}\,. \end{aligned} \tag{3.71}$$

The thermodynamics can be summarised by

$$\begin{aligned} \mu_i &= \frac{4\pi T \prod_j (1+\kappa_j)}{(3+2\sum_j \kappa_j + \sum_{j<k} \kappa_j \kappa_k - \prod_j \kappa_j)} \left(\frac{\sqrt{\kappa_i}}{1+\kappa_i}\right)\,, \\ \ln \mathcal{Z}_{\rm gc} &= \frac{64\pi^6 N^3 T^5 \prod_j (1+\kappa_j)^4}{3\prod_a (1-\Omega_a^2)(3+\sum_j \kappa_j - \prod_j \kappa_j)^3}\,. \end{aligned} \tag{3.72}$$

The mean free path in fluid dynamics is given by

$$\begin{aligned} l_{\rm mfp} \sim \left[\frac{S}{4\pi E}\right]_{\Omega=0} &= \frac{B}{(d-1)4\pi T A} = \frac{\left(3+\sum_j \kappa_j - \prod_j \kappa_j\right)}{10\pi T \prod_j (1+\kappa_j)} \\ &= \frac{1}{10\pi T}\left[\sum_j \frac{2}{1+\kappa_j} - 1\right]. \end{aligned} \tag{3.73}$$

It is evident that the thermodynamic equations of state listed above allow a set of extremal fluid configurations very similar to those discussed in §3.5.2. The analysis of §3.5.2 can be easily extended to fluids on S^5.

3.6.2 Black holes in AdS_4 with pairwise equal charges

The relevant solution was found in [72]. Its thermodynamics have been computed in [73]. We consider the limit of large r_+ with $\frac{2ms_i^2}{r_+} = k_i$ fixed. In this limit m can be written as

$$m = \frac{r_+^3}{2}(1+k_1)^2(1+k_2)^2,$$

and therefore $s_i \sim \frac{1}{r_+}$.

After multiplying integrals by $\frac{R_{\rm AdS}^2}{G_4} = \frac{(2N)^{3/2}}{3}$, the thermodynamic quantities can be expressed as

$$\begin{aligned} T &= \frac{r_+(3+\sum_j k_j - \prod_j k_j)}{4\pi}\,, \qquad\qquad \Omega = a\,, \\ \mu_1 = \mu_3 &= 4\pi T \frac{(1+k_2)\sqrt{k_1}}{(3+\sum_j k_j - \prod_j k_j)}\,, \quad \mu_2 = \mu_4 = 4\pi T \frac{(1+k_1)\sqrt{k_2}}{(3+\sum_j k_j - \prod_j k_j)}\,, \\ \ln \mathcal{Z}_{\rm gc} &= \frac{16\pi^3 (2N)^{3/2} T^2}{3}\left(\frac{\prod_j (1+k_j)^2}{(3+\sum_j k_j - \prod_j k_j)^3}\right)\frac{1}{1-a^2}\,. \end{aligned} \tag{3.74}$$

If one identifies $k_1 = \kappa_1 = \kappa_3$ and $k_2 = \kappa_2 = \kappa_4$, then these formulae match with (3.68). It is not difficult to verify that the first corrections to the thermodynamic equations above occur at $\mathcal{O}(1/r_+^2)$.

It is clear from (3.74) that the black holes of this subsection admit a zero temperature (extremal) limit with nonsingular thermodynamics at any every value of r_+. These extremal black holes are dual to extremal solutions of fluid dynamics analogous to those described in the previous section in the context of $\mathcal{N} = 4$ Yang-Mills.

The fluid dynamical mean free path may easily be computed as a function of black hole parameters. From (3.69) we find

$$l_{\rm mfp} \sim \frac{1}{2r_+ \prod_j (1+\kappa_j)}\,.$$

As in the previous section, the $l_{\rm mfp} \sim 1/r_+$ away from thermodynamically suspect limits of parameters.

3.6.3 Black holes in AdS_7 with equal rotation parameters

The relevant solution was found in [71]. Its thermodynamics have been computed in [73].[16]

[16] We believe that [73] has the following typos: equation (4.7) should read

$$S = \frac{\pi^3 (r^2+a^2)\sqrt{f_1}}{4\Xi^3} \quad T = \frac{Y'}{4\pi r (r^2+a^2)\sqrt{f_1}} \quad \Phi_i = \frac{2ms_i}{\rho^4 \Xi H_i}\left[\Xi_- \alpha_i + \beta_i(\Omega - g)\right].$$

We set the parameter g in [73] to be unity and consider the limit

$$\rho_+ \gg 1\,, \qquad \text{and} \quad H_i = 1 + \frac{2ms_i^2}{\rho_+^6} \quad \text{fixed},$$

where i=1,2. In this limit, the parameter m is given by

$$2m = \rho_+^6 H_1 H_2\,.$$

In this limit, after multiplying integrals by $\frac{R^5_{\rm AdS}}{G_7} = \frac{16N^3}{3\pi^2}$, the thermodynamics can be summarised by

$$\begin{aligned}
&\Omega = a\,, && T = \frac{\rho_+}{2\pi}\left(\frac{2\sum_j H_j - \prod_j H_j}{\prod_j \sqrt{H_j}}\right),\\
&\mu_1 = 2\pi T \frac{H_2\sqrt{H_1-1}}{2\sum_j H_j - \prod_j H_j}\,, && \mu_2 = 2\pi T \frac{H_1\sqrt{H_2-1}}{2\sum_j H_j - \prod_j H_j}\,,\\
&&& \ln \mathcal{Z}_{\rm gc} = \frac{64\pi^6 N^3 T^5}{3(1-\Omega^2)^3}\left(\frac{\prod_j H_j^4}{(2\sum_j H_j - \prod_j H_j)^6}\right).
\end{aligned} \tag{3.75}$$

These formulae agree with (3.72) upon identifying $\kappa_i = H_i - 1$ and setting $\Omega_1 = \Omega_2 = \Omega_3 \equiv \Omega = a$. The first corrections to these thermodynamic formulae occur at $\mathcal{O}(1/r_+^2)$.

Expressing the fluid mechanical mean free path (3.73) as a function of black hole parameters we find

$$l_{\rm mfp} \sim \frac{1}{5\rho_+ \prod_j \sqrt{1+\kappa_j}}\,.$$

Once again $l_{\rm mfp} \sim 1/r_+$, away from thermodynamically suspect limits.

3.7 Discussion

As we have explained in this chapter, the classical properties of large black holes in AdS spaces enjoy a large degree of universality, summarised by (3.2). However the reasoning that led to (3.2) applies equally to all classical theories of gravity, not just to those theories that are governed by the two derivative effective action. For instance, $\mathcal{N} = 4$ Yang-Mills theory at finite λ is dual to IIB theory on $AdS_5 \times S^5$ of finite radius in string units. Even though thermodynamics of black holes in this background will receive contributions from each of the infinite sequence of α' corrections to the Einstein-Hilbert action, we expect (3.2) to be exact in the large horizon radius limit.[17]

We find it particularly interesting that (at least in several particular contexts) our fluid dynamical picture applies not just to non-extremal black holes but also to large radius

[17]Away from the supergravity limit, the mean free path $l_{\rm mfp} = \eta/\rho$ is expected to be given by $f(\lambda)s/4\pi\rho$ where $f(\lambda)$ is a monotonically decreasing function that interpolates between infinity at $\lambda = 0$ to unity at infinite λ. Thus the condition for the validity of fluid mechanics is modified at finite λ; in the uncharged case, for instance, it is $T \gg f(\lambda)$.

extremal black holes. This fact might allow us to make connections between our approach and the interesting recent investigations of the properties of extremal black holes. In particular, Astefanesei, Goldstein, Jena, Sen and Trivedi [80] have recently argued that the attractor mechanism applies to rotating extremal black holes, and have derived a differential equation that determines the attractor geometry (and gauge field distribution, etc.) of the near horizon region of such black holes. It would be very interesting to investigate the connection, if any, between these rotating attractor equations and our equations of rotating fluid dynamics.

It would be conceptually simple (though perhaps technically intricate) to compute the spectrum of small fluctuations about the fluid dynamical solutions presented in this chapter. This spectrum should match the spectrum of the (lowest) quasinormal modes about the relevant black holes (the decay of fluid fluctuations due to viscosity maps to the decay of quasi normal modes as they fall into the black hole horizon). It would be interesting to check if this is indeed the case.

It would be interesting to better understand, purely in bulk terms, why our proposal works. Roughly speaking, it should be possible to understand the metric of a black hole in global AdS and in the large radius limit, as a superposition of patches of the metric of black branes of various different temperatures and moving at various different velocities, where the temperatures and velocities are given by the solutions to the fluid dynamical equations presented in this chapter. It would be interesting and useful if these words could be converted into the first term of a systematic approximation procedure to generate black hole solutions in AdS spaces in a power series in $1/r_+$. Such a construction would constitute a bulk derivation of the boundary Navier-Stokes equations (and corrections thereof).

Relatedly, it would be interesting to ask if there are any gravitational interpretations of the local properties of fluids in our solutions. For instance, fluid mechanics yields a sharp prediction for the velocity and entropy density of the fluid as a function of position on the sphere. We have not yet been able to verify these predictions, because we do not know what gravitational construction we should compare them to. The entropy of the fluid is an integral over the boundary. The entropy of the black hole is an integral over the horizon. Perhaps there exists a natural map from the horizon to the boundary that allows one to convert horizon densities to boundary densities and vice versa. Such a map (for which we have no conjecture) would permit a gravitational interpretation for s, the local entropy density of the fluid.

The fluid velocity is another quantity for which it would be useful to have a gravitational definition. We do not really have a serious proposal for such a definition: nonetheless, in the next few paragraphs we outline a caricature proposal, in order to give the reader a sense of the types of relations that might exist (we emphasise that we do not have any physical reason to believe that this caricature has any truth to it).

In the black hole solutions, there is one special Killing vector, $K = \partial_t + \Omega_a \partial_{\phi_a}$, that is also the null generator of the horizon. It has the norm

$$\|K\|^2 \equiv -K^\mu K_\mu = \begin{cases} r^2\gamma^{-2} & \text{at the boundary,} \\ 0 & \text{at the horizon.} \end{cases}$$

If we were to normalise it with respect to the metric of the conformal boundary, the result

would be $\widetilde{K} = \gamma K$. This could be identified with the fluid velocity u^μ. However, as γ is not constant, $\widetilde{K}$ is not a Killing vector. It also seems unnatural to use a normalisation factor that depends on θ but not r. Nonetheless, this much maligned vector field has an interesting property.

Recall that black hole temperature and chemical potentials can be computed from the formulae

$$T = \frac{\kappa}{2\pi} = \left.\frac{\sqrt{(\partial_\mu \|K\|)(\partial^\mu \|K\|)}}{2\pi}\right|_{\text{horizon}}, \qquad \mu_i = A^i_\mu K^\mu\big|_{\text{horizon}}\,.$$

If one were to replace K with $\widetilde{K}$ in the formulae above, one would obtain $\mathcal{T}$ and μ_i, the local temperature and chemical potentials of the fluid.

We end this chapter by reminding the reader that, while our proposal has passed many checks, our work has left one significant puzzle unresolved. While the thermodynamics and stress tensors of uncharged rotating black holes in every dimension, plus all known black holes in $AdS_7 \times S^4$ and $AdS_4 \times S^7$, deviate from the predictions of the Navier-Stokes equations only at second order in l_{mfp}, the situation is more complex for black holes in $AdS_5 \times S^5$. In this case, black holes with at least one SO(6) charge equal to zero also agree with the results of the Navier-Stokes equations up to $\mathcal{O}(l^2_{\text{mfp}})$. However the thermodynamics of rotating black holes with all SO(6) charges nonzero, appears to deviate from our fluid mechanical predictions at $\mathcal{O}(l_{\text{mfp}})$ (see §3.5.8).

We consider this a significant puzzle as our fluid dynamical configurations solve the Navier-Stokes equations including $\mathcal{O}(l_{\text{mfp}})$ dissipative contributions. Moreover, in appendix 3.A we have checked by direct enumeration that all possible parity invariant vectors and traceless symmetric tensors that transform homogeneously under conformal transformation and contain a single derivative simply vanish on our solution, so it is difficult to see how any one derivative modification to the equations of fluid dynamics could help resolve this puzzle.[18] There is a proposed resolution to this puzzle in [74, 75]. They propose adding a term proportional to $\epsilon^{\lambda\mu\nu\sigma}\omega_{\mu\nu}u_\sigma$ to the heat flux, q^λ, and or the diffusion current j^λ_i. However, if we look at (2.11), we see that we would not be able to guarantee the increase of entropy (not using the same q^λ and j^λ_i in the stress tensor and charge currents as in the entropy current would violate the first law of thermodynamics). We emphasise that our reason for excluding these terms *was not* parity invariance, but the laws of thermodynamics.

Once this puzzle is resolved it would be interesting to attempt to reproduce the $\mathcal{O}(l^2_{\text{mfp}})$ corrections to black hole thermodynamics from appropriate additions to the equations of fluid dynamics. It is perhaps worth emphasising that black holes in AdS represent exact (to all orders in l_{mfp}) solutions to a dynamical flow. A detailed study of these solutions might lead to new insights into the nature of the fluid dynamical approximations of

[18] It has been suggested that certain pathologies in relativistic fluid dynamics lead to the breakdown of the derivative expansion [81] (See also [52] and the references therein). As any such pathology should apply equally to two charge and three charge black holes, we find it difficult to see how this issue could have bearing on our puzzle. We thank S. Gupta and H. Liu for discussions on this issue. Another possibility is that the formulae of black hole thermodynamics receive corrections – perhaps from Wess-Zumino type terms – that are nonzero only in an even dimensional bulk (and so in ten but not in eleven dimensions) and only when all charges are nonzero. We thank O. Aharony for suggesting this possibility.

the high energy regime of quantum field theories.

Appendices

3.A Conformal fluid mechanics

Consider a conformal fluid in d dimensions. We seek the conformal transformations of various observables of such a fluid. To this end, consider a conformal transformation which replaces the old metric $g_{\mu\nu}$ with $\tilde{g}_{\mu\nu}$ given by

$$g_{\mu\nu} = \mathrm{e}^{2\phi}\tilde{g}_{\mu\nu}; \qquad g^{\mu\nu} = \mathrm{e}^{-2\phi}\tilde{g}^{\mu\nu}.$$

The Christoffel symbols transform as

$$\Gamma^{\nu}_{\lambda\mu} = \widetilde{\Gamma}^{\nu}_{\lambda\mu} + \delta^{\nu}_{\lambda}\partial_{\mu}\phi + \delta^{\nu}_{\mu}\partial_{\lambda}\phi - \tilde{g}_{\lambda\mu}\tilde{g}^{\nu\sigma}\partial_{\sigma}\phi\,.$$

Let u^{μ} be the four-velocity describing the fluid motion. Using the normalisation condition $g_{\mu\nu}u^{\mu}u^{\nu} = \tilde{g}_{\mu\nu}\tilde{u}^{\mu}\tilde{u}^{\nu} = -1$, we get $u^{\mu} = \mathrm{e}^{-\phi}\tilde{u}^{\mu}$. It follows that the projection tensor transforms as $P^{\mu\nu} = g^{\mu\nu} + u^{\mu}u^{\nu} = \mathrm{e}^{-2\phi}\widetilde{P}^{\mu\nu}$. The transformation of the covariant derivative of u^{μ} is given by

$$\nabla_{\mu}u^{\nu} = \partial_{\mu}u^{\nu} + \Gamma^{\nu}_{\mu\lambda}u^{\lambda} = \mathrm{e}^{-\phi}\left[\widetilde{\nabla}_{\mu}\tilde{u}^{\nu} + \delta^{\nu}_{\mu}\tilde{u}^{\sigma}\partial_{\sigma}\phi - \tilde{g}_{\mu\lambda}\tilde{u}^{\lambda}\tilde{g}^{\nu\sigma}\partial_{\sigma}\phi\right]. \tag{3.76}$$

The above equation can be used to derive the transformation of various related quantities

$$\begin{aligned}
\vartheta = \nabla_{\mu}u^{\mu} &= \mathrm{e}^{-\phi}\left[\tilde{\vartheta} + (d-1)\tilde{u}^{\sigma}\partial_{\sigma}\phi\right],\\
a^{\nu} = u^{\mu}\nabla_{\mu}u^{\nu} &= \mathrm{e}^{-2\phi}\left[\tilde{a}^{\nu} + \widetilde{P}^{\nu\sigma}\partial_{\sigma}\phi\right],\\
\sigma^{\mu\nu} &= \frac{1}{2}\left(P^{\mu\lambda}\nabla_{\lambda}u^{\nu} + P^{\nu\lambda}\nabla_{\lambda}u^{\mu}\right) - \frac{1}{d-1}\vartheta P^{\mu\nu} = \mathrm{e}^{-3\phi}\tilde{\sigma}^{\mu\nu},\\
\omega^{\mu\nu} &= \frac{1}{2}\left(P^{\mu\lambda}\nabla_{\lambda}u^{\nu} - P^{\nu\lambda}\nabla_{\lambda}u^{\mu}\right) = \mathrm{e}^{-3\phi}\widetilde{\omega}^{\mu\nu}.
\end{aligned} \tag{3.77}$$

Further, the transformation of the temperature and the chemical potential can be written as $\mathcal{T} = \mathrm{e}^{-\phi}\widetilde{\mathcal{T}}$ and $\mathfrak{m} = \mathrm{e}^{-\phi}\tilde{\mathfrak{m}}$. The transformation of spatial gradient of temperature (appearing in the Fourier law of heat conduction) is

$$P^{\mu\nu}(\partial_{\nu}\mathcal{T} + a_{\nu}\mathcal{T}) = \mathrm{e}^{-3\phi}\widetilde{P}^{\mu\nu}(\partial_{\nu}\widetilde{\mathcal{T}} + \tilde{a}_{\nu}\widetilde{\mathcal{T}})\,.$$

The viscosity, conductivity etc. scale as $\kappa = \mathrm{e}^{-(d-2)\phi}\tilde{\kappa}$, $\eta = \mathrm{e}^{-(d-1)\phi}\tilde{\eta}$, $\mu_i = \mathrm{e}^{-\phi}\tilde{\mu}_i$ and $D_{ij} = \mathrm{e}^{-(d-2)\phi}\widetilde{D}_{ij}$.

For a fluid with c charges, there are $2c+2$ vector quantities involving no more than a single derivative which transform homogeneously[19]. They are

$$u^{\mu}, \quad \partial_{\mu}\nu_i, \quad \partial_{\mu}\mathcal{T} + \left(a_{\mu} - \frac{\vartheta}{d-1}u_{\mu}\right)\mathcal{T}, \quad u^{\mu}u^{\sigma}\partial_{\sigma}\nu_i \quad \text{and} \quad \left(u^{\sigma}\partial_{\sigma}\mathcal{T} + \frac{\vartheta}{d-1}\mathcal{T}\right)u^{\mu}.$$

[19]In the following analysis, we will neglect pseudo-tensors which can be formed out of $\epsilon_{\mu\nu\lambda\ldots}$. Additional tensors appear if such pseudo-tensors are included in the analysis.

In the kind of solutions we consider in this chapter, all of them vanish except u^μ.

The transformation of the stress tensor is $T^{\mu\nu} = \mathrm{e}^{-(d+2)\phi}\widetilde{T}^{\mu\nu}$, from which it follows that

$$\nabla_\mu T^{\mu\nu} = \mathrm{e}^{-(d+2)\phi}(\widetilde{\nabla}_\mu \widetilde{T}^{\mu\nu} - \tilde{g}_{\lambda\sigma}\widetilde{T}^{\lambda\sigma}\tilde{g}^{\nu\sigma}\partial_\sigma\phi)\,.$$

So, for the stress tensor to be conserved in both the metrics, it is necessary that $T^{\mu\nu}$ is traceless.

To consider the possible terms that can appear in the stress tensor, we should look at the traceless symmetric second rank tensors which transform homogeneously. The tensors formed out of single derivatives which satisfy the above criterion are easily enumerated. For a fluid with c charges, there are $2c+4$ such tensors and they are

$$\begin{aligned} &u^\mu u^\nu + \frac{1}{d}g^{\mu\nu}, \quad \sigma^{\mu\nu}, \quad q^\mu u^\nu + q^\nu u^\mu, \quad \left(u^\sigma\partial_\sigma\mathcal{T} + \frac{\vartheta}{d-1}\mathcal{T}\right)\left(u^\mu u^\nu + \frac{1}{d}g^{\mu\nu}\right), \\ &\frac{1}{2}\left(u^\mu\partial^\lambda\nu_i + u^\lambda\partial^\mu\nu_i\right) - \frac{g^{\mu\nu}}{d}u^\sigma\partial_\sigma\nu_i \quad \text{and} \quad u^\sigma\partial_\sigma\nu_i\left(u^\mu u^\nu + \frac{1}{d}g^{\mu\nu}\right). \end{aligned} \tag{3.78}$$

Among these possibilities, the stress tensor we employ just contains the tensors in the first line. It can be shown that the other tensors which appear in the above list can be removed by a redefinition of the temperature etc. Even if they were to appear in the stress tensor, for the purposes of this chapter, it suffices to notice that all such tensors except $u^\mu u^\nu + \frac{1}{d}g^{\mu\nu}$ vanish on our solutions. Hence, they would not contribute to any of the thermodynamic integrals evaluated on our solutions.

3.B Free thermodynamics on spheres

In (3.26) above, we have presented a general expression for the grand canonical partition function for any conformal fluid on a sphere. In this appendix , we compare this expression with the conformal thermodynamics of a free complex scalar field on a sphere.

Strictly speaking, the fluid dynamical description never applies to free theories on a compact manifold, as the constituents of a free gas have a divergent mean free path (they never collide). Nonetheless, as we demonstrate in this subsection, free thermodynamics already displays some of the features of (3.26) - in its dependence on angular velocities, for example - together with certain pathologies unique to free theories.

Consider a free complex scalar field on $S^{d-1}\times$ time. This system has a $U(1)$ symmetry, under which ϕ has unit charge and ϕ^* has charge minus one. We define the 'letter partition function' [82] $Z_{\rm let}$ as $\mathrm{Tr}\exp\left[-\beta E + \nu R + \beta\Omega_a L_a\right]$ evaluated over all spherical harmonic modes of the scalar field

$$Z_{\rm let} = (\mathrm{e}^{\nu} + \mathrm{e}^{-\nu})\mathrm{e}^{-\beta\frac{d-2}{2}}\left(\frac{1-\mathrm{e}^{-2\beta}}{\prod_{a=1}^{n}(1-\mathrm{e}^{-\beta-\beta\Omega_a})(1-\mathrm{e}^{-\beta+\beta\Omega_a})}\right) \tag{3.79}$$

(this formula, and some of the others in this section, are valid only for even d; the generalisation to odd d is simple). We will now examine the high temperature limit of the grand-canonical partition function separately for $\nu = 0$ and $\nu \neq 0$.

3.B.1 Zero chemical potential: ($\nu = 0$) case

The second quantised partition function, $\mathcal{Z}_{\rm gc}$ for the scalar field on the sphere is given by

$$\mathcal{Z}_{\rm gc} = \exp\left(\sum_N \frac{Z_{\rm let}(N\beta, N\nu, \Omega_a)}{N}\right). \tag{3.80}$$

For small β, we have

$$Z_{\rm let} \approx \frac{4}{\beta^{d-1}\prod_a(1-\Omega_a^2)}\,.$$

It follows that[20]

$$\ln \mathcal{Z}_{\rm gc} = \frac{4\zeta(d)}{\beta^{d-1}\prod_a(1-\Omega_a^2)}\,. \tag{3.81}$$

Upon identifying $V_d h|_{\nu=0} = 4\zeta(d)$, we find that (3.80) is in perfect agreement with (3.26).

3.B.2 Nonzero chemical potential: ($\nu \neq 0$) case

The high temperature limit of the thermodynamics of a free, charged, massless field is complicated by the occurrence of Bose condensation. This phenomenon occurs already when $\Omega_a = 0$; this is the case we first focus on.

It is useful to rewrite the letter partition function as

$$Z_{\rm let} = (2\cosh\nu)\ \ \mathrm{e}^{-\beta\frac{d-2}{2}}\sum_N m(N)\mathrm{e}^{-\beta N}, \tag{3.82}$$

where $m(N) \approx 2N^{d-2}/(d-2)!$ for $N \gg 1$. The logarithm of the grand canonical partition function may then be written as a sum over Bose factors (one per 'letter')

$$\ln \mathcal{Z}_{\rm gc} = -\sum_N m(N)\left[\ln(1-\mathrm{e}^{-\beta(N+(d-2)/2)+\nu}) + \ln(1-\mathrm{e}^{-\beta(N+(d-2)/2)-\nu})\right]. \tag{3.83}$$

The total charge in this ensemble is given by

$$R = \frac{\partial}{\partial\nu}\ln\mathcal{Z}_{\rm gc} = \sum_N m(N)\left(\frac{1}{\mathrm{e}^{\beta(N+(d-2)/2)-\nu}-1} - \frac{1}{\mathrm{e}^{\beta(N+(d-2)/2)+\nu}-1}\right). \tag{3.84}$$

In order to compare with fluid dynamics, we should take β to zero while simultaneously scaling to large R as $R = \frac{q}{\beta^{d-1}}$ with q held fixed. As we will see below, in order to make the total charge R large, we will have to choose the chemical potential to be large. However it is clear from (3.83) that $|\nu| < \beta(d-2)/2$. Consequently, the best we can do is to set $\nu = \beta((d-2)/2) - \epsilon$ where ϵ will be taken to be small. We are interested in the limit when β is also small. We may approximate (3.84) by

$$\frac{q}{\beta^{d-1}} = \frac{1}{\epsilon} - \frac{1}{\mathrm{e}^{\beta(d-2)-\epsilon}-1} + \sum_{N=1}^{\infty}\left(\frac{1}{\mathrm{e}^{\beta N+\epsilon}-1} - \frac{1}{\mathrm{e}^{\beta(N+(d-2))-\epsilon}-1}\right). \tag{3.85}$$

[20] This formula has been derived before in many contexts, for example [83] have derived this in $d = 4$ and compared it with the thermodynamics of black holes in AdS_5.

The only solution to (3.85) is

$$\epsilon = \frac{\beta^{d-1}}{q}\left(1 + \mathcal{O}(\beta)\right).$$

Substituting this solution into the partition function, we find

$$\ln Z_q = \frac{4\zeta(d)}{\beta^{d-1}}\left(1 + \mathcal{O}(\beta)\right). \tag{3.86}$$

Consequently, to leading order the partition function is independent of the charge q ! What is going on here is that almost all of the charge of the system resides in a Bose condensate of the zero mode of the field ϕ. This zero mode contributes very little entropy or energy to the system at leading order in β.[21] At high temperatures, the zero mode is simply a sink that absorbs the system charge, leaving the other thermodynamic parameters unaffected.

Upon generalising our analysis to include angular velocities, we once again find that the leading order partition function (in the limit of high temperatures and a charge $R = q/\beta^{d-1}$) is independent of q and in fact is given by (3.81). Consequently, there is a slightly trivial (or pathological) sense in which the thermodynamics of a free charged scalar field agrees with the predictions of fluid mechanics - we find agreement upon setting $h(\nu)$ to a constant.

[21] In particular, the contribution of the zero mode to the energy is proportional to the charge, which is suppressed by a factor of β relative to the contribution to the energy from nonzero modes.

Chapter 4

Plasmarings as dual black rings

In this chapter, we will study the plsamaball system, discussed in §1.3 in $d = 2+1$ in detail. In most of this chapter we will study $d = 4$, $SU(N)$, $\mathcal{N} = 4$ Yang-Mills at 't Hooft coupling $g_{YM}^2 N = \lambda$, compactified on a Scherk-Schwarz S^1 (the remaining $2+1$ dimensions are non-compact). Our analysis will apply equally well to the Scherk-Scwarz compactification of any strongly coupled, large N, conformal field theory. The low energy dynamics of this theory is that of a $2+1$ dimensional Yang-Mills system that undergoes deconfining phase transition at a finite temperature [49]. At large N and strong 't Hooft coupling this system admits supergravity dual description; as discussed in §1.3, the low temperature confining phase is dual to a gas of IIB supergravitons on the so called AdS soliton background [49]

$$\mathrm{d}s^2 = \frac{R_{\mathrm{AdS}}^2}{z^2}\left(-\mathrm{d}t^2 + \left[1-(\pi \mathcal{T}_{\mathrm{c}} z)^4\right]\,\mathrm{d}\theta^2 + \mathrm{d}x_i^2 + \frac{\mathrm{d}z^2}{\left[1-(\pi \mathcal{T}_{\mathrm{c}} z)^4\right]}\right), \tag{4.1}$$

where $i = 1, 2$, $\theta \sim \theta + {\mathcal{T}_{\mathrm{c}}}^{-1}$, $R_{\mathrm{AdS}}^2 = \sqrt{\lambda}\alpha'$.

The high temperature phase of the same system (at temperature $\mathcal{T}$) is dual to the the black brane

$$\mathrm{d}s^2 = \frac{R_{\mathrm{AdS}}^2}{z^2}\left(-\left[1-(\pi \mathcal{T} z)^4\right]\,\mathrm{d}t^2 + \mathrm{d}\theta^2 + \mathrm{d}x_i^2 + \frac{\mathrm{d}z^2}{\left[1-(\pi \mathcal{T} z)^4\right]}\right). \tag{4.2}$$

The thermodynamics of the high temperature phase can be computed using the usual constitutive equations of black brane thermodynamics [50]

$$\mathcal{P} = \frac{\pi^2 N^2}{8\mathcal{T}_{\mathrm{c}}}\left(\mathcal{T}^4 - {\mathcal{T}_{\mathrm{c}}}^4\right). \tag{4.3}$$

This system undergoes a deconfinement phase transition at temperature $\mathcal{T} = \mathcal{T}_{\mathrm{c}}$.

Just as the mean equilibrium properties of the deconfined phase are well described by the equations of thermodynamics, the statistically averaged near-equilibrium dynamics of this phase is governed by the equations of fluid dynamics – the relativistic generalisation

of the Navier-Stokes equations. These equations accurately describe the time evolution of fluid configurations whose space time derivatives are all small in units of the mean free path, which is of the same order as the mass gap of the theory [25, 50]. The same equations, augmented by appropriate surface terms, may also be used to study the dynamics of large lumps of plasma localised in the gauge theory vacuum (see §2.3).

The properties of the surface that separates the plasma from the vacuum, may be studied in the context of the simplest plasma profile with a surface; a configuration in which half of space, $x < 0$, is filled with the plasma. The surface at $x = 0$ is a domain wall that separates the plasma from the vacuum. The net force on this domain wall vanishes (and so the system is in equilibrium) when the plasma that fills $x < 0$ has vanishing pressure, i.e. at $\mathcal{T} = \mathcal{T}_c$ in the large N limit. The bulk gravity dual of this solution was constructed numerically in [50]; this configuration interpolates between the black brane at $\mathcal{T} = \mathcal{T}_c$ for $x < 0$ and the vacuum at $x > 0$, via a domain wall. The thickness and surface tension of this domain wall may be read off from this gravitational solutions, and were estimated, in [50] at approximately $6 \times \frac{1}{2\pi\mathcal{T}_c}$ and $\sigma = 2.0 \times \frac{\pi^2 N^2 \mathcal{T}_c{}^2}{2}$.

More generally, one would expect a finite lump of plasma that evolves according to the relativistic Navier-Stokes equations map in the bulk to a 'black hole' that evolves according to the Einstein equations. Provided all length scales in the plasma solution are small compared to the gauge theory mass gap (which is of the same order as the domain wall thickness), the dual bulk solution is well approximated by a superposition of patches of the black brane solution (with temperature varying across the patches) in the bulk and patches of the domain wall solution described in the previous paragraph. It follows (at least for stationary solutions) that the 3 dimensional black hole horizon topology (at any given time) is given by an S^1 (physically this is the θ circle) fibred over the two dimensional fluid configuration at the same time, subject to the condition that the S^1 contracts at all fluid surfaces (see fig.1.4). Consequently, fluid configurations with different topologies yield bulk dual black hole configurations with distinct horizon topologies. We will return to this point below.

This chapter is devoted to a detailed study of certain 'stationary' configurations of the plasma fluid; i.e. time independent, steady state solutions to the relativistic Navier-Stokes equations. The simplest configurations of this sort was studied already in [50]; the plasmaball is a static, spherically symmetric lump of fluid at constant local pressure P with $P = \sigma/R$ where R is the radius of the lump and σ its surface tension. In this chapter we study the more intricate spinning lumps of stationary fluid. These lumps carry angular momentum in addition to their mass.

It turns out that the relativistic Navier-Stokes equations admit two distinct classes of solutions of these sort. The first class of solution is a simple deformation of the static plasmaball; it is given by plasmaballs that spin at a constant angular velocity. The centripetal force needed to keep the configuration rotating in this solution is provided by a pressure gradient. The local plasma pressure (and hence local temperature and density) decreases from the edge (where it is a positive number set by the radius, surface tension and rotation speed) to the centre. As large enough angular velocity the pressure goes sufficiently negative in the core of the solution to allow for a second kind of solution of these equations; an annulus of plasma fluid rotating at constant angular velocity Ω. The local plasma pres-

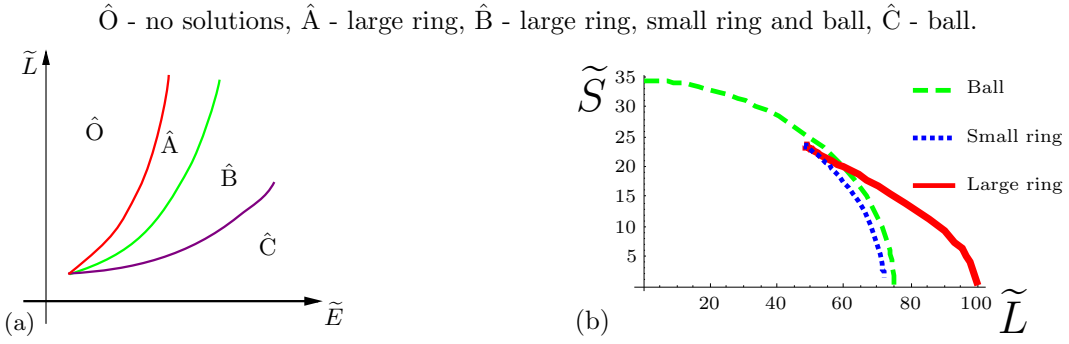

Figure 4.1: (a) Regions where ball and ring solutions exist, (b) their entropy as a function of angular momentum at fixed energy.

sure is positive on the outer surface and negative at the inner surface; the numerical value of the pressure in each case precisely balances the surface tensions at these boundaries.

We now describe the moduli space of spinning plasmaball and plasma ring solutions in a little more detail. In fig.4.1(a) we have plotted the energy-angular momentum plane, which we have divided up into 4 regions. In region Ĉ (low angular momentum at fixed energy) the only rigidly rotating solution to the equations of fluid dynamics is the rotating plasmaball. At higher angular momentum (region B̂) in addition to the rotating plasmaball there exist two new annulus type solutions which we call large and small ring solutions. As their names makes clear, the solutions are distinguished by their size; the large ring has a larger outer radius than the small one. On further raising angular momentum (region Â), the small ring and the ball cease to exist; in this region the large ring is the only solution. Finally, at still larger angular momentum (region Ô) there exist no solutions.

In fig.4.1(b) we have plotted the entropy of the three different kinds of solutions as a function of their angular momentum at a particular fixed energy. At angular momenta for which all three solutions coexist (region B̂) the entropy of the small ring is always smaller than the entropy of either the large ring or the black hole. Upon raising the angular momentum, the solution with dominant entropy switches from being the ball to the large ring; the first order transition between these solutions occurs at an angular momentum that lies on a 'phase transition line' in the bulk of region B̂. This picture suggests - and we conjecture - that the ball and the large ring are locally stable with respect to axisymmetric fluctuations, while the small ring is locally unstable to such fluctuations.[1] In §4.3.5 we perform a 'turning point' analysis of our solutions, to find some evidence for this guess. We will analyse the stability of these solutions in more detain in Ch.5.

Let us now turn to the bulk dual interpretation of our solutions. The fluid for the spinning plasmaball is topologically a disk; consequently the horizon topology for the dual bulk solution - the S^1 fibration over this disk - yields an S^3. The bulk dual of the spinning

[1]It is possible that the large ring exhibits Plateau-Rayleigh type instabilities that break rotational invariance; such modes would map to Gregory-Laflamme type instabilities of the bulk solution (see also [29]). We thank T. Wiseman for suggesting this possibility.

plasmaball is simply a rotating five dimensional black hole. On the other hand the fluid configuration of the plasmaring has the topology of $S^1\times$ interval; the S^1 fibration over this configuration yields $S^1 \times S^2$; i.e. a five dimensional black ring! Notice that in addition to the isometry along the S^1, these ring solutions all have a isometry on the S^2 corresponding to translations along the Scherk-Schwarz circle. This additional isometry, that does not appear to be required by symmetry considerations, appears to be a feature of all known black ring solutions in flat space as well.

Using the gauge theory / gravity duality, the quantitative versions of the fig.4.1 give precise quantitative predictions for the existence, thermodynamic properties and stability of sufficiently big black holes and black rings in Scherk-Schwarz compactified AdS_5 spaces. While these gravitational solutions have not yet been constructed, their analogues in flat 5 dimensional space are known, and have been well studied. The general qualitative features (and some quantitative features) of fig.4.1 are in remarkably good agreement with the analogous plots for black holes and black rings in flat five dimensional space (see §4.3.4 for a detailed discussion).

The constructions we have described above admit simple generalisations to plasma solutions dual to black holes and black rings in Scherk-Schwarz compactified AdS_6 space.[2] We postpone this analysis to Ch.6.

Finally, we should point out that there has been a long history within the General Relativity literature of treating black hole horizons as surfaces associated with fluids. In one of the most recent discussion within this framework, the authors of [31] have modelled spinning black holes in $d+1$ dimensional (flat space) gravity by $d+1$ dimensional lumps of incompressible fluid; here the fluid surface represents the black hole horizon. Within this framework the 4+1 dimensional black ring, for instance, is modelled by a 4+1 dimensional stationary fluid lump of topology $B^3 \times S^1$ [30]. This description is rather different from the AdS/CFT induced description of black rings in Scherk Schwarz compactified AdS_5 as a 2+1 dimensional annulus of fluid. It would be interesting to better understand the interconnections between these approaches.

4.1 Confining fluid

4.1.1 Equations of state

To solve the equations of fluid mechanics, one also needs expressions for the various coefficients that appear in the stress tensor above in terms of the density. For our purposes, we only need to know the thermodynamic properties of the fluid, which could be determined from the static black brane solution (4.2). In this subsection we discuss thermodynamics of the plasma at rest. This is different from the overall thermodynamics of the plasmaball/plasmaring that we will discuss in §4.2.4. We will be restricting attention to plasmas with all chemical potentials and conserved charges set to zero.

[2]Note that the spinning plasmaring has no analogue in 1+1 dimensional fluid dynamics, for the excellent reason that there is no spin. This tallies with the fact that there are no black rings in four dimensions (at least in flat space).

Recall from §2.1 that the thermodynamics of a fluid is completely specified once we express the pressure, $\mathcal{P}$, in terms of the temperature $\mathcal{T}$. For a conformal theory in d dimensions with no conserved charges, dimensional analysis determines

$$\mathcal{P} = \alpha \mathcal{T}^d, \tag{4.4}$$

with α an arbitrary constant. In our situation, the plasma is dual to the same black brane, so it doesn't know about any capping off in the IR except that the energy is measured with respect to a different zero. Before reducing on the Scherk-Schwarz circle, it behaves like a conformal theory in $d+1$ dimensions plus a vacuum energy density. After dimensional reduction on the Scherc-Scwarz circle of radius $1/\mathcal{T}_c$,[3] we have

$$\mathcal{P} = \frac{\alpha}{\mathcal{T}_c}\mathcal{T}^{d+1} - \rho_0. \tag{4.5}$$

The phase transition occurs when the confined and deconfined phase have the same free energy density, and hence the same pressure. As the deconfined plasma has a pressure of order N^2 (if we are considering a gauge theory) and the confined phase has a pressure of order N^0, to leading order at large N this phase transition occurs when $\mathcal{P} = 0$:

$$\rho_0 = \alpha {\mathcal{T}_c}^d. \tag{4.6}$$

Using (2.2), this gives

$$\mathcal{P} = \frac{\alpha}{\mathcal{T}_c}\left(\mathcal{T}^{d+1} - {\mathcal{T}_c}^{d+1}\right), \qquad \rho = \frac{\alpha}{\mathcal{T}_c}\left(d\mathcal{T}^{d+1} + {\mathcal{T}_c}^{d+1}\right), \qquad s = \frac{(d+1)\alpha}{\mathcal{T}_c}\mathcal{T}^d. \tag{4.7}$$

or, in three dimensions

$$\mathcal{P} = \frac{\alpha}{\mathcal{T}_c}\left(\mathcal{T}^4 - {\mathcal{T}_c}^4\right), \qquad \rho = \frac{\alpha}{\mathcal{T}_c}\left(3\mathcal{T}^4 + {\mathcal{T}_c}^4\right), \qquad s = \frac{4\alpha}{\mathcal{T}_c}\mathcal{T}^3. \tag{4.8}$$

Note that the critical density (the density at the phase transition) is *not* ρ_0, but is given by

$$\rho_c = (d+1)\rho_0 = (d+1)\alpha {\mathcal{T}_c}^d = s_c \mathcal{T}_c\,. \tag{4.9}$$

The thermalisation length scale can be estimated from (2.16):

$$l_{\text{mfp}} \sim \frac{s}{4\pi\rho} = \frac{(d+1)\mathcal{T}^d}{4\pi(d\mathcal{T}^{d+1} + {\mathcal{T}_c}^{d+1})}\,. \tag{4.10}$$

For the black-brane equation of state (4.3)

$$\alpha = \frac{\pi^2 N^2}{8}\,. \tag{4.11}$$

However, the values of this constant will not be important below.

[3]Strictly speaking, it is not a dimensional reduction as we will have plasma temperature of the same order as the Kaluza-Klein scale. Rather, we are restricting attention to classical solutions that do not vary in this compact dimension.

4.1.2 Surface tension

The surface tension at $\mathcal{T} = \mathcal{T}_c$ can be computed from the domain wall solutions constructed in [50].

$$\sigma = \begin{cases} 2.0 \times \dfrac{\rho_c}{\mathcal{T}_c} & \text{for } d = 3, \\ 1.7 \times \dfrac{\rho_c}{\mathcal{T}_c} & \text{for } d = 4. \end{cases} \tag{4.12}$$

Unfortunately, we do not know the surface tension at any other temperature, so we will assume that it is constant. This will hopefully be a reasonable approximation, provided that $\mathcal{T} - \mathcal{T}_c$ is small.

We can estimate the thickness of the surface using (2.27)

$$\xi = \frac{\sigma}{\rho_c} = \frac{\sigma}{(d+1)\alpha {\mathcal{T}_c}^d} = \begin{cases} \dfrac{2.0}{\mathcal{T}_c} & \text{for } d = 3, \\ \dfrac{1.7}{\mathcal{T}_c} & \text{for } d = 4. \end{cases} \tag{4.13}$$

This compares well with the thickness of the domain wall taken from the gravity solution: $6 \times \frac{1}{2\pi\mathcal{T}_c}$ in $d = 3$ and $5 \times \frac{1}{2\pi\mathcal{T}_c}$ in $d = 4$.

For the purposes of this and subsequent chapters, it is useful to define the related length scale

$$\xi' = (d+1)\xi = \frac{\sigma}{\rho_0} = \frac{\sigma}{\alpha {\mathcal{T}_c}^d}\,. \tag{4.14}$$

This length scale is of order N^0, and is similar to l_{mfp} and the surface thickness (provided that $\mathcal{T}$ is close to $\mathcal{T}_c$), all of which are $\sim 1/\mathcal{T}_c$.

4.2 Rigidly rotating configurations

In this section, we study stationary, axially symmetric rotating fluid configurations in 2+1 dimensions, whose equation of state is presented in §4.1.1. As discussed in §2.4, the velocity should be proportional to a time-like Killing vector, and we can always boost to a frame where this Killing vector describes rigid rotation. In order to be stationary, the fluid configuration must ne axially symmetric.

We choose the axis of rotation as our origin in polar coordinates; in these coordinates the fluid temperature is a function only of the radial coordinate r, and the (t, r, ϕ) components of the velocity are given by $u^\mu = \gamma(1, 0, \Omega)$ with the normalisation factor $\gamma = \left(1 - \Omega^2 r^2\right)^{-1/2}$. We will find two distinct kinds of solutions; rotating plasmaballs with the topology of a two dimensional disk, and plasmarings with the topology of a two dimensional annulus. The configurations we find are exact solutions to the equations of relativistic fluid dynamics; in §4.3.2 we will demonstrate that these equations accurately represent plasma dynamics for large enough plasmaballs and plasmarings.

4.2.1 Solving the equations of motion

Our fluid propagates in flat 2+1 dimensional space. In polar coordinates

$$\mathrm{d}s^2 = -\mathrm{d}t^2 + \mathrm{d}r^2 + r^2\mathrm{d}\phi^2\,. \tag{4.15}$$

As discussed above, we choose a velocity profile

$$u = \gamma(\partial_t + \Omega\partial_\phi), \quad \gamma = \left(1-\Omega^2 r^2\right)^{-1/2}. \tag{4.16}$$

Following (2.30), we must choose the temperature profile

$$\mathcal{T} = \gamma T. \tag{4.17}$$

which, using (4.7), leads to the pressure profile

$$\mathcal{P} = \frac{\alpha}{\mathcal{T}_{\rm c}}\left(\gamma^4 T^4 - {\mathcal{T}_{\rm c}}^4\right). \tag{4.18}$$

Outer and inner surfaces can be described, as in §2.3, by the functions

$$\begin{aligned} f_{\rm o} &= r_{\rm o} - r, \qquad & \Theta &= \frac{1}{r_{\rm o}}\,, \\ f_{\rm i} &= r - r_{\rm i}, \qquad & \Theta &= -\frac{1}{r_{\rm i}}\,. \end{aligned} \tag{4.19}$$

4.2.2 Spinning ball

Let us first study a fluid configuration with a single outer surface at $r = r_{\rm o}$. Using the (4.18) and (4.19), the boundary condition (2.31) can be written as

$$\frac{\alpha}{\mathcal{T}_{\rm c}}\left(\frac{T^4}{(1-\Omega^2 r_{\rm o}^2)^2} - {\mathcal{T}_{\rm c}}^4\right) = \frac{\sigma}{r_{\rm o}}\,. \tag{4.20}$$

If we define dimensionless variables

$$\widetilde{\Omega} = \xi'\Omega\,, \qquad \tilde{r} = \frac{r}{\xi'}\,, \qquad v = \Omega r = \widetilde{\Omega}\tilde{r}\,, \qquad \widetilde{T} = \frac{T}{\mathcal{T}_{\rm c}}\,, \tag{4.21}$$

where ξ' is defined in (4.14), then (4.20) can be written as

$$\widetilde{T}^4 = \left(1 + \frac{\widetilde{\Omega}}{v_{\rm o}}\right)\left(1 - v_{\rm o}^2\right)^2 \equiv g_+(v_{\rm o}). \tag{4.22}$$

Note that the range of v is $[0,1]$ and $\widetilde{T}^4$ is always positive for this solution, as is required for this to make sense.

It is convenient to take the two independent parameters of the ball solution to be $v_{\rm o}$ and $\widetilde{\Omega}$, with (4.22) determining $\widetilde{T}$.

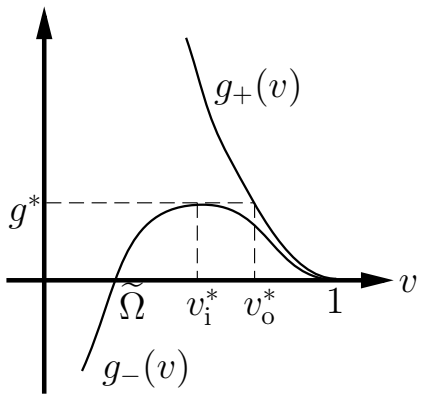

Figure 4.2: Graph of $g_\pm(v)$ showing possible values of $v_{o,i}$

4.2.3 Spinning ring

We now turn to solutions that have an inner surface well an outer surface. In addition to the boundary condition at the outer radius (4.20) we now have

$$\frac{\alpha}{\mathcal{T}_{\rm c}}\left(\frac{T^4}{(1-\Omega^2 r_{\rm i}^2)^2}-\mathcal{T}_{\rm c}^{\,4}\right)=-\frac{\sigma}{r_{\rm i}}\,. \tag{4.23}$$

So the positions of the boundaries are related to the temperature and angular velocity by

$$\begin{aligned}\widetilde{T}^4&=\left(1+\frac{\widetilde{\Omega}}{v_{\rm o}}\right)\left(1-v_{\rm o}^2\right)^2\equiv g_+(v_{\rm o})\\ &=\left(1-\frac{\widetilde{\Omega}}{v_{\rm i}}\right)\left(1-v_{\rm i}^2\right)^2\equiv g_-(v_{\rm i}).\end{aligned} \tag{4.24}$$

Note that $\widetilde{T}^4\geq 0$ provided that $v_{\rm i}\geq\widetilde{\Omega}$.

It is convenient to take the two independent parameters of the ring solution to be $v_{\rm o}$ and $v_{\rm i}$, using (4.22) to eliminate $\widetilde{T}$ and $\widetilde{\Omega}$:

$$\begin{aligned}\widetilde{\Omega}&=\frac{v_{\rm o}v_{\rm i}(v_{\rm o}-v_{\rm i})(2-v_{\rm o}^2-v_{\rm i}^2)}{1-v_{\rm o}v_{\rm i}(2-v_{\rm o}^2+v_{\rm o}v_{\rm i}-v_{\rm i}^2)}\,,\\ \widetilde{T}^4&=\frac{(1-v_{\rm o}^2)^2(1-v_{\rm i}^2)^2}{1-v_{\rm o}v_{\rm i}(2-v_{\rm o}^2+v_{\rm o}v_{\rm i}-v_{\rm i}^2)}\,.\end{aligned} \tag{4.25}$$

The two functions, $g_\pm(v)$ are schematically plotted in fig.4.2 for some value of $\widetilde{\Omega}$, where we have labelled special velocities $v_{\rm i}^*$ and $v_{\rm o}^*$. As $v_{\rm i}<1$, it is necessary that $\widetilde{\Omega}<1$.

We can see that there are no solutions to $g_+(v_{\rm o})=g_-(v_{\rm i})$ for $v_{\rm o}<v_{\rm o}^*$ and two solutions for $v_{\rm o}>v_{\rm o}^*$. One of these has $v_{\rm i}<v_{\rm i}^*$ (the thick ring) and one has $v_{\rm i}>v_{\rm i}^*$ (the thin ring). The distinction between 'thin' and 'thick' rings will not prove physically important.

In §4.3.1 we will find it physically useful to distinguish between distinct ring solutions (we will call these large and small rings) at the same values of conserved charges (energy and angular momentum), rather than the parameters $v_{\rm o}$ and $\widetilde{\Omega}$.

4.2.4 Thermodynamic potentials

In this subsection, we compute the thermodynamic potentials (energy, angular momentum, entropy, etc.) for the spinning plasmaball and plasmarings themselves, rather than their constituent plasma. This includes contributions from the kinetic energy of the plasma as well as its internal energy.

The constitutive relations we find are predictions for, e.g., entropy as a function of mass and angular momentum of the dual gravity solutions.

We can define some dimensionless variables

$$\ln\widetilde{\mathcal{Z}}_{\rm gc}=\frac{\ln\mathcal{Z}_{\rm gc}}{\pi\alpha{\mathcal{T}_{\rm c}}^2(\xi')^2}\,,\quad \widetilde{E}=\frac{E}{\pi\alpha{\mathcal{T}_{\rm c}}^3(\xi')^2}\,,\quad \widetilde{L}=\frac{L}{\pi\alpha{\mathcal{T}_{\rm c}}^3(\xi')^3}\,,\quad \widetilde{S}=\frac{S}{\pi\alpha{\mathcal{T}_{\rm c}}^2(\xi')^2}\,, \tag{4.26}$$

This ensures that $\mathrm{d}\widetilde{E}=\widetilde{T}\mathrm{d}\widetilde{S}+\widetilde{\Omega}\mathrm{d}\widetilde{L}$ and $-\widetilde{T}\ln\widetilde{\mathcal{Z}}_{\rm gc}=\widetilde{E}-\widetilde{\Omega}\widetilde{L}-\widetilde{T}\widetilde{S}$.

These can be computed using (2.39) and (2.40). It is helpful to note that

$$\begin{aligned}
\widetilde{S}&=\left(\frac{\partial(\widetilde{T}\ln\widetilde{\mathcal{Z}}_{\rm gc})}{\partial\widetilde{T}}\right)_{\widetilde{\Omega}}=\frac{\begin{vmatrix}\left(\frac{\partial(\widetilde{T}\ln\widetilde{\mathcal{Z}}_{\rm gc})}{\partial\alpha}\right)_\beta & \left(\frac{\partial\widetilde{\Omega}}{\partial\alpha}\right)_\beta\\ \left(\frac{\partial(\widetilde{T}\ln\widetilde{\mathcal{Z}}_{\rm gc})}{\partial\beta}\right)_\alpha & \left(\frac{\partial\widetilde{\Omega}}{\partial\beta}\right)_\alpha\end{vmatrix}}{\begin{vmatrix}\left(\frac{\partial\widetilde{T}}{\partial\alpha}\right)_\beta & \left(\frac{\partial\widetilde{\Omega}}{\partial\alpha}\right)_\beta\\ \left(\frac{\partial\widetilde{T}}{\partial\beta}\right)_\alpha & \left(\frac{\partial\widetilde{\Omega}}{\partial\beta}\right)_\alpha\end{vmatrix}}\,,\\
\widetilde{L}&=\left(\frac{\partial(\widetilde{T}\ln\widetilde{\mathcal{Z}}_{\rm gc})}{\partial\widetilde{\Omega}}\right)_{\widetilde{T}}=\frac{\begin{vmatrix}\left(\frac{\partial\widetilde{T}}{\partial\alpha}\right)_\beta & \left(\frac{\partial(\widetilde{T}\ln\widetilde{\mathcal{Z}}_{\rm gc})}{\partial\alpha}\right)_\beta\\ \left(\frac{\partial\widetilde{T}}{\partial\beta}\right)_\alpha & \left(\frac{\partial(\widetilde{T}\ln\widetilde{\mathcal{Z}}_{\rm gc})}{\partial\beta}\right)_\alpha\end{vmatrix}}{\begin{vmatrix}\left(\frac{\partial\widetilde{T}}{\partial\alpha}\right)_\beta & \left(\frac{\partial\widetilde{\Omega}}{\partial\alpha}\right)_\beta\\ \left(\frac{\partial\widetilde{T}}{\partial\beta}\right)_\alpha & \left(\frac{\partial\widetilde{\Omega}}{\partial\beta}\right)_\alpha\end{vmatrix}}\,,
\end{aligned} \tag{4.27}$$

where α and β are the two parameters of the solutions.

We present the results of these computations in the next two subsections.

Spinning ball

Partition function

$$\ln\widetilde{\mathcal{Z}}_{\rm gc}=-\frac{v_{\rm o}^{5/4}(\widetilde{\Omega}v_{\rm o}^2+\widetilde{\Omega}+v_{\rm o}^3)}{\widetilde{\Omega}^2(\widetilde{\Omega}+v_{\rm o})^{1/4}\sqrt{1-v_{\rm o}^2}}\,. \tag{4.28}$$

Energy

$$\widetilde{E}=\frac{4v_{\rm o}^2-v_{\rm o}^4+5\widetilde{\Omega}v_{\rm o}-\widetilde{\Omega}v_{\rm o}^3}{\widetilde{\Omega}^2}\,. \tag{4.29}$$

Angular momentum

$$\widetilde{L} = \frac{2v_{\rm o}^4 + 2\widetilde{\Omega}v_{\rm o}^3}{\widetilde{\Omega}^3}\,. \tag{4.30}$$

Entropy

$$\widetilde{S} = \frac{4v_{\rm o}^2}{\widetilde{\Omega}^2}\sqrt{1-v_{\rm o}^2}\left(1+\frac{\widetilde{\Omega}}{v_{\rm o}}\right)^{3/4}\,. \tag{4.31}$$

Spinning ring

Partition function

$$\ln\widetilde{\mathcal{Z}}_{\rm gc} = -\frac{(v_{\rm o}+v_{\rm i})^3(1-v_{\rm o}v_{\rm i})[1-v_{\rm o}v_{\rm i}(2-v_{\rm o}^2+v_{\rm o}v_{\rm i}-v_{\rm i}^2)]^{5/4}}{v_{\rm o}^2v_{\rm i}^2(v_{\rm o}-v_{\rm i})\sqrt{(1-v_{\rm o}^2)(1-v_{\rm i}^2)}(2-v_{\rm i}^2-v_{\rm o}^2)^2}\,. \tag{4.32}$$

Energy

$$\widetilde{E} = \frac{(2-v_{\rm o}-v_{\rm i})(2+v_{\rm o}+v_{\rm i})(v_{\rm o}+v_{\rm i})(v_{\rm o}v_{\rm i}+1)[1-v_{\rm o}v_{\rm i}(2-v_{\rm o}^2+v_{\rm o}v_{\rm i}-v_{\rm i}^2)]}{v_{\rm o}^2v_{\rm i}^2(v_{\rm o}-v_{\rm i})(2-v_{\rm o}^2-v_{\rm i}^2)^2}\,. \tag{4.33}$$

Angular momentum

$$\widetilde{L} = \frac{2(v_{\rm o}+v_{\rm i})(v_{\rm o}^2+v_{\rm i}^2-2v_{\rm o}^2v_{\rm i}^2)[1-v_{\rm o}v_{\rm i}(2-v_{\rm o}^2+v_{\rm o}v_{\rm i}-v_{\rm i}^2)]^2}{v_{\rm o}^3v_{\rm i}^3(v_{\rm o}-v_{\rm i})^2(2-v_{\rm o}^2-v_{\rm i}^2)^3}\,. \tag{4.34}$$

Entropy

$$\widetilde{S} = \frac{4\sqrt{(1-v_{\rm o}^2)(1-v_{\rm i}^2)}(v_{\rm o}+v_{\rm i})[1-v_{\rm o}v_{\rm i}(2-v_{\rm o}^2+v_{\rm o}v_{\rm i}-v_{\rm i}^2)]^{5/4}}{v_{\rm o}^2v_{\rm i}^2(v_{\rm o}-v_{\rm i})(2-v_{\rm o}^2-v_{\rm i}^2)^2}\,. \tag{4.35}$$

4.3 Solutions at fixed energy and angular momentum

4.3.1 Existence

The various regions of existence of the plasmaball, thin plasmaring and thick plasmaring in the $\widetilde{E}$-$\widetilde{L}$ plane are drawn schematically in fig.4.3.

The ball solution exists over a region C in the $\widetilde{E}$-$\widetilde{L}$ plane. At the boundary of the region C the ball solution $v_{\rm o}$ attains its maximum value of unity. Using (4.29,4.30) we find an analytic expression for the boundary of C:

$$\widetilde{L} = \frac{2}{27}\left[(3\widetilde{E}+4)^{3/2} - 9\widetilde{E} - 8\right] \sim \frac{2\widetilde{E}^{3/2}}{3^{3/2}} \quad \text{for large } \widetilde{E}\,. \tag{4.36}$$

From (4.22), we see that balls on this boundary saturate the extremality bound (i.e. have zero temperature).

Like the balls, rings of a fixed energy have a maximum value of angular momentum. Rings at the edge of this bound (the boundary between O and A in fig.4.3b) have $v_{\rm o} = v_{\rm i} = 1$

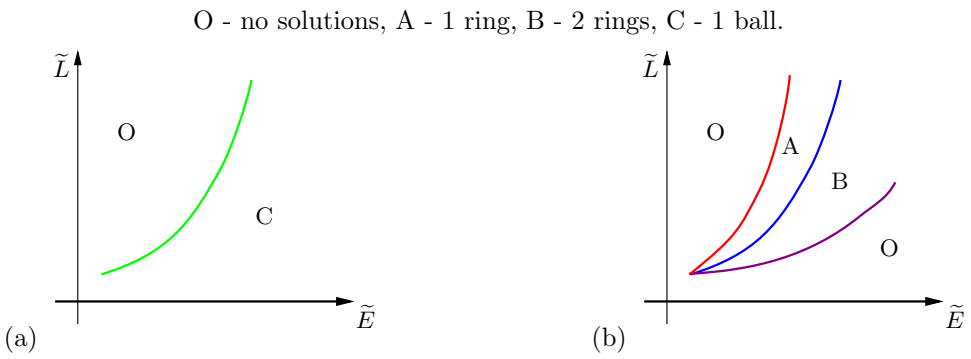

Figure 4.3: Regions where (a) ball and (b) ring solutions exist.

and so are extremal (see (4.25)) and of zero width. Using (4.33,4.34) the O-A boundary is given by

$$\widetilde{L} = \frac{\widetilde{E}^2}{16}\,, \tag{4.37}$$

(this expression is valid only for $\widetilde{E} > 8$, $\widetilde{L} > 2$; at lower energies $\widetilde{\Omega}$ exceeds unity).

As we lower angular momentum of the solution, this ring moves away from extremality and increases in width. At a particular angular momentum (the boundary between region A and region B) a new ring solution comes into existence. The corresponding solution has $v_{\rm o} = 1$, $v_{\rm i} = \widetilde{\Omega}$ and so is extremal (see (4.24). Using (4.33,4.34), the analytic expression for the A-B boundary is given by

$$\widetilde{L} = \frac{2}{27}\left[(3\widetilde{E}+1)^{3/2} - 9\widetilde{E} + 1\right] \sim \frac{2\widetilde{E}^{3/2}}{3^{3/2}} \quad \text{for large } \widetilde{E}\,, \tag{4.38}$$

(for $\widetilde{E} > 8$, $\widetilde{L} > 2$ as above). In the high energy limit $\widetilde{E} \gg 1$ the ratio of angular momentum for the new extremal rings (at the A-B boundary) and extremal plasmaball tends to unity, (even though the the difference between angular momenta does not go to zero). Consequently the leading high energy behaviour of (4.38) and (4.36) is the same in this limit, as is also clear from fig.4.5. We emphasise that, for our solutions, the extremal ball and extremal thick ring are not quite identical (as is the case for black holes and small black rings [20] in flat space) as the inner radius of our extremal thick rings does not vanish. However, the inner radius of the extremal thick ring is always (for all values of energy) of the same order as the thickness of the domain wall. As the fluid dynamics approximations fail precisely under these conditions, it could well be that the new extremal plasmaring and extremal plasmaball are actually identical configurations.

As we further lower angular momentum, the new ring solution moves away from extremality; this new solution always has a smaller outer radius than the 'original' ring solution (the solutions that also exists in region A), as shown in fig.4.4. As a consequence, we refer to these two ring solutions as small and large respectively.

Further lowering angular momentum, we hit the boundary between regions B and O where the two ring solutions merge into each other. At still lower angular momentum,

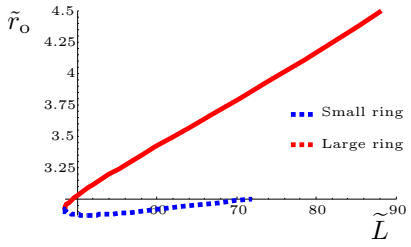

Figure 4.4: Outer radius of large and small rings as a function of angular momentum, $\widetilde{L}$, at fixed energy, $\widetilde{E} = 40$.

we have no ring solutions. We can think of this as follows: as we vary (v_o, v_i) for the ring, (4.33) and (4.34) map out a surface in the $\widetilde{E}$-$\widetilde{L}$ plane. At some point, this surface turns over, so we have a region of the $\widetilde{E}$-$\widetilde{L}$ plane where there are two branches of ring solutions. These can be distinguished by the sign of the Jacobian:

$$\begin{aligned} \text{large ring:} \quad & \frac{\partial(\widetilde{E},\widetilde{L})}{\partial(v_o,v_i)} < 0, \\ \text{small ring:} \quad & \frac{\partial(\widetilde{E},\widetilde{L})}{\partial(v_o,v_i)} > 0, \end{aligned} \tag{4.39}$$

where

$$\begin{aligned} \frac{\partial(\widetilde{E},\widetilde{L})}{\partial(v_o,v_i)} \equiv & \left(\frac{\partial\widetilde{E}}{\partial v_o}\right)_{v_i}\left(\frac{\partial\widetilde{L}}{\partial v_i}\right)_{v_o} - \left(\frac{\partial\widetilde{L}}{\partial v_o}\right)_{v_i}\left(\frac{\partial\widetilde{E}}{\partial v_i}\right)_{v_o} \\ = & \frac{2(v_o+v_i)(1-v_o v_i(2-v_o^2+v_o v_i-v_i^2))^2}{v_o^6 v_i^6 (v_o-v_i)^4(2-v_o^2-v_i^2)^6}\, V(v_o,v_i) \end{aligned} \tag{4.40}$$

where $V(v_o, v_i)$ is a degree 16 polynomial. The place where the two solutions meet, and hence the B-O boundary, can be found by setting it to zero. In the high energy/angular momentum limit, one has

$$\begin{aligned} & v_o \to 0, \qquad v_i \to 0, \qquad \frac{v_i}{v_o} \to \frac{1}{4}\left(1+\sqrt{33}-\sqrt{2\left(9+\sqrt{33}\right)}\right), \\ & \widetilde{E} \sim \frac{\text{const.}}{v_o^4}, \quad \widetilde{L} \sim \frac{\text{const.}}{v_o^5}, \quad \frac{\widetilde{L}}{\widetilde{E}^{5/4}} \to \frac{\sqrt[8]{\frac{1}{2}\left(11133+1837\sqrt{33}\right)}}{4\sqrt[4]{3}}. \end{aligned} \tag{4.41}$$

The existence of plasmaball and plasmaring solutions in the $\widetilde{E}$-$\widetilde{L}$ plane may thus be summarised as in fig.4.5.

4.3.2 Validity

As we have described above, plasmaballs and plasmarings are exact solutions to the relativistic Navier-Stokes equations (supplemented by sharp surface boundary conditions).

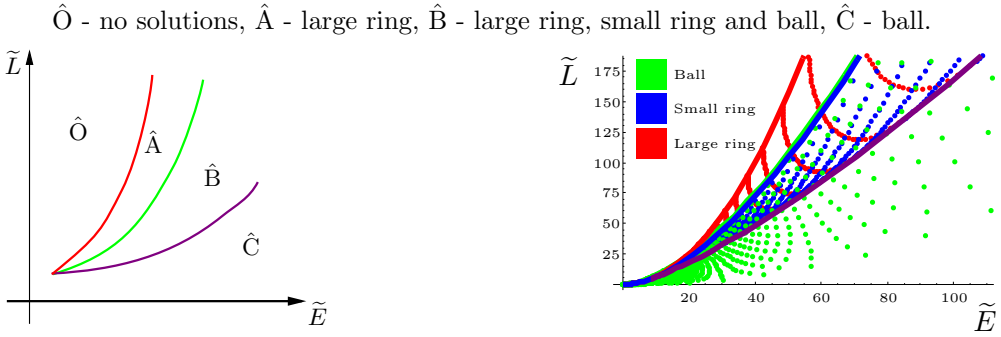

Figure 4.5: Regions where ball and ring solutions exist.

However these equations of fluid dynamics accurately capture the dynamics of the fluid plasma only under certain conditions. In our discussion we have assigned a well defined pressure and temperature to the fluid at each point in space. Clearly this procedure is valid only when the variation of these thermodynamic quantities is small over the thermalisation length scale of the fluid (4.10).

Second, we have treated the surface of the plasma as sharp; in reality this surface has a thickness of order ξ (see (4.13)). Consequently, our treatment of the surface is valid only when its deviation from a straight line occurs on scales large compared to $\xi \sim \xi'$ (higher derivative contributions to the surface stress tensor, which we have ignored in our treatment, would become important if this were not the case); further we must also require that only a small fraction of the fluid should reside in surfaces.

Thirdly, we have ignored the fact that the surface tension is a function of the fluid temperature at the surface, and simply set $\sigma = \sigma(\mathcal{T}_c)$. This is valid provided that $\mathcal{T}/\mathcal{T}_c \approx 1$ at all surfaces. When this is the case, the pressure will be small compared to ρ_c (see (4.8)). Then, (2.31) tells us that the extrinsic curvature of the surface must be small compared to $1/\xi$, which is the same as the previous condition.

Finally, the fluid evolution equations, by their very nature, track mean velocities and energy densities, ignoring fluctuations. In our context this approximation is justified by large N; fluctuations are suppressed by powers of $1/N^2$, dual to the suppression of quantum metric fluctuations in the bulk.

We can estimate the scale over which thermodynamic quantities vary as the distance over which the fractional change in the temperature is one. As the temperature is proportional to γ, we should look at

$$\frac{1}{\|\nabla \ln \gamma\|} = \frac{1-v^2}{\Omega v} \,.$$

At temperatures close to $\mathcal{T}_c$, where our other approximations are valid, we have $l_{\rm mfp} \sim \xi'$. Therefore, we require that the ratio of the above quantity to ξ' is large. As this takes its minimum value at the outer surface, the condition for the validity of the equations of fluid

dynamics may be estimated to be

$$(\Delta u)^{-1} \equiv \frac{1-v_{\rm o}^2}{\widetilde{\Omega} v_{\rm o}} \gg 1\,. \tag{4.42}$$

Our treatment of the surface as a zero-thickness object is valid if

$$\{r_{\rm o}, r_{\rm i}, r_{\rm o}-r_{\rm i}\} \gg \xi'.$$

(for the ring, the $r_{\rm o}$ inequality in the equation above follows automatically from the either of the other two inequalities). This condition can be rewritten in terms of our dimensionless variables as

$$\tilde{r}_{\rm o} \gg 1 \qquad \text{for the ball,} \qquad \{\tilde{r}_{\rm i}, \tilde{r}_{\rm o}-\tilde{r}_{\rm i}\} \gg 1 \qquad \text{for the ring.} \tag{4.43}$$

In fig.4.6, we have plotted a sample of the quantities $\ln(1/\Delta u)$, $\ln(\tilde{r}_{\rm i})$, $\ln(\tilde{r}_{\rm o}-\tilde{r}_{\rm i})$ and $\ln(\tilde{r}_{\rm o})$ as a function of energy and angular momentum for the thin ring, thick ring and ball. The full set of plots can be found in [2]. From the figure we observe that these quantities are large (and so the fluid dynamics approximations of this chapter are accurate) when our rings and balls have large energy and we stay away from the extremality bounds.

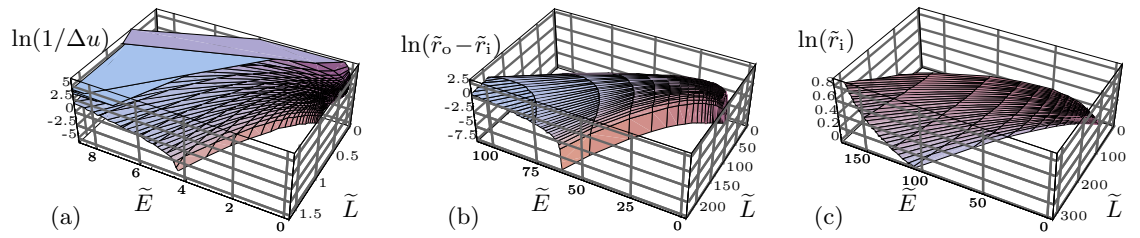

Figure 4.6: Plots of (a) $\ln(1/\Delta u)$ for balls, (b) $\ln(\tilde{r}_{\rm o}-\tilde{r}_{\rm i})$ for (a) large rings, and (c) $\ln(\tilde{r}_{\rm i})$ for small rings.

4.3.3 Global stability and phase diagram

Recall that (see fig.4.5) at fixed values of energy and angular momentum, we have either 0, 1 or 3 plasmaball / plasmaring solutions. At those values of charges for which multiple solutions exist, it is natural to inquire which of these solutions is entropically favoured. In fig.4.7(a) we have plotted the entropy of plasma ball and plasmaring solutions as a function of angular momentum at fixed energy.

Note that, when it exists, the small ring always carries lower entropy than both the big ring and the plasmaball. At low enough angular momentum the plasmaball is the only solution. This solution continues to be entropically dominant (upon raising the angular momentum) over an interval, even after the new ring solutions are nucleated. At a critical angular momentum, however, the entropy of the large ring equals and then exceeds the entropy of the plasmaball (all three ring solutions continue to exist in a neighbourhood

PH–phase boundary, ELR–extreme large ring, EB–extreme ball, ESR– extreme small ring, LSM–large/small ring merger.

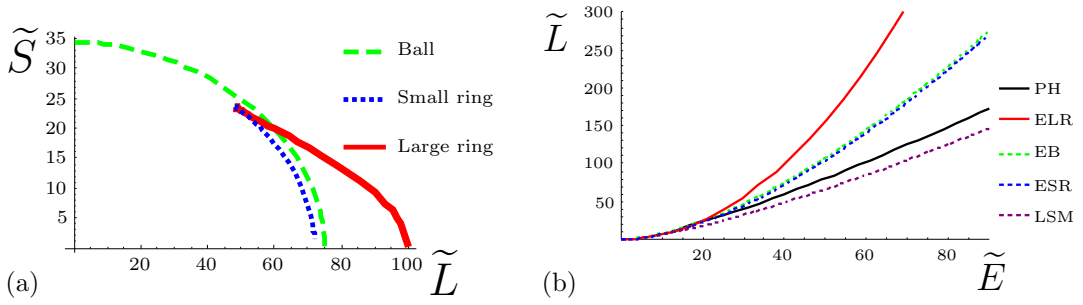

Figure 4.7: (a) Entropy, $\widetilde{S}$, as a function of angular momentum, $\widetilde{L}$ for fixed energy, $\widetilde{E} = 40$. (b) Phase boundary with existence boundaries.

about this point). The large ring is the entropically dominant solution at all larger angular momenta.

The phase boundary can be seen in fig.4.7(b). In the high energy/angular momentum limit[4]

$$\begin{aligned} &\text{Ball:} \quad v_{\rm o} \to 0, \quad \widetilde{\Omega} \to 0, \quad \frac{\widetilde{\Omega}}{v_{\rm o}^3} \to a = 0.273243, \\ &\text{Ring:} \quad v_{\rm o} \to 0, \quad v_{\rm i} \to 0, \quad \frac{v_{\rm i}}{v_{\rm o}} \to b = 0.506128, \end{aligned} \tag{4.44}$$

with $\frac{v_{\rm o}(\text{ring})}{v_{\rm o}(\text{ball})} = \sqrt[4]{\frac{a^2(b+1)}{4b^2(1-b)}} = 0.68658$. We have

$$\widetilde{E} \sim \frac{\text{const.}}{v_{\rm o}^4}\,, \quad \widetilde{L} \sim \frac{\text{const.}}{v_{\rm o}^5}\,, \quad \frac{\widetilde{L}}{\widetilde{E}^{5/4}} \to \frac{1}{2\sqrt{2a}} = 0.676364\,. \tag{4.45}$$

4.3.4 Comparison with black rings in flat 5D space

As we have explained in the introduction, the plasmaball and plasmaring solutions of this chapter are dual to black holes and black rings in the background (4.1). Unfortunately the corresponding gravitational solutions have not yet been constructed; however exact black ring solutions to the vacuum Einstein equations in 5 dimensions, were obtained in [20] (see [21] for a review). These solutions were further studied in [84]. In this subsection we compare the properties these black rings and black holes with our plasmaballs and plasmarings, and find broad qualitative agreement between the two. While we expect the properties of plasmaballs and plasmarings to match quantitatively with those of black holes and black rings in the background (4.1), we could not hope to find better than qualitative agreement with the properties of the same objects in flat space.

In fig.4.8 we have presented a schematic plot for the existence regions and phase diagram of black hole and black ring solutions in 5 dimensional flat space. This figure looks

[4] Analytically, $a = \frac{2b\left(4b(1-b)+\sqrt{1-b^2}(1+4b+b^2)\right)}{1+9b+10b^2+42b^3+9b^4+b^5}$ and $4 - 7b - 8b^2 + 10b^3 + 4b^4 + b^5 = 0$.

A' - thin black ring, B' - thin black ring, thick black ring and black hole, C' - black hole.

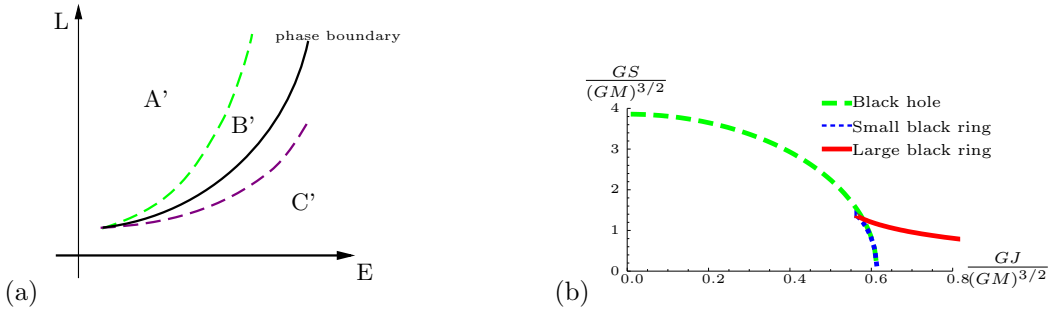

Figure 4.8: (a) Existence regions and (b) phase diagram for black holes/rings in five dimensional flat space.

fairly similar to figs.4.5,4.7. The major qualitative difference is the absence of the analogue of the region O (see fig. 4.5) in fig. 4.8. Thus unlike thin black rings in flat 5 dimensional space, plasmarings (and so black rings in Scherk-Schwarz AdS_5) have an upper bound to their angular momentum at fixed energy.[5]

It is interesting to pursue the comparison between these solutions in more detail. The gravitational analogue of fig.4.7 (presented as [20, fig.3] AND fig.4.8(B)) looks fairly similar to our figure. The main qualitative differences are: unlike for plasmarings, the entropy of the large flat space black ring doesn't go to zero at a finite angular momentum (it asymptotes to zero at infinity) and the entropy of the small flat space black ring and black hole go to zero at exactly the same point instead of the slightly different values that we see. We expect that first of these differences reflects a physical difference between black rings in flat space and Scherk-Schwarz compactified AdS_5, the second difference is an artefact of the breakdown of the fluid dynamics approximation for extremal small rings (whose inner radius is always of order the surface thickness).

In even greater detail, we could quantitatively compare the boundaries between regions O, A, B and C (see fig.4.3) which correspond to th phase boundary (PH), the extreme large ring (ELR), the extreme ball (EB), the extreme small ring (ESR) and the large/small ring merger (LSM). These curves, as well as the phase boundary, may be parameterised by $L = xE^y$ at large energies.

For black holes and black rings in flat space $y_{LSM} = y_{EB} = y_{ESR} = y_{PH} = \frac{3}{2}$. For our plasmaballs and plasmarings, as one can see in (4.36-4.41) and (4.45) ,for large energy, we get $y_{ELR} = 2$, $y_{ESR} = y_{EB} = \frac{3}{2}$, $y_{LSM} = 5/4$ and $y_{PH} = 5/4$ (see table 4.1).

It is meaningless to compare the x's directly, as they are dimensionful quantities. However, when two y's have the same value, the ratio of the corresponding x's is dimensionless and may be compared. For black rings $x_{ESR} = x_{EB} = \sqrt{32G/27\pi}$, $x_{LSM} = \sqrt{G/\pi}$ and $x_{PH} = \sqrt{256G/243\pi}$, so $x_{ESR}/x_{EB} = 1$, $x_{EB}/x_{LSM} = \sqrt{32/27}$ and $x_{LSM}/x_{PH} = 9\sqrt{3}/16$. For plasmaballs and plasmarings, if we used the dimensionless quantities (4.26), we find

[5]This upper bound was expected for black rings in AdS. The negative cosmological constant has a similar effect to the dipole charge of [85]. We thank R. Emparan for explaining this to us.

Quantity	Black rings	Plasmarings
y_{ELR}	N/A	2
y_{ESR}	3/2	3/2
y_{EB}	3/2	3/2
y_{LSM}	3/2	5/4
y_{PH}	3/2	5/4
x_{ESR}/x_{EB}	1	1
x_{EB}/x_{LSM}	$\sqrt{32/27}$	N/A
x_{LSM}/x_{PH}	$9\sqrt{3}/16 \approx 0.97$	0.91

Table 4.1: Comparison of scalings of boundaries for black rings and plasmarings.

$x_{ELR} = \frac{1}{16}$, $x_{ESR} = x_{EB} = 2/3^{3/2}$, $x_{LSM} \approx 0.60$ and $x_{PH} \approx 0.69$. Therefore $x_{ESR}/x_{EB} = 1$ and $x_{LSM}/x_{PH} \approx 0.90$.

This is summarised in table 4.1. Note that the extremality boundaries, ELR, EB and ESR, occur precisely where at least one of the approximations discussed in §4.3.2 breaks down. Therefore, nothing quantitative about these boundaries should be trusted.

4.3.5 Turning point stability

We have seen in §4.3.3 that the spinning plasma solution of maximal entropy is the plasmaball (at low angular momentum) or the large plasmaring (at high angular momentum). The 'phase transition' between these two solutions may be thought of as being of first order (in the sense that the two competing solutions are different at the phase transition point). The small plasmaring is entropically subdominant to both the plasmaball and the large plasmaring whenever it exists.

This situation appears to lend itself to a description in terms of a Landau diagram, with the entropy given by a function of the (unidentified) order parameter that has two maxima (the plasmaball and the large plasmaring) separated by a single minimum (the small plasmaring). This analogy suggests - and we conjecture that - the small plasmaring is always dynamically unstable, while the plasmaball and large plasmarings are dynamically stable with respect to axisymmetric fluctuations.

An honest verification of our conjecture would require a study of the spectrum of linear fluctuations about our plasmaball and plasmaring solutions, an analysis that we have not carried out. In this subsection, however, we present some evidence for our conjecture, using the 'turning point' stability analysis of [86] (see [87] for discussion and references).

Consider a (not necessarily stable) equilibrium configuration that changes from being stable to unstable under continuous variation. The configurations we apply these considerations to are plasmarings; according to our conjecture these rings are stable to axisymmetric fluctuations when large but become unstable to the same modes when small. At the boundary of stability, the matrix of second derivatives of the entropy with respect to off shell variations (or 'order parameters') of the configuration under question develops a zero eigenvalue. In the neighbourhood of this special point, a small change in the thermodynamic potentials of the solution give rise to a large change in the order parameter along the zero

eigenvalue direction (as such a change is entropically inexpensive). As argued in [88–91], this results in a divergent contribution to the second derivative of the equilibrium entropy as a function of equilibrium thermodynamic quantities (for instance the angular momentum at fixed energy) proportional to the negative inverse of the small eigenvalue.

It follows that a configuration that changes stability has divergent second derivatives of entropy with respect to - say - angular momentum. Moreover the sign of this second derivative is positive in the 'more stable' phase and negative in the 'less stable' phase. Note that the turning point method gives information about the change in the number of unstable directions about a solution, but does not yield information about the absolute number of instabilities. Moreover, this method only links vertical tangents - and not vertical asymptotes - in the graph of the first derivative of entropy with respect to (say) angular momentum vs. angular momentum (a conjugacy diagram) to instabilities, as vertical asymptotes occur at boundaries of equilibrium solution space instead of separating solutions of differing degrees of stability.

The turning point method is useful because it yields information about stability properties, with respect to off shell fluctuations, of phases, using information only about on shell variations. It is especially useful in the study of nonextensive systems like black holes, for which negative specific heats do not necessarily imply dynamical instability (note that we're working with the microcanonical ensemble, unlike the grand-canonical considerations of [92]). This method has been used to study the stability of black rings in 5 dimensions [87, 93]; it suggests that small black rings are always unstable, while large black rings are more stable in that context. This result corroborates the explicit linear fluctuation analysis about the flat space black rings [84].

We now proceed to apply the turning point method to our plasmarings. quantities β and ψ via

$$\mathrm{d}\widetilde{S} = \beta\,\mathrm{d}\widetilde{E} + \psi\,\mathrm{d}\widetilde{L}. \tag{4.46}$$

One can show that

$$\left(\frac{\partial\beta}{\partial\widetilde{E}}\right)_{\widetilde{L}} = \frac{\frac{\partial(\beta,\widetilde{L})}{\partial(v_{\mathrm{o}},v_{\mathrm{i}})}}{\frac{\partial(\widetilde{E},\widetilde{L})}{\partial(v_{\mathrm{o}},v_{\mathrm{i}})}}, \qquad \left(\frac{\partial\psi}{\partial\widetilde{L}}\right)_{\widetilde{E}} = \frac{\frac{\partial(\widetilde{E},\psi)}{\partial(v_{\mathrm{o}},v_{\mathrm{i}})}}{\frac{\partial(\widetilde{E},\widetilde{L})}{\partial(v_{\mathrm{o}},v_{\mathrm{i}})}}. \tag{4.47}$$

Therefore, one would expect a vertical tangent to occur at the small-ring/large-ring boundary as discussed in (4.40).

In fig.4.9 we have plotted ψ against angular momentum at fixed energy for our ring solutions. This graph has a single turning point, precisely at the point at which the large ring turns into a small ring. The slope of the curve turns from positive (for the large ring) to negative (for the small ring) in upon passing through the turning point, consistent with our conjecture about the stability properties of plasmarings. More generally, fig.4.9 is qualitatively similar to the equivalent graph of [87, fig.6(b)] for black hole and black rings in flat 5 dimensional space, except that the large black ring curves back down as we increase $\widetilde{L}$. This difference has no impact on stability analysis, as the turning point method links instabilities to vertical tangents rather than horizontal tangents (even though a heat capacity/susceptibility changes sign as one crosses a horizontal tangent).

In conclusion, the turning point method indicates that the small ring has an additional instability as compared to the large ring. Note that it is perfectly possible that both

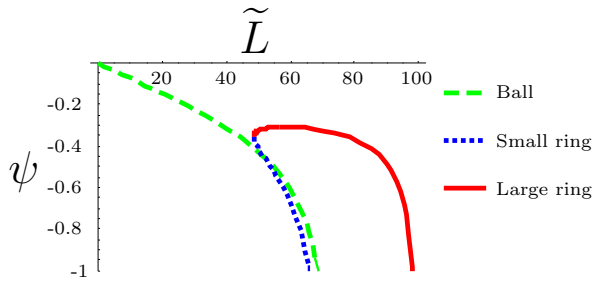

Figure 4.9: Conjugacy diagram: ψ as a function of angular momentum, $\widetilde{L}$ for fixed energy, $\widetilde{E} = 40$.

the large and the small ring are unstable, for example to fluctuations that break rotational symmetry.

4.4 Discussion

In this chapter we have emphasised that the AdS/CFT correspondence implies a duality between nonsingular classical gravitational solutions with horizons, and solutions to the boundary equations of fluid dynamics. This connection has previously been utilised by several authors to obtain gravitational predictions for various fluid viscosities and conductivities (see, for instance, [25] and references therein). The new element in our work is the incorporation of boundaries separating the fluid from the vacuum into the Navier-Stokes equations. This feature (which relies on the explicit gravitational construction of the domain wall in [50]) allowed us to study stationary *finite energy* lumps of plasma, which are dual to localised black holes and black rings in the bulk.

All our work (and easily imagined generalisations) apply to confining field theories. Stationary black holes in such backgrounds sit at the IR ends of the geometry; the boundary shadow of such black holes is a lump of deconfined fluid of size $R + \mathcal{O}(\Lambda_{\rm gap}^{-1})$. The fluid dynamic equations accurately describe such lumps only when $R \gg \Lambda_{\rm gap}^{-1}$, in the same limit the fluid yields an approximately local representation of the horizon. Consequently, the AdS/CFT correspondence provides an approximately local fluid description of horizon dynamics in the long wavelength limit.

All the specific results of this chapter are based on the equations of state (4.7), which are valid for the high temperature phase of Scherk-Schwarz compactified conformal field theories (dual to gravity in Scherk-Schwarz compactified AdS space). However the only qualitative feature of this equation of state that was important for the existence of the solutions of this chapter is that the fluid pressure vanishes at finite energy density. As discussed is §4.3.2, our solutions are only valid for temperature close to this critical temperature. As a consequence such solutions 'sample' only the fluid equation of state only in the neighbourhood around the zero pressure point, and so would exist in any fluid whose pressure vanishes at finite energy density.

Our results suggest several directions for future research. It would be interesting to

analyse the stability of small fluctuations about the solutions presented in this chapter. As we have mentioned in §4.3.5, we expect the small ring to be unstable to axisymmetric fluid fluctuations, while we expect the ball and the large ring to be stable to such fluctuations. However, it is quite possible that such an analysis would reveal that the large ring solutions of this chapter have a Plateau-Rayleigh type instability that maps to Gregory-Laflamme instabilities (see also [29])[6] of the dual bulk solutions.

Although we have not mentioned this in the text, there exists a scaling limit in which the thin plasmarings solutions simplify greatly.[7] In this limit ($\widetilde{\Omega} \to 0$ with $v_{\rm i}$ fixed), the 3D plasmaring reduces to a straight strip of moving fluid. The fluid pressure vanishes on this strip, and the fluid velocity is constant across the strip (more precisely $v_{\rm o} = v_{\rm i} + \frac{1-v_{\rm i}^2}{2v_{\rm i}^2}\widetilde{\Omega} + \mathcal{O}(\widetilde{\Omega}^2)$ so that $\tilde{r}_{\rm o} - \tilde{r}_{\rm i} = \frac{1-v_{\rm i}^2}{2v_{\rm i}^2} + \mathcal{O}(\widetilde{\Omega})$). Similarly, there should exist scaling limit under which the 4 dimensional plasmaring reduces to an infinite stationary cylinder, with fluid flow along the axis. Various dynamical properties of large rings (e.g. the potential Gregory-Laflamme type instability alluded to in the previous paragraph) will probably prove easiest to study in this scaling limit. We will present an analysis of the fluctuations of these solutions in Ch.5.

In five dimensional gravity there are a number of interesting solutions with disconnected horizons, such as black saturns [94], with a black hole surrounded by a black ring, and di-rings [95–98]. These solutions play a significant role in the phase diagram [99]. We note that the construction of such solutions in fluid mechanics is trivial – disconnected lumps of plasma do not affect each other at all. This may sound surprising from the gravitational perspective, as one would expect black holes to attract each other. However, in the AdS soliton background the spectrum of the graviton has a gap $\Lambda_{\rm gap} \sim \xi^{-1}$. Therefore one would expect the gravitational attraction to die off exponentially rather than the usual power law, $\mathrm{e}^{-\Lambda_{\rm gap} r} \sim \mathrm{e}^{-r/\xi}$. As the surface tension approximations is only valid when the separation of these lumps of plasma is much larger than the surface thickness, $r \gg \xi$, the gravitational attraction would be negligible.

One issue concerning saturns is thermal equilibrium between the components [99]. This would require the temperature and angular velocity of the components to be equal (see also [100]). It was pointed out in [100] that such solutions do not exist in our framework – the temperature and angular velocity determine the outer radius of the ball/ring components in exactly the same way (see (4.22) and (4.24)) so the components would have to overlap. However, demanding thermal equilibrium between the disconnected components is only reasonable when the time scale of energy/angular momentum exchange between the components is much shorter than the rate of Hawking leakage to infinity. This limit may not be compatible with the demand that the separation of the components is much larger than the surface thickness.

[6] We thank T. Wiseman for suggesting this.

[7] We thank T. Wiseman again for pointing this out to us.

Chapter 5

The stability of plasmarings and strings in 2+1 dimensions

In this chapter we will study small fluctuations about the plsamaball and plasma ring solutions discussed in Ch.4, warming up with a study of the fluctuations of the 2+1 dimensional plasmastring – an infinite strip of deconfined plasma surrounded be the confined phase.

Of particular interest are fluctuations whose frequency have a positive imaginary part. As mentioned in §1.1, the question of instabilities of extended black objects has been one of the most controversial issues in general relativity, in particular the question of their endpoint (see [40] for a review). The difficult nature of these questions in the gravitational setting leads us to see if we can get any insight into these questions using our holographic fluid mechanics approach. There is a well known instability in fluid mechanics, the Plateau-Rayleigh instability, for a tube of fluid to split into droplets. Most of the previous discussion has been for non-relativistic incompressible fluids, for which it boils down to minimising surface area at fixed volume. In our situation, the fluid is very much compressible and relativistic corrections could be significant, so we will perform the analysis anew.

We will only be working at the linearised level, so we will not be able to answer any questions regarding the endpoint of any instabilities, we will only be able to see if the instabilities exist. It is worth noting that, when the fluid is water, the issue of the endpoint of the Plateau-Rayleigh instability was settled experimentally by Savart. We have all seen a stream of water falling from a tap split into droplets, however one might worry that there is a thin neck of water connecting the droplets that one fails to see. Savart ruled this out by quickly flicking "a narrow metal object" (probably his sword) between the droplets and seeing if it was wet afterwards. As it came out dry, he concluded that there was no such neck. This is a remarkably simple way of arguing that the evolution of black strings will lead to a naked singularity!

We will also be restricting attention to fluctuations for which ω^2 is real, i.e. the frequency has either real or imaginary parts but not both. Studying complex frequencies would require solving the real and imaginary parts of our equations simultaneously, which would require much more work.

In addition, we will also be ignoring the dissipative part of the stress tensor (2.13).

This is common in elementary treatments of the Plateau-Rayleigh instability [101] and should be a reasonable approximation for low enough frequencies. In any case, one would only expect dissipation to slow down instabilities and not create them. Note that when we keep only the perfect fluid part of the stress tensor, (2.25) reduces to (2.31)

$$\mathcal{P}|_{\text{surface}} = \sigma\Theta. \tag{5.1}$$

This is slightly different to the situation of (2.31). In that case there was no time dependence, so Θ could be interpreted as a spatial intrinsic curvature. In this case we do have time dependence, so Θ is a space-time extrinsic curvature.

When it is simply a matter of minimising surface area, the Plateau-Rayleigh instability does not exist in 2+1 dimensions. For a wavy fluctuation in higher dimensions one can compensate for the increase in surface area due to a wavy line being longer than a straight line with the decrease in surface area due to the smaller radius of the tube in the trough of the wave. In 2+1 dimensions one only has the increase in surface area due to a wavy line being longer than a straight line. As our fluid is compressible, this reasoning cannot be taken over directly, however we will find that all fluctuations are stable in §5.2.

In §4.3.5, we presented a thermodynamic argument that suggested that the ball and large ring are stable to axisymmetric fluctuations, whereas the small ring is unstable, much like their asymptotically flat gravitational counterparts. This is almost confirmed in §5.3, we find no axisymmetric instabilities for the ball and large ring and we do find an axisymmetric instability for the small ring. However, this instability does not appear exactly where the large ring and small ring meet. We do not see any sign of wavy instabilities. A wavy instability with complex frequency was found for the plasmaball in [102], which was missed by our restriction to pure real or pure imaginary frequencies. We note that the usual argument that there must be a zero mode must occur when the instability develops doesn't apply to complex frequencies, so their conclusion that there is a branch of lobed configurations need not be true.

The plan of this chapter is as follows: In §5.1, we collect some definitions for the thermodynamic properties of a generic fluid that is close to a first order deconfinement phase transition that will be useful in §5.2, where we look at the stability of the plasmastring in 2+1 dimensions. In that section we will consider arbitrary equations of state that have first order deconfinement phase transitions as well as the Scherk-Schwarz black-brane equations of state considered previously (4.8). In §5.3 we will look at the fluctuations of the plasmaball and plasma ring solutions discussed in Ch.4.

5.1 Thermodynamics near the phase transition

In §5.2, we will look at infinitesimal fluctuations of a generic fluid that is at the temperature of its first order deconfinement phase transition. It will be useful to collect a few formulae describing the thermodynamics close to the phase transition here.

Consider a large N confining gauge theory with a first order deconfining phase transition. As the free energy of the deconfined phase is of order N^2 compared to the confined phase, the phase transition occurs when the free energy of the deconfined phase

vanishes to leading order in N. At this temperature $\mathcal{T}_c$ (see (2.2)):

$$\mathcal{P} = 0, \qquad \rho = \rho_c, \qquad s = s_c = \frac{\rho_c}{\mathcal{T}_c}. \tag{5.2}$$

For a small deviation, $\mathcal{T} = \mathcal{T}_c(1 + \delta\tau)$,

$$\mathcal{P} = \rho_c\,\delta\tau + \mathcal{O}(\delta\tau^2), \qquad \rho = \rho_c + C\,\mathcal{T}_c\,\delta\tau + \mathcal{O}(\delta\tau^2), \qquad s = \frac{\rho_c}{\mathcal{T}_c} + C\,\delta\tau + \mathcal{O}(\delta\tau^2), \tag{5.3}$$

where $C = \mathcal{T}_c\, s'(\mathcal{T}_c)$ is the heat capacity at the critical temperature. We also define the speed of sound

$$c_s^2 = \frac{\rho_c}{C\mathcal{T}_c}. \tag{5.4}$$

For thermodynamically stable fluids, with $C > 0$, c_s is real. For unstable fluids, with $C < 0$, c_s is imaginary.

The fluids we consider in §5.2.2 and §5.3, constructed from a Scherk-Schwarz compactification of a strongly coupled 4 dimensional conformal theory, have equations of state of the given by (4.8). With this equation of state

$$\rho_c = 4\alpha\mathcal{T}_c{}^3, \qquad C = 12\alpha\mathcal{T}_c{}^2, \qquad c_s = \frac{1}{\sqrt{3}}. \tag{5.5}$$

5.2 Plasmastring in 2+1 dimensions

In this section we will study the stability of a strip of plasma of width W. When the extended direction is infinite, this has topology $B^1 \times \mathbb{R}$. Following the usual circle-fibration method, the dual black object has topology $S^2 \times \mathbb{R}$, i.e. it is a black string.

We work in 2+1 dimensions with one direction compactified, $y \sim y + 2\pi l$. We study the stability of the plasmastring: a strip of plasma that wraps the y direction and fills $0 < x < W$. We assume that $l, W \gg l_{\rm mfp}, \xi$. The fluid and surfaces are described by

$$\begin{aligned} f_0 &= x, & f_1 &= W - x, \\ u^\mu &= (1,0,0) & \mathcal{T} &= \mathcal{T}_c. \end{aligned} \tag{5.6}$$

5.2.1 Thermodynamics

In this section, we compare the thermodynamics of the plasmastring to an array of n plasmaballs of radius R. In particular, we ask which has the larger entropy at fixed energy.

Note that there are no static wavy strings in 2+1 dimensions. For a static fluid, the temperature and velocity are constant and the dissipative part of the stress tensor vanishes. This means that, using (2.31) as a boundary condition, we see that the surface must have constant curvature. In two dimensions, the only surface of constant curvature is a circle (or a line).

From (2.31), we see that the plasmastring must have zero pressure, therefore $\mathcal{T} = \mathcal{T}_c$. This means

$$\begin{aligned} E_{\text{string}} &= 8\pi\alpha{\mathcal{T}_c}^3 Wl + 4\pi\sigma l = 8\pi\alpha{\mathcal{T}_c}^3(Wl + 2\xi l), \\ S_{\text{string}} &= 8\pi\alpha{\mathcal{T}_c}^2 Wl. \end{aligned} \tag{5.7}$$

For the balls, (2.31) gives

$$\mathcal{P} = \frac{\alpha}{\mathcal{T}_c}\left(\mathcal{T}^4 - {\mathcal{T}_c}^4\right) = \frac{\sigma}{R} \quad \Longrightarrow \mathcal{T}^4 = {\mathcal{T}_c}^4\left(1 + \frac{4\xi}{R}\right),$$

therefore

$$\begin{aligned} E_{\text{ball}} &= \frac{\alpha}{\mathcal{T}_c}\left(3\mathcal{T}^4 + {\mathcal{T}_c}^4\right) n\pi R^2 + 2n\pi\sigma R = 4n\pi\alpha{\mathcal{T}_c}^3(R^2 + 5\xi R), \\ S_{\text{ball}} &= 4\frac{\alpha}{\mathcal{T}_c}\mathcal{T}^3 n\pi R^2 = 4n\pi\alpha{\mathcal{T}_c}^2\left(R + 4\xi\right)^{3/4} R^{5/4}. \end{aligned} \tag{5.8}$$

Equating the energies determines the radius of the ball

$$R = \sqrt{\frac{2Wl + 4\xi l}{n} + \frac{25\xi^2}{4}} - \frac{5\xi}{2}. \tag{5.9}$$

Introducing variables $w = W/l$ and $\epsilon = \xi/l$, the entropy difference is

$$\begin{aligned} \frac{S_{\text{ball}} - S_{\text{string}}}{4\pi\alpha{\mathcal{T}_c}^2 l^2} &= n\left(\sqrt{\frac{2w + 4\epsilon}{n} + \frac{25\epsilon^2}{4}} - \frac{5\epsilon}{2}\right)^{5/4}\left(\sqrt{\frac{2w + 4\epsilon}{n} + \frac{25\epsilon^2}{4}} + \frac{3\epsilon}{2}\right)^{3/4} - 2w \\ &= 2\epsilon\left(2 - \sqrt{2nw}\right) + \mathcal{O}\left(\epsilon^2\right). \end{aligned} \tag{5.10}$$

We see that, for $w > 2$ the plasmastring is entropically favoured, whereas for $w < 2$ a single plasmaball is preferred. An array of n balls becomes preferable to a string when $w < 2/n$, though it is always preferable to have $n = 1$.

This discussion was for the microcanonical ensemble. For the canonical ensemble, the corresponding question is trivial: we cannot put the string and the ball at the same temperature, as the string always has $\mathcal{T} = \mathcal{T}_c$ and the ball has $\mathcal{T} > \mathcal{T}_c$.

5.2.2 Fluctuations

We now turn to a time-dependent analysis of small fluctuations of the plasmastring. We will see if the frequency these fluctuations can have positive imaginary part, corresponding to instabilities.

We work to fist order in small fluctuations of the form

$$\begin{aligned} f_0 &= x - \mathrm{e}^{-\mathrm{i}\omega t + \mathrm{i}k_y y}\delta x_0, & f_1 &= W + \mathrm{e}^{-\mathrm{i}\omega t + \mathrm{i}k_y y}\delta x_1 - x, \\ u^\mu &= \left(1, \mathrm{e}^{-\mathrm{i}\omega t + \mathrm{i}k_y y}\delta u(x), \mathrm{e}^{-\mathrm{i}\omega t + \mathrm{i}k_y y}\delta v(x)\right) & \mathcal{T} &= \mathcal{T}_c\left(1 + \mathrm{e}^{-\mathrm{i}\omega t + \mathrm{i}k_y y}\delta\tau(x)\right), \end{aligned} \tag{5.11}$$

where $k_y = n/l$. To first order, the normalisation $u^2 = -1$ is maintained.

Ignoring dissipative terms, to first order in the fluctuations, we have

$$\begin{aligned} T^{\mu\nu}_{\text{perfect}} &= \begin{pmatrix} \rho_{\text{c}} & 0 & 0 \\ 0 & 0 & 0 \\ 0 & 0 & 0 \end{pmatrix} + \begin{pmatrix} c_{\text{s}}^{-2}\delta\tau(x) & \delta u(x) & \delta v(x) \\ \delta u(x) & \delta\tau(x) & 0 \\ \delta v(x) & 0 & \delta\tau(x) \end{pmatrix} \rho_{\text{c}} \mathrm{e}^{-\mathrm{i}\omega t + \mathrm{i}k_y y}, \\ \nabla_\mu T^{\mu\nu}_{\text{perfect}} &= \begin{pmatrix} \mathrm{i}k_y\delta v(x) - \mathrm{i}c_{\text{s}}^{-2}\omega\delta\tau(x) + \delta u'(x) \\ \delta\tau'(x) - \mathrm{i}\omega\delta u(x) \\ -\mathrm{i}(\omega\delta v(x) - k_y\delta\tau(x)) \end{pmatrix} \rho_{\text{c}} \mathrm{e}^{-\mathrm{i}\omega t + \mathrm{i}k_y y}. \end{aligned} \tag{5.12}$$

So, to zeroth order in l_{mfp}, (2.3) is solved by

$$\begin{aligned} \delta\tau(x) &= \mathrm{e}^{\mathrm{i}k_x x}\delta\tau_+ + \mathrm{e}^{-\mathrm{i}k_x x}\delta\tau_-, \\ \delta u(x) &= \frac{k_x}{\omega}\left(\mathrm{e}^{\mathrm{i}k_x x}\delta\tau_+ - \mathrm{e}^{-\mathrm{i}k_x x}\delta\tau_-\right), \qquad \text{where} \quad k = \sqrt{\frac{\omega^2}{c_{\text{s}}^2} - k_y^2}. \\ \delta v(x) &= \frac{k_y}{\omega}\left(\mathrm{e}^{\mathrm{i}k_x x}\delta\tau_+ + \mathrm{e}^{-\mathrm{i}k_x x}\delta\tau_-\right), \end{aligned} \tag{5.13}$$

Using the notation of (2.27), the boundary conditions (2.20) and (5.1), to first order in the fluctuations, become

$$\begin{aligned} u^\mu\partial_\mu f_0\Big|_{f_0=0} &= \left[\mathrm{i}\omega\delta x_0 + \frac{k_x}{\omega}(\delta\tau_+ - \delta\tau_-)\right]\mathrm{e}^{-\mathrm{i}\omega t + \mathrm{i}k_y y}, \\ \mathcal{P} - \sigma\Theta\Big|_{f_0=0} &= \left[\xi(k_y^2 - \omega^2)\delta x_0 + (\delta\tau_+ + \delta\tau_-)\right]\rho_{\text{c}}\mathrm{e}^{-\mathrm{i}\omega t + \mathrm{i}k_y y}, \\ u^\mu\partial_\mu f_1\Big|_{f_1=0} &= \left[-\mathrm{i}\omega\delta x_1 - \frac{k_x}{\omega}(\mathrm{e}^{\mathrm{i}k_x W}\delta\tau_+ - \mathrm{e}^{-\mathrm{i}k_x W}\delta\tau_-)\right]\mathrm{e}^{-\mathrm{i}\omega t + \mathrm{i}k_y y}, \\ \mathcal{P} - \sigma\Theta\Big|_{f_1=0} &= \left[\xi(k_y^2 - \omega^2)\delta x_1 - (\mathrm{e}^{\mathrm{i}k_x W}\delta\tau_+ + \mathrm{e}^{-\mathrm{i}k_x W}\delta\tau_-)\right]\rho_{\text{c}}\mathrm{e}^{-\mathrm{i}\omega t + \mathrm{i}k_y y}. \end{aligned} \tag{5.14}$$

We can eliminate $\delta\tau_\pm$

$$\delta\tau_+ = \left[\frac{\xi k_x(\omega^2 - k_y^2) - \mathrm{i}\omega^2}{2k_x}\right]\delta x_0, \quad \delta\tau_- = \left[\frac{\xi k_x(\omega^2 - k_y^2) + \mathrm{i}\omega^2}{2k_x}\right]\delta x_0 \tag{5.15}$$

leaving

$$\begin{aligned} \left[\frac{\xi k_x(k_y^2 - \omega^2)}{\omega}\sin(k_x W) + \omega\cos(k_x W)\right]\delta x_0 \quad &- \quad \omega\,\delta x_1 = 0 \\ \left[\xi(k_y^2 - \omega^2)\cos(k_x W) - \frac{\omega^2}{k_x}\sin(k_x W)\right]\delta x_0 \quad &+ \quad \xi(k_y^2 - \omega^2)\,\delta x_1 = 0 \end{aligned} \tag{5.16}$$

which has nontrivial solutions when

$$2\xi k_x\omega^2(k_y^2 - \omega^2)\cos(k_x W) + \left[\xi^2 k_x^2(k_y^2 - \omega^2)^2 - \omega^4\right]\sin(k_x W) = 0. \tag{5.17}$$

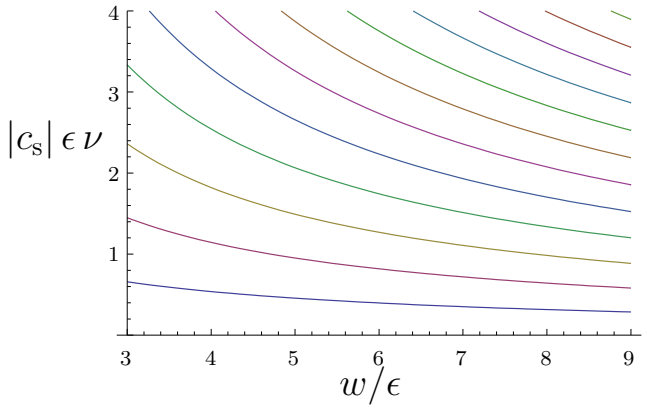

Figure 5.1: Values of ν vs. w for unstable homogenous modes.

Note that there is always a trivial solution with $k_y = \omega = 0$. This has $\delta\tau(x) = \delta u(x) = \delta v(x) = 0$ and δx_0, δx_1 arbitrary. This just corresponds to changing which static solution we're perturbing from. We will ignore this solution from now on.

We will now look for unstable modes (i.e. with $\omega = \mathrm{i}\nu/l$, $\nu > 0$) in two special cases: $k_y = 0$ with c_s^2 arbitrary; and k_y arbitrary with $c_s^2 = 1/3$ from (5.5).

Homogeneous mode, arbitrary equation of state

In this section, we will look at modes that are homogeneous in the y direction, i.e. we set $k_y = 0$, but we leave the equation of state (that appears via c_s^2) arbitrary. We look for unstable modes, i.e. we take (5.17), substitute k from (5.13) and look for solutions of the form $\omega = \mathrm{i}\nu/l$, $\nu > 0$:

$$2c_s\epsilon\nu\cosh\left(\frac{\nu w}{c_s}\right) + \left(c_s^2 + \epsilon^2\nu^2\right)\sinh\left(\frac{\nu w}{c_s}\right) = 0. \tag{5.18}$$

For thermodynamically stable fluids with $C > 0$, there are no real solutions to this equation, as both terms have the same sign. For thermodynamically unstable fluids with $C < 0$, we have

$$2\,|c_s|\,\epsilon\nu\cos\left(\frac{\nu w}{|c_s|}\right) + \left(|c_s|^2 - \epsilon^2\nu^2\right)\sin\left(\frac{\nu w}{|c_s|}\right) = 0. \tag{5.19}$$

We plot some of the roots in fig.5.1. Note that the regime of validity is $w/\epsilon \gg 1$ and $\epsilon\nu \ll 1$, which corresponds to the bottom right of the graph.

The fact that thermodynamically stable strings are mechanically stable and thermodynamically unstable strings are mechanically unstable agrees with the Gubser-Mitra conjecture [77, 103]. This instability is essentially due to the unstable sound mode, as pointed out in [104] this occurs when the heat capacity is negative.

Wavy modes, black brane equation of state

In this section, we will look at modes that are wavy in the y direction, i.e. we allow $k_y \neq 0$, but we use the special equation of state (4.8), i.e. we set $c_{\rm s}^2 = 1/3$ as in (5.5). We look for unstable modes, i.e. we take (5.17), substitute k_x from (5.13), $k_y = n/l$ and look for solutions of the form $\omega = {\rm i}\nu/l$, $\nu > 0$. We also use the notation of (2.27) and (5.10):

$$2\epsilon\,\nu^2(\nu^2+n^2)\sqrt{3\nu^2+n^2}\cosh\left(w\sqrt{3\nu^2+n^2}\right) + \left[\nu^4+\epsilon^2(\nu^2+n^2)^2(3\nu^2+n^2)\right]\sinh\left(w\sqrt{3\nu^2+n^2}\right) = 0, \quad (5.20)$$

which has no real solutions.

Note that this does not mean that the dual black string is stable. We have been restricting attention to a particular subset of fluctuations — those that do not involve the Scerk-Schwarz circle — as all others are outside the regime of validity of fluid mechanics. This only tells us that any Gregory-Laflamme instabilities of these black strings must involve the Scherk-Schwarz circle.

5.3 Plasmaballs and plasmarings

In this section we will apply the methods of §5.2.2 to the plasmaball and plasmaring solutions of Ch.4. In §4.3.5, a turning point analysis, along the lines of [87, 93], suggested that the small ring is unstable to an axisymmetric fluctuation. The point where the large ring turns into the small ring, where we expect this instability to develop, can be found by setting the jacobian in (4.40) to zero. We will look for such an instability in §5.3.1. In flat space, black rings with the radius of the S^1 much larger than the S^2 are expected to have non-axisymmetric instabilities [84], as they start to look like boosted black strings. As we saw above, our plasmastrings do not have these instabilities in 2+1 dimensions, so this reasoning does not follow through, but we will look for such instabilities in §5.3.1.

We use coordinates (t, r, ϕ)

$$ds^2 = -dt^2 + dr^2 + r^2 d\phi^2.$$

The interior of the fluid in the unperturbed solution is described by

$$\mathcal{T} = \gamma T, \quad u^\mu = \gamma(1, 0, \Omega), \quad \gamma = (1-\Omega^2 r^2)^{-1/2}. \quad (5.21)$$

The ball and ring have outer surfaces at $r = r_{\rm o}$. The ring also has an inner surface at $r = r_{\rm i}$. These parameters are related to T and Ω by (4.25).

5.3.1 Fluctuations

We look at fluctuations of the form

$$\begin{aligned}
\mathcal{T} &= \gamma T\left(1+\delta\tau(v)e^{-i\omega t+in\phi}\right),\\
u^\mu &= \gamma(1,0,\Omega) + \gamma(\Omega^2 r^2\delta v(v), i\delta u(v), \Omega\delta v(v))\, e^{-i\omega t+in\phi},\\
f_{\rm o} &= r_{\rm o} - r + \delta r_{\rm o}\, e^{-i\omega t+in\phi},\\
f_{\rm i} &= r - r_{\rm i} - \delta r_{\rm i}\, e^{-i\omega t+in\phi}.
\end{aligned} \quad (5.22)$$

It is convenient to define

$$\delta\tilde{r}_{\rm o} = \frac{\delta r_{\rm o}}{\xi'}, \quad \delta\tilde{r}_{\rm i} = \frac{\delta r_{\rm i}}{\xi'}, \quad \widetilde{\omega} = \xi'\omega, \quad \varpi = \omega - n\Omega, \quad \widetilde{\varpi} = \widetilde{\omega} - n\widetilde{\Omega}. \tag{5.23}$$

The equation of motion (2.3), to first order in the fluctuations and zeroth order in $l_{\rm mfp}$, gives

$$\nabla_\mu T^{\mu\nu}_{\rm perfect} = \frac{4{\rm i}\alpha\mathcal{T}^4}{\mathcal{T}_{\rm c}}\gamma^2 {\rm e}^{-{\rm i}\omega t+{\rm i}n\phi}\times \begin{pmatrix} [\frac{n\Omega}{\gamma^2} - 2v^2\varpi]\delta v(v) + [\frac{n\Omega-(4\gamma^2-1)\varpi}{\gamma^2}]\delta\tau(v) + \frac{(6\gamma^2-5)}{v}\Omega\delta u(v) + \Omega\delta u'(v) \\ 2{\rm i}v\Omega\delta v(v) - {\rm i}\varpi\delta u(v) - {\rm i}\frac{\Omega}{\gamma^2}\delta\tau'(v) \\ [\frac{n\Omega-(2\gamma^2-1)\varpi}{\gamma^2}]\Omega\delta v(v) + [\frac{n\Omega}{\gamma^2 v^2} - 4\varpi]\Omega\delta\tau(v) + \frac{3(2\gamma^2-1)}{v}\Omega^2\delta u(v) + \Omega^2\delta u'(v) \end{pmatrix}. \tag{5.24}$$

We can eliminate $\delta v(v)$

$$\delta v(v) = \frac{(n\Omega - \gamma^2 v^2\varpi)\delta\tau(v) + 2v\gamma^4\Omega\delta u(v)}{\varpi\gamma^2 v^2}, \tag{5.25}$$

leaving

$$\frac{\rm d}{{\rm d}v}\begin{pmatrix}\delta\tau\\ \delta u\end{pmatrix} = \begin{pmatrix} \frac{2}{v\widetilde{\varpi}}\left[n\widetilde{\Omega} - \gamma^2 v^2\widetilde{\varpi}\right] & \frac{\gamma^2}{\Omega\widetilde{\varpi}}\left[4\gamma^2\widetilde{\Omega}^2 - \widetilde{\varpi}^2\right] \\ \frac{\gamma^2(3\gamma^2-2)\widetilde{\varpi}^2 - [n\widetilde{\Omega}-\gamma^2 v^2\widetilde{\varpi}]^2}{v^2\gamma^4\widetilde{\Omega}\widetilde{\varpi}} & -\frac{1}{v\widetilde{\varpi}}\left[(2\gamma^2-1)\widetilde{\varpi} + 2n\widetilde{\Omega}\right] \end{pmatrix}\begin{pmatrix}\delta\tau\\ \delta u\end{pmatrix}. \tag{5.26}$$

The boundary conditions (2.20) and (5.1), to first order in the fluctuations, are

$$\begin{aligned} u^\mu\partial_\mu f_{\rm o}\Big|_{f_{\rm o}=0} &= [\widetilde{\varpi}\,\delta\tilde{r}_{\rm o} + \delta u(v_{\rm o})]\,{\rm i}\gamma_{\rm o}{\rm e}^{-{\rm i}\omega t+{\rm i}n\phi}, \\ \mathcal{P}-\sigma\Theta\Big|_{f_{\rm o}=0} &= \left[\frac{4v_{\rm o}^3\gamma_{\rm o}^2\widetilde{\Omega} + v_{\rm o}^2\widetilde{\omega}^2 - n^2\widetilde{\Omega}^2 + (1+3v_{\rm o}^2)\gamma_{\rm o}^2\widetilde{\Omega}^2}{4v_{\rm o}^2}\,\delta\tilde{r}_{\rm o} + \gamma_{\rm o}^4\widetilde{T}^4\delta\tau(v_{\rm o})\right] \\ &\quad\times\rho_{\rm c}{\rm e}^{-{\rm i}\omega t+{\rm i}n\phi}, \\ u^\mu\partial_\mu f_{\rm i}\Big|_{f_{\rm i}=0} &= [\widetilde{\varpi}\,\delta\tilde{r}_{\rm i} + \delta u(v_{\rm i})]\,{\rm i}\gamma_{\rm i}{\rm e}^{-{\rm i}\omega t+{\rm i}n\phi}, \\ \mathcal{P}-\sigma\Theta\Big|_{f_{\rm i}=0} &= \left[\frac{4v_{\rm i}^3\gamma_{\rm i}^2\widetilde{\Omega} - v_{\rm i}^2\widetilde{\omega}^2 + n^2\widetilde{\Omega}^2 - (1+3v_{\rm i}^2)\gamma_{\rm i}^2\widetilde{\Omega}^2}{4v_{\rm i}^2}\,\delta\tilde{r}_{\rm i} + \gamma_{\rm i}^4\widetilde{T}^4\delta\tau(v_{\rm i})\right] \\ &\quad\times\rho_{\rm c}{\rm e}^{-{\rm i}\omega t+{\rm i}n\phi}. \end{aligned} \tag{5.27}$$

Solving these gives

$$\begin{aligned} \delta\tau(v_{\rm o}) &= \frac{(v_{\rm o}^4 - v_{\rm o}^2)\widetilde{\omega}^2 - 4v_{\rm o}^3\widetilde{\Omega} + (1-v_{\rm o}^2)n^2\widetilde{\Omega}^2 - (1+3v_{\rm o}^2)\widetilde{\Omega}^2}{4v_{\rm o}(1-v_{\rm o}^2)(v_{\rm o}+\widetilde{\Omega})}\,\delta\tilde{r}_{\rm o}, \\ \delta u(v_{\rm o}) &= -\widetilde{\varpi}\,\delta\tilde{r}_{\rm o}, \\ \delta\tau(v_{\rm i}) &= \frac{(v_{\rm i}^2 - v_{\rm i}^4)\widetilde{\omega}^2 - 4v_{\rm i}^3\widetilde{\Omega} - (1-v_{\rm i}^2)n^2\widetilde{\Omega}^2 + (1+3v_{\rm i}^2)\widetilde{\Omega}^2}{4v_{\rm i}(1-v_{\rm i}^2)(v_{\rm i}-\widetilde{\Omega})}\,\delta\tilde{r}_{\rm i} \\ \delta u(v_{\rm i}) &= -\widetilde{\varpi}\,\delta\tilde{r}_{\rm i}. \end{aligned} \tag{5.28}$$

For the ball, we have no boundary conditions at $f_\mathrm{i} = 0$. Instead, we require $\delta u(0) = 0$.

We can write the solution to (5.26) as

$$\begin{pmatrix}\delta\tau\\ \delta u\end{pmatrix} = \delta\tau(v_\mathrm{o})\begin{pmatrix}\alpha_1(v)\\ \beta_1(v)\end{pmatrix} + \delta u(v_\mathrm{o})\begin{pmatrix}\alpha_2(v)\\ \beta_2(v)\end{pmatrix}, \tag{5.29}$$

where

$$\begin{pmatrix}\alpha_1(v_\mathrm{o})\\ \beta_1(v_\mathrm{o})\end{pmatrix} = \begin{pmatrix}1\\ 0\end{pmatrix}, \qquad \begin{pmatrix}\alpha_2(v_\mathrm{o})\\ \beta_2(v_\mathrm{o})\end{pmatrix} = \begin{pmatrix}0\\ 1\end{pmatrix}, \tag{5.30}$$

which also solves the boundary conditions (5.28) at $v = v_\mathrm{o}$.

For the ball, the boundary condition at $v = 0$ will have a non-trivial solution when

$$\Delta_\mathrm{ball} \equiv \beta_1(0)\frac{\delta\tau(v_\mathrm{o})}{\delta\tilde{r}_\mathrm{o}} + \beta_2(0)\frac{\delta u(v_\mathrm{o})}{\delta\tilde{r}_\mathrm{o}} = 0. \tag{5.31}$$

For the ring, the boundary conditions at $v = v_\mathrm{i}$ will have a non-trivial solution when

$$\Delta_\mathrm{ring} \equiv \begin{vmatrix}\alpha_1(v_\mathrm{i})\frac{\delta\tau(v_\mathrm{o})}{\delta\tilde{r}_\mathrm{o}} + \alpha_2(v_\mathrm{i})\frac{\delta u(v_\mathrm{o})}{\delta\tilde{r}_\mathrm{o}} & \frac{\delta\tau(v_\mathrm{i})}{\delta\tilde{r}_\mathrm{i}}\\ \beta_1(v_\mathrm{i})\frac{\delta\tau(v_\mathrm{o})}{\delta\tilde{r}_\mathrm{o}} + \beta_2(v_\mathrm{i})\frac{\delta u(v_\mathrm{o})}{\delta\tilde{r}_\mathrm{o}} & \frac{\delta u(v_\mathrm{i})}{\delta\tilde{r}_\mathrm{i}}\end{vmatrix} = 0. \tag{5.32}$$

Axisymmetric modes

In this section, we will concentrate on modes with $n = 0$. There is always a mode at $\widetilde{\omega} = 0$:

$$\begin{aligned}\delta\tau(v) &= A(1-v^2),\\ \delta u(v) &= 0,\\ \delta v(v) &= -A(1-v^2),\end{aligned} \tag{5.33}$$

with (5.28) determining A in terms of $\delta\tilde{r}_\mathrm{o}$. For the ring, $\delta\tilde{r}_\mathrm{i}$ will be determined in terms of $\delta\tilde{r}_\mathrm{o}$. Surprisingly, this does not correspond to changing which solution we expand about. That would be

$$\begin{aligned}\delta\tau(v) &= \frac{\delta\widetilde{T}}{\widetilde{T}} + \frac{v^2}{1-v^2}\frac{\delta\widetilde{\Omega}}{\widetilde{\Omega}},\\ \delta u(v) &= 0,\\ \delta v(v) &= \frac{1}{1-v^2}\frac{\delta\widetilde{\Omega}}{\widetilde{\Omega}}.\end{aligned} \tag{5.34}$$

These are a solution to (5.24), but they do not appear to be the $\widetilde{\omega} \to 0$ limit of fluctuations of the form (5.22).

We can ignore this boring mode by changing variables

$$\delta u(v) = -\widetilde{\omega}\delta\hat{u}(v). \tag{5.35}$$

Now the differential equation is

$$\frac{\mathrm{d}}{\mathrm{d}v}\begin{pmatrix}\delta\tau\\ \delta\hat{u}\end{pmatrix} = \begin{pmatrix}-\frac{2v}{1-v^2} & \frac{(1-v^2)\widetilde{\omega}^2 - 4\widetilde{\Omega}^2}{(1-v^2)^2\widetilde{\Omega}}\\ -\frac{3-v^2}{\widetilde{\Omega}} & -\frac{1+v^2}{v(1-v^2)}\end{pmatrix}\begin{pmatrix}\delta\tau\\ \delta\hat{u}\end{pmatrix}, \tag{5.36}$$

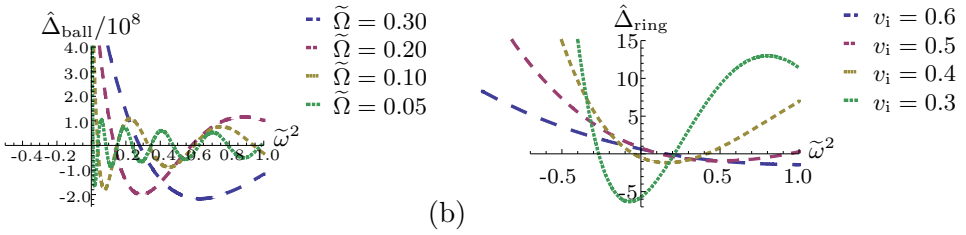

Figure 5.2: Plot of the conditions (5.40) and (5.41) vs. $\widetilde{\omega}^2$ for (a) the ball and (b) the ring with $v_{\rm o} = 0.8$. The fluctuations correspond to positive roots, the unstable modes correspond to negative roots.

and the boundary conditions are

$$\begin{aligned}
\delta\tau(v_{\rm o}) &= \frac{(v_{\rm o}^4 - v_{\rm o}^2)\widetilde{\omega}^2 - 4v_{\rm o}^3\widetilde{\Omega} - (1+3v_{\rm o}^2)\widetilde{\Omega}^2}{4v_{\rm o}(1-v_{\rm o}^2)(v_{\rm o}+\widetilde{\Omega})}\,\delta\tilde{r}_{\rm o}, \\
\delta\hat{u}(v_{\rm o}) &= \delta\tilde{r}_{\rm o}, \\
\delta\tau(v_{\rm i}) &= \frac{(v_{\rm i}^2 - v_{\rm i}^4)\widetilde{\omega}^2 - 4v_{\rm i}^3\widetilde{\Omega} + (1+3v_{\rm i}^2)\widetilde{\Omega}^2}{4v_{\rm i}(1-v_{\rm i}^2)(v_{\rm i}-\widetilde{\Omega})}\,\delta\tilde{r}_{\rm i} \\
\delta\hat{u}(v_{\rm i}) &= \delta\tilde{r}_{\rm i}.
\end{aligned} \tag{5.37}$$

We write the solution to (5.36) as

$$\begin{pmatrix}\delta\tau \\ \delta\hat{u}\end{pmatrix} = \delta\tau(v_{\rm o})\begin{pmatrix}\alpha_1(v) \\ \hat{\beta}_1(v)\end{pmatrix} + \delta u(v_{\rm o})\begin{pmatrix}\alpha_2(v) \\ \hat{\beta}_2(v)\end{pmatrix}, \tag{5.38}$$

where

$$\begin{pmatrix}\alpha_1(v_{\rm o}) \\ \hat{\beta}_1(v_{\rm o})\end{pmatrix} = \begin{pmatrix}1 \\ 0\end{pmatrix}, \qquad \begin{pmatrix}\alpha_2(v_{\rm o}) \\ \hat{\beta}_2(v_{\rm o})\end{pmatrix} = \begin{pmatrix}0 \\ 1\end{pmatrix}, \tag{5.39}$$

which also solves the boundary conditions (5.37) at $v = v_{\rm o}$.

For the ball, the boundary condition at $v = 0$ will have a non-trivial solution when

$$\hat{\Delta}_{\rm ball} \equiv \hat{\beta}_1(0)\frac{\delta\tau(v_{\rm o})}{\delta\tilde{r}_{\rm o}} + \hat{\beta}_2(0)\frac{\delta\hat{u}(v_{\rm o})}{\delta\tilde{r}_{\rm o}} = 0. \tag{5.40}$$

For the ring, the boundary conditions at $v = v_{\rm i}$ will have a non-trivial solution when

$$\hat{\Delta}_{\rm ring} \equiv \det\begin{pmatrix}\alpha_1(v_{\rm i})\frac{\delta\tau(v_{\rm o})}{\delta\tilde{r}_{\rm o}} + \alpha_2(v_{\rm i})\frac{\delta\hat{u}(v_{\rm o})}{\delta\tilde{r}_{\rm o}} & \frac{\delta\tau(v_{\rm i})}{\delta\tilde{r}_{\rm i}} \\ \hat{\beta}_1(v_{\rm i})\frac{\delta\tau(v_{\rm o})}{\delta\tilde{r}_{\rm o}} + \hat{\beta}_2(v_{\rm i})\frac{\delta\hat{u}(v_{\rm o})}{\delta\tilde{r}_{\rm o}} & \frac{\delta\hat{u}(v_{\rm i})}{\delta\tilde{r}_{\rm i}}\end{pmatrix} = 0. \tag{5.41}$$

We plot these two conditions in fig.5.2. We see that the ring has unstable modes for certain values of $(v_{\rm o}, v_{\rm i})$, but not for others. For the ball, we see no signs of any instabilities.

At the point where a new instability develops, we will have an additional zero-mode. We can look for this zero-mode by setting $\widetilde{\omega} = 0$. The solution of (5.36) is

$$\begin{aligned}\delta\tau &= A\left[\frac{v^2+1}{v^2-1}\right] + B\left[\frac{(v^2+1)\log(v)+2}{v^2-1}\right],\\ \delta\hat{u} &= A\left[\frac{2v^3+6v}{4\widetilde{\Omega}}\right] + B\left[\frac{2\log(v)v^4 - v^4 + 6\log(v)v^2 + 8v^2 + 1}{4v\widetilde{\Omega}}\right].\end{aligned} \tag{5.42}$$

The boundary conditions (5.37) at $v = v_{\rm o}$ give

$$\begin{aligned}A &= \frac{4v_{\rm o}^5 + 3\widetilde{\Omega}v_{\rm o}^4 - 28v_{\rm o}^3 - 20\widetilde{\Omega}v_{\rm o}^2 - 2(4v_{\rm o}^3 + 3\widetilde{\Omega}v_{\rm o}^2 + 8v_{\rm o} + 5\widetilde{\Omega})v_{\rm o}^2\log(v_{\rm o}) + \widetilde{\Omega}}{4v_{\rm o}(1-v_{\rm o}^2)^2(v_{\rm o}+\widetilde{\Omega})}\,\widetilde{\Omega}\delta\tilde{r}_{\rm o},\\ B &= \frac{4v_{\rm o}^3 + 3\widetilde{\Omega}v_{\rm o}^2 + 8v_{\rm o} + 5\widetilde{\Omega}}{2(1-v_{\rm o}^2)^2(v_{\rm o}+\widetilde{\Omega})}\,v_{\rm o}\widetilde{\Omega}\delta\tilde{r}_{\rm o}.\end{aligned} \tag{5.43}$$

For the ball, if we try to impose the boundary condition at $v = 0$, we find

$$\lim_{v\to 0}\delta\hat{u} = \frac{v_{\rm o}(4v_{\rm o}^3 + 3\widetilde{\Omega}v_{\rm o}^2 + 8v_{\rm o} + 5\widetilde{\Omega})}{8v(1-v_{\rm o}^2)^2(v_{\rm o}+\widetilde{\Omega})}, \tag{5.44}$$

so the putative new zero-mode doesn't exist.

For the ring, imposing the boundary condition at $v = v_{\rm i}$ gives

$$\begin{aligned}A &= \frac{4v_{\rm i}^5 - 3\widetilde{\Omega}v_{\rm i}^4 - 28v_{\rm i}^3 + 20\widetilde{\Omega}v_{\rm i}^2 - 2(4v_{\rm i}^3 - 3\widetilde{\Omega}v_{\rm i}^2 + 8v_{\rm i} - 5\widetilde{\Omega})v_{\rm i}^2\log(v_{\rm i}) - \widetilde{\Omega}}{4v_{\rm i}(1-v_{\rm i}^2)^2(v_{\rm i}-\widetilde{\Omega})}\,\widetilde{\Omega}\delta\tilde{r}_{\rm i},\\ B &= \frac{4v_{\rm i}^3 - 3\widetilde{\Omega}v_{\rm i}^2 + 8v_{\rm i} - 5\widetilde{\Omega}}{2(1-v_{\rm i}^2)^2(v_{\rm i}-\widetilde{\Omega})}\,v_{\rm i}\widetilde{\Omega}\delta\tilde{r}_{\rm i}.\end{aligned} \tag{5.45}$$

Consistency of this equation and (5.43) for non-trivial $\delta\tilde{r}_{\rm o}$ and $\delta\tilde{r}_{\rm i}$ requires that

$$\begin{aligned}0 &= \frac{A}{\widetilde{\Omega}\delta\tilde{r}_{\rm o}}\frac{B}{\widetilde{\Omega}\delta\tilde{r}_{\rm i}} - \frac{A}{\widetilde{\Omega}\delta\tilde{r}_{\rm i}}\frac{B}{\widetilde{\Omega}\delta\tilde{r}_{\rm o}}\\ &= \frac{v_{\rm o}-v_{\rm i}}{8v_{\rm o}v_{\rm i}(1-v_{\rm o}^2)^4(1-v_{\rm i}^2)^4}\left[X(v_{\rm o},v_{\rm i})\frac{2v_{\rm o}^2v_{\rm i}^2\log(v_{\rm o}/v_{\rm i})}{v_{\rm o}-v_{\rm i}} + Y(v_{\rm o},v_{\rm i})\right]\end{aligned} \tag{5.46}$$

where X and Y are polynomials of degree 12 and 13 respectively.

We see that this is not exactly the same as the place where the small ring turns into the large ring, as discussed near (4.47). However, in fig.5.3, we have plotted $\widetilde{L}$ vs. $\widetilde{E}$ for this zero mode, as well as the existence boundaries for balls and rings. We see that this instability develops very close to that line.

Evaluating the jacobian in (4.40) along the curve where this zero mode exists shows that it is positive there, i.e. this zero mode occurs for the small ring. Looking at fig.5.2, we see that for fixed $v_{\rm o}$ the instability occurs for smaller values of $v_{\rm i}$, i.e. the small rings, and both rings are stable in the small gap between the existence of the zero mode and the large/small ring merger.

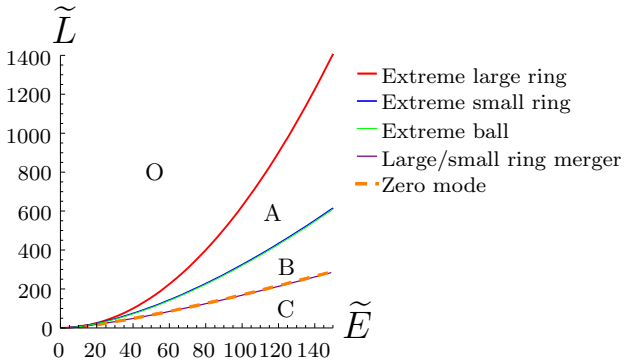

O – no solutions, A – large ring only, B – large ring, small ring, ball, C – ball only.

Figure 5.3: Graph showing $\widetilde{L}$ vs. $\widetilde{E}$ for the axisymmetric zero mode, as well as the existence boundaries for balls and rings.

Wavy modes

Now we will look at modes with ϕ dependance, in particular with $n = 1, 2$.

Things become complicated when we try to look at unstable modes. It seems tha the correct approach is to make ϖ imaginary rather than ω. The former corresponds to modes that rotate around the ball/ring and grow, the latter to modes that simply grow.

When we make ϖ imaginary, the differential equation (5.26) becomes complex. Therefore, the conditions (5.31) and (5.32) become complex. This means that we need two real variables to play with to find solutions, if we simply try to make ϖ imaginary, generically there will be no solutions. We would have to adjust both the real and imaginary parts to find solutions. We will not do that here. An instability at complex $\widetilde{\varpi}$ has been found in [102], but we note that the usual argument that there must be a zero mode must occur when the instability develops doesn't apply to complex frequencies as one can pass from positive to negative imaginary parts without passing through zero.

We verify this in fig.5.4, where we plot the absolute values of the conditions (5.31) and (5.32) vs. $\widetilde{\varpi}^2$ for $n = 1, 2$. We see that there are zeroes for positive $\widetilde{\varpi}^2$, corresponding to oscillating fluctuations, but not for negative $\widetilde{\varpi}^2$, corresponding to instabilities.

5.4 Discussion

We have seen that the 2+1 dimensional plasmastring does not have Plateau-Rayleigh instabilities. A very thorough study of the Plateau-Rayleigh instability for higher dimensional plasmastrings was performed in [105], where the instability was shown to exist. Note that large black strings in AdS do not have the Gregory-Laflamme instability [48, 106–108], whereas their asymptotically flat counterparts do. This fits with the idea that plasmaballs will behave more and more like flat space black holes (and less like AdS black holes) as we increase the number of dimensions, as discussed in §1.3.

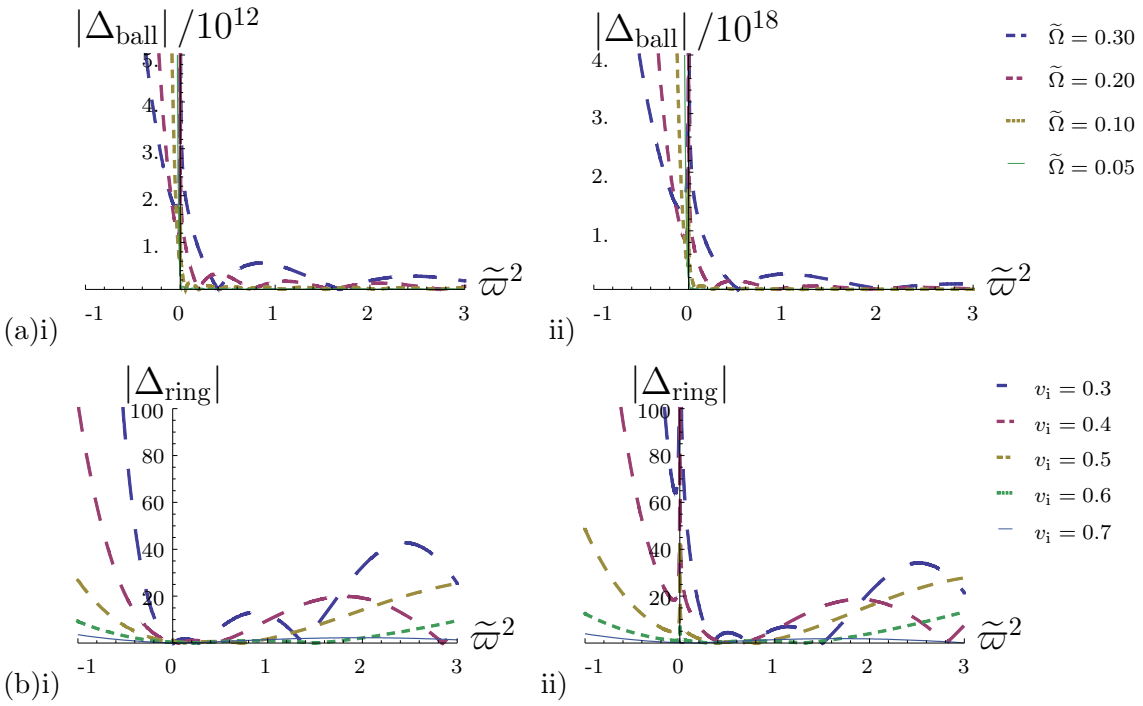

Figure 5.4: Plot of the conditions (a)(5.31) and (b)(5.32) vs. $\widetilde{\varpi}^2$ for (i) $n = 1$ and (ii) $n = 2$ with $v_{\rm o} = 0.8$. Positive roots correspond to fluctuations, negative roots correspond to instabilities.

One interesting direction for further study would be following the instabilities found to their endpoint. This would require numerical simulations, but one would expect these to be much simpler than the corresponding gravitational simulations. Although the surface tension approximation will break down when the tubes pinch off, it is possible that the code may get closer to the pinch without braking down like in the gravitational setting [43, 44] and one might be able to extrapolate to the pinch more reliably and see if it takes place in finite time.

We have also seen that the small plasmarings are unstable with respect to axisymmetric fluctuations, whereas the large plasmarings are stable. This confirms the thermodynamic prediction of §4.3.5. It is still puzzling that the instability does not appear at the exact place predicted thermodynamically, although it appears very close. This could be an artefact of the approximations made – surface tension, neglecting viscosity etc. However, the thermodynamic predictions were made under many of the same approximations and it would be surprising if the precise values of the transport coefficients were relevant for the discrepancy.

Chapter 6

Higher dimensional plasmarings

In this chapter we turn to a consideration of localised plasma configurations in certain massive 4 and 5 dimensional field theories obtained by compactifying related 5 and 6 dimensional CFTs on a Scherk-Schwarz circle. Although the field theories in question are not gauge theories (e.g. the 5 dimensional massive theory could be obtained by compactifying the (0,2) theory on the world volume of an M5 brane on a Scherk-Schwarz circle) they undergo first order 'deconfining' transitions and the high temperature phase of these theories admits a fluid dynamical description. The fluid configurations we will construct are dual to localised black holes and black rings in Scherk-Schwarz compactified AdS_6 and AdS_7 respectively.

The constructions we have described in Ch.4 admit simple generalisations to plasma solutions dual to black holes and black rings in Scherk-Schwarz compactified AdS_6 space. As the qualitative nature of the moduli space of black hole like solutions in six dimensional gravity is poorly understood, this study is of interest. The boundary duals of these objects, in the long wavelength limit, are stationary solutions to the equations of fluid dynamics of a 4 dimensional field theory. In §6.1 we construct such solutions. Our study will be less thorough than our 3 dimensional analysis above; we find solutions analogous to those in 3 dimensions, but we postpone the complete parameterisation and study of the thermodynamic properties of these solutions to future work. It turns out that these solutions occur in two qualitatively distinct classes. The simplest solutions are simply spinning balls of plasma; the fact that these balls spin causes them to flatten out near the 'poles'. As these balls are spun up, their profile begins to 'dip' near the poles (see fig.6.1). As these balls are further spun up, they pinch off at the centre and turn into doughnut shaped rings (see fig.6.1).

As discussed in §1.3, the horizon topology of the black objects dual to the rotating plasmaballs and plasmarings described above, is obtained by fibering the fluid configuration with an S^1 that shrinks to zero at the fluid edges. This procedure yields a horizon topology S^4 for the dual to the rotating plasmaball, and topology $S^3 \times S^1$ for the dual to the plasmaring. As plasmaball and plasmaring configurations appear to exhaust the set of stationary fluid solutions to the equations of fluid dynamics, it follows that arbitrarily large stationary black objects in Scherk-Schwarz compactified AdS_6 all have one of these two horizon topologies. $S^2 \times S^2$ is an example of another topology one could have imagined for black objects in this space; these would have been dual to hollow shells of rotating fluid;

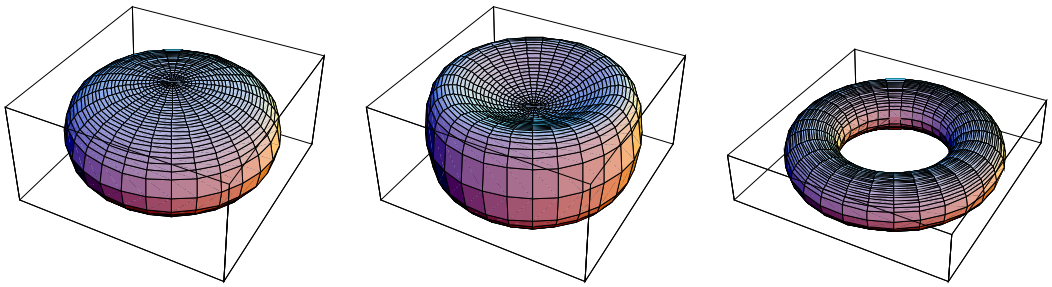

Figure 6.1: Spinning ball and ring solutions.

however, there are no such stationary solutions to the equations of fluid dynamics.

The analysis of four dimensional fluid configurations, described above, demonstrates the power of the fluid dynamical method. In simple contexts, the Navier-Stokes equations are much easier to solve than the full set of Einstein's equations, and rather easily reveal interesting and nontrivial information. It would be interesting to extend our analysis of fluid dynamical models in various directions to obtain information about the moduli space and stability of classes of black solutions in AdS spaces.

An obvious extension would be to move to higher dimensions. In §6.2 we have derived the equations relevant to stationary fluid flow in 5 dimensions, but we leave the study of their solutions (and their higher dimensional counterparts) to future work. A complete analysis of these equations would yield the spectrum of black holes in Scherk-Schwarz compactified AdS_7 spaces, in terms of the fluid dynamics of the deconfined phase of the M5 brane theory on a Scherk-Schwarz circle.

6.1 Four dimensional plasmarings

We now turn to the study of spinning lumps of plasma in four dimensions. As discussed previously, this is dual to the study of black objects in Scherk-Schwarz compactified AdS_6. The equation of state of this fluid is given by (4.7) restricted to $d = 4$.

$$\mathcal{P} = \frac{\alpha}{\mathcal{T}_c}\left(\mathcal{T}^5 - \mathcal{T}_c{}^5\right). \tag{6.1}$$

6.1.1 Equations of motion

In this section we set up the equations of motion of our fluid. We proceed in direct imitation of our analysis of $d = 3$ above. We use the metric

$$\mathrm{d}s^2 = -\mathrm{d}t^2 + \mathrm{d}r^2 + r^2\mathrm{d}\phi^2 + \mathrm{d}z^2\,. \tag{6.2}$$

We choose the origin so that $r = 0$ is the axis of rotation and there is a reflection symmetry in the plane $z = 0$.

For our configurations, $u^\mu = \gamma(1,0,\Omega,0)$ with $\gamma = \left(1-\Omega^2 r^2\right)^{-1/2}$. We describe the upper surface by $f(r,z) = h(r) - z$. Following (2.30), as usual, this leads to the temperature and pressure profile

$$\mathcal{T} = \frac{T}{\sqrt{1-\Omega^2 r^2}}\,, \qquad \mathcal{P} = \frac{\alpha}{\mathcal{T}_{\rm c}}\left(\frac{T^5}{(1-\Omega^2 r^2)^{5/2}} - \mathcal{T}_{\rm c}{}^5\right). \tag{6.3}$$

The extrinsic curvature of the surface is

$$\Theta = \mp \frac{r h'' + h'(1+h'^2)}{r(1+h'^2)^{3/2}} \tag{6.4}$$

where the upper sign refers to the upper ($z > 0$) surface.

We define dimensionless variables as before (with ξ' defined in (4.14))

$$\widetilde{\Omega} = \xi' \Omega\,, \qquad v = \Omega r\,, \qquad \tilde{h}(v) = \Omega h(r)\,, \qquad \widetilde{T} = \frac{T}{\mathcal{T}_{\rm c}} \tag{6.5}$$

The boundary condition (2.31) for an upper surface gives

$$\frac{\widetilde{T}^5}{(1-v^2)^{5/2}} - 1 = -\widetilde{\Omega}\frac{v\tilde{h}'' + \tilde{h}'(1+\tilde{h}'^2)}{v(1+\tilde{h}'^2)^{3/2}}\,. \tag{6.6}$$

This can be integrated once to give

$$\frac{v\tilde{h}'}{\sqrt{1+\tilde{h}'^2}} = -\frac{\widetilde{T}^5}{3\widetilde{\Omega}(1-v^2)^{3/2}} + \frac{v^2}{2\widetilde{\Omega}} + \frac{\mathcal{C}}{\widetilde{\Omega}}\,, \tag{6.7}$$

where $\mathcal{C}$ is an integration constant.

6.1.2 Solutions

Now we will discuss the space of solutions to (6.7). We will find several types of solutions, dual to black objects with different horizon topologies.

The differential equation (6.7) can be written as

$$\frac{\mathrm{d}\tilde{h}}{\mathrm{d}v} = -\frac{2\widetilde{T}^5 - 3(v^2+2\mathcal{C})(1-v^2)^{3/2}}{\sqrt{36\widetilde{\Omega}^2 v^2(1-v^2)^3 - \left[2\widetilde{T}^5 - 3(v^2+2\mathcal{C})(1-v^2)^{3/2}\right]^2}}\,. \tag{6.8}$$

It follows that the outer surface of our plasma configuration is given by

$$\tilde{h}(v) = \int_{v_{\rm o}}^{v} \mathrm{d}x \left(-\frac{2\widetilde{T}^5 - 3(x^2+2\mathcal{C})(1-x^2)^{3/2}}{\sqrt{36\widetilde{\Omega}^2 x^2(1-x^2)^3 - \left[2\widetilde{T}^5 - 3(x^2+2\mathcal{C})(1-x^2)^{3/2}\right]^2}}\right) \tag{6.9}$$

Of course this only makes sense provided

$$6\widetilde{\Omega}x(1-x^2)^{3/2} \geq \left|2\widetilde{T}^5 - 3(x^2+2\mathcal{C})(1-x^2)^{3/2}\right| \quad \forall\, x \in (v, v_{\rm o}). \tag{6.10}$$

Inner boundaries to the plasma configuration (if they exist) are described by a function $f(r,z) = z - h(r)$. The equivalent of (6.8), with a new integration constant $\mathcal{D}$ replacing $\mathcal{C}$, is

$$\frac{\mathrm{d}\tilde{h}}{\mathrm{d}v} = \frac{2\widetilde{T}^5 - 3(v^2+2\mathcal{D})(1-v^2)^{3/2}}{\sqrt{36\widetilde{\Omega}^2 v^2(1-v^2)^3 - \left[2\widetilde{T}^5 - 3(v^2+2\mathcal{D})(1-v^2)^{3/2}\right]^2}}\,. \tag{6.11}$$

The profiles of such boundaries may be obtained by integrating the equation above.

Even before doing any analysis, we will find it useful to give names to several easily visualised, topologically distinct fluid configurations.

Ordinary ball: $v'(l) = \tilde{h}(l) = 0$ at $v = v_{\rm o}$. $\tilde{h}'(l) > 0$ for $0 < v < v_{\rm o}$. $\tilde{h}'(l) = 0$ at $v = 0$.

Pinched ball: $v'(l) = \tilde{h}(l) = 0$ at $v = v_{\rm o}$. $\tilde{h}'(l) > 0$ for $0 < v < v_{\rm m}$. $\tilde{h}'(l) = 0$ at $v = v_{\rm m}$. $\tilde{h}'(l) < 0$ for $0 < v < v_{\rm m}$. $\tilde{h}'(l) = 0$ at $v = 0$.[1]

Ring: $v'(l) = \tilde{h}(l) = 0$ at $v = v_{\rm o}$. $\tilde{h}'(l) > 0$ for $v_{\rm m} < v < v_{\rm o}$. $\tilde{h}'(l) = 0$ at $v = v_{\rm m}$. $\tilde{h}'(l) < 0$ for $v_{\rm i} < v < v_{\rm m}$. $v'(l) = \tilde{h}(l) = 0$ at $v = v_{\rm i}$, where $v_{\rm i} < v_{\rm m} < v_{\rm o}$.

Examples of these surfaces can be seen in figs.6.4-6.5. Each of these solutions could have lumps of fluid eaten out of them. We will use the terms

Hollow ball: A ball (pinched or ordinary) with a ball cut out from its inside.

Hollow ring: A ring with a ring cut out from its inside.

Toroidally hollowed ball: A ball with a ring cut out from its inside.

It is easy to work out the horizon topology of the gravitational solutions dual to the plasma topologies listed above. [32, 33] have obtained a restriction on the topologies of horizons of stationary black holes in any theory of gravity that obeys the dominant energy condition; any product of spheres obeys the conditions from their analysis. Although the dominant energy condition is violated in AdS space, in table 6.1, we have listed all 4 dimensional horizons that are topologically products of lower dimensional spheres, and note that all but one of these configurations is obtained from the dual to plasma objects named above (B^3 is a ball, B^2 is a disc and B^1 is an interval). The last one, T^4, is a marginal case of the theorem and is probably ruled out anyway.

In the rest of this section we will determine all stationary, rigidly spinning solutions of the equations of fluid dynamics described above.

Ordinary ball

We search for solutions of (6.9) for which $\tilde{h}'(l)$ vanishes at $v = 0$ and $v'(l)$ vanishes at the outermost point of the surface $v = v_0$; we also require that $\tilde{h}$ decrease monotonically

[1] Black holes with wavy horizons in six dimensions and above were predicted in [36].

Horizon topology	Plasma topology	Object
S^4	B^3	Ball
$S^3 \times S^1$	$B^2 \times S^1$	Ring
$S^2 \times S^2$	$B^1 \times S^2$	Hollow ball
$S^2 \times T^2$	$B^1 \times T^2$	Hollow ring
T^4	None	None

Table 6.1: Topologies of gravity and plasma solutions

from 0 to v_o. The first condition sets $\widetilde{T}^5 = 3\mathcal{C}$. The condition that $v'(l)$ is zero at v_o may be used to determine $\widetilde{\Omega}$ as a function of v_o and $\widetilde{T}^5$:

$$\widetilde{\Omega} = \frac{2\widetilde{T}^5 - (3v_o^2 + 2\widetilde{T}^5)(1-v_o^2)^{3/2}}{6v_o(1-v_o^2)^{3/2}}\,. \tag{6.12}$$

Note that the numerator of the formula for $\tilde{h}'(v)$ be written as

$$2\left[1-(1-v^2)^{3/2}\right]\left(\widetilde{T}^5 - \frac{3v^2(1-v^2)^{3/2}}{2\left[1-(1-v^2)^{3/2}\right]}\right)$$

and $2\left(1-(1-v^2)^{3/2}\right) \geq 3v^2(1-v^2)^{3/2}$. Thus, $\widetilde{T}^5 > 1$ guarantees our monotonicity requirement. From (6.3), we see that this also ensures that the pressure is positive throughout the ball.

In summary, the full set of ordinary ball solution is obtained by substituting $\mathcal{C} = \widetilde{T}^5/3$ and $\Omega = \Omega(\widetilde{T}^5, v_o)$ (obtained from (6.12)) into (6.9). This procedure gives us a ball solution for any choice of $\widetilde{T}^5 > 1$ and $v_o > 0$.

In figs.6.4,6.5 we present a plot of the profile $\tilde{h}(v)$ for the ball solution at $v_o = 0.8$, $\widetilde{T}^5 = 1.5$.

Pinched ball

The pinched ball satisfies all the conditions of the ordinary ball except for the monotonicity requirement on $\tilde{h}(v)$; in fact the function $\tilde{h}(v)$ is required to first increase and then decrease as v runs from 0 to v_o. It follows that $\mathcal{C}$ and $\widetilde{\Omega}$ for these solutions are determined as in the previous subsubsection ($\mathcal{C} = \widetilde{T}^5/3$ and Ω from (6.12)) however the requirement $\tilde{h}''(v) > 0$ at $v = 0$ forces $\widetilde{T}^5 < 1$. This ensures that $\tilde{h}'(v) > 0$ at small v and $\tilde{h}'(v) < 0$ at larger v. It also ensures that the solution has negative pressure at the origin and positive pressure at the outermost radius.

Not every choice of $(\widetilde{T}^5, v_o) \in [0,1]$, however, yields an acceptable pinched ball solution. As we decrease v_o from 1, at fixed $\widetilde{T}^5$, it turns out that $\tilde{h}(0)$ decreases, and in fact vanishes at a critical value of v_o. Solutions at smaller v_o are unphysical. The physical

domain,in $(\widetilde{T}^5, v_\mathrm{o})$ space is given by the inequality

$$\tilde{h}(0) = -\int_0^{v_\mathrm{o}} \frac{\mathrm{d}\tilde{h}}{\mathrm{d}v}\,\mathrm{d}v = \int_0^{v_\mathrm{o}} \frac{2\widetilde{T}^5 - (3v^2+2\widetilde{T}^5)(1-v^2)^{3/2}}{\sqrt{36\widetilde{\Omega}^2 v^2(1-v^2)^3 - \left[2\widetilde{T}^5 - (3v^2+2\widetilde{T}^5)(1-v^2)^{3/2}\right]^2}}\,\mathrm{d}v \geq 0\,. \quad (6.13)$$

The boundary of the domain permitted by (6.13) is plotted in fig.6.2. The full set of pinched ball solutions is parameterised by values of v_o and $\widetilde{T}^5$ in the region indicated in fig.6.2.

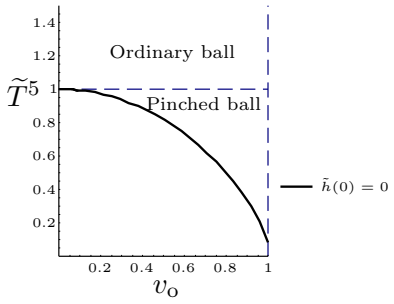

Figure 6.2: Domain of ball solutions.

In figs.6.4,6.5 we present an example of the profile $\tilde{h}(v)$ for the pinched ball solution at parameters $v_\mathrm{o} = 0.8$, $\widetilde{T}^5 = 0.55$.

Ring

The plasma of the ring configuration excludes the region $v < v_\mathrm{i}$; as this region omits $v = 0$, $\widetilde{T}^5$ and $\mathcal{C}$ are not constrained as before.

As $v'(l)$ vanishes at $v_\mathrm{i}, v_\mathrm{o}$ we have the following constraints

$$\begin{aligned} 2\widetilde{T}^5 - 3(v_\mathrm{i}^2+2\mathcal{C})(1-v_\mathrm{i}^2)^{3/2} &= -6\widetilde{\Omega} v_\mathrm{i}(1-v_\mathrm{i}^2)^{3/2}\,, \\ 2\widetilde{T}^5 - 3(v_\mathrm{o}^2+2\mathcal{C})(1-v_\mathrm{o}^2)^{3/2} &= 6\widetilde{\Omega} v_\mathrm{o}(1-v_\mathrm{o}^2)^{3/2}\,. \end{aligned} \quad (6.14)$$

the choice of negative/positive square roots comes from the requirements that $\tilde{h}'(l) < 0$ at $v = v_\mathrm{i}$ and $\tilde{h}'(l) > 0$ at $v = v_\mathrm{o}$. These equations may be used to solve for $\mathcal{C}$ and $\widetilde{\Omega}$ as a function of $\widetilde{T}^5, v_\mathrm{i}, v_\mathrm{o}$. $\widetilde{T}^5(v_\mathrm{o}, v_\mathrm{i})$ may then be determined from the requirement that $\tilde{h}(v_\mathrm{i}) = \tilde{h}(v_\mathrm{o}) = 0$, i.e.

$$\int_{v_\mathrm{i}}^{v_\mathrm{o}} \frac{\mathrm{d}\tilde{h}}{\mathrm{d}v}\,\mathrm{d}v = -\int_{v_\mathrm{i}}^{v_\mathrm{o}} \frac{2\widetilde{T}^5 - 3(v^2+2\mathcal{C})(1-v^2)^{3/2}}{\sqrt{36\widetilde{\Omega}^2 v^2(1-v^2)^3 - \left[2\widetilde{T}^5 - 3(v^2+2\mathcal{C})(1-v^2)^{3/2}\right]^2}}\,\mathrm{d}v = 0\,. \quad (6.15)$$

In practice, it is easier to first eliminate $\widetilde{T}^5$ and $\mathcal{C}$ using (6.14), then substitute $v_\mathrm{i} = \widetilde{\Omega}\tilde{r}_\mathrm{i}$, $v_\mathrm{o} = \widetilde{\Omega} r_\mathrm{o}$ and use (6.15) to solve for $\widetilde{\Omega}$ at fixed $\tilde{r}_\mathrm{i}$ and $\tilde{r}_\mathrm{o}$. after this, one can determine $\widetilde{T}^5$,

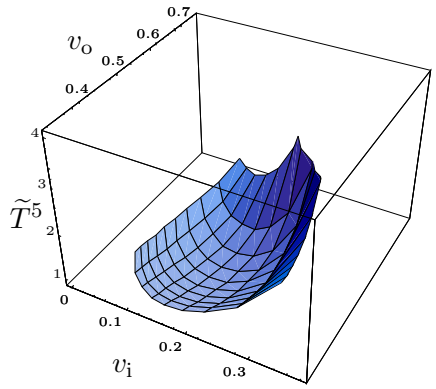

Figure 6.3: $\widetilde{T}^5$ as a function of v_i and v_o for ring solutions.

v_i and v_o from $\widetilde{\Omega}$, $\tilde{r}_i$ and $\tilde{r}_o$. We present a 3 dimensional plot of $\widetilde{T}^5$ as a function of v_i and v_o for $1 < \tilde{r}_o < 10$, $0.1 < \tilde{r}_i/\tilde{r}_o < 0.9$ in fig.6.3. All of these solutions have $\widetilde{T}^5 > 0$, as required. Unfortunately, with this method, one cannot see if there is a physically acceptable solution for the whole range of $0 < v_i < v_o < 1$. It appears that there is a solution for every value of $\tilde{r}_i < \tilde{r}_o$.

In figs.6.4,6.5 we plot the profile function $\tilde{h}(v)$ for the ring solution at parameters $\tilde{r}_i = 10$, $\tilde{r}_o = 20$.

Hollow ball

In this subsection we will demonstrate the non-existence of rigidly rotating hollow ball solutions to the equations of fluid dynamics. Let us suppose such a solution did exist. The inner surface must have vanishing gradient at $v = 0$; this sets $\mathcal{D} = \widetilde{T}^5/3$. Now let the outermost point of the eaten out region be $v = \tilde{v}_o$. The inner surface must have a vertical tangent at $\tilde{v}_o$. This also implies that the outer surface also has a vertical tangent at $\tilde{v}_o$ (the condition for a vertical tangent is identical for an outer or inner surface). However, such points saturate the inequality (6.10) and, as discussed in §6.1.2, this never happens in the interior of a ball. It follows that hollow ball solutions do not exist.

Hollow ring and toroidally hollowed ball

Let us first consider the possibility of the existence of a toridally hollowed ball solution. Let the innermost and outermost part of the hollowed out region occur at $v = \tilde{v}_i$ and $v = \tilde{v}_o$ respectively. Let us define $a(v) = 6\widetilde{\Omega}v(1-v^2)^{3/2}$ and $b(v) = -2\widetilde{T}^5 + 3(v^2 + 2\mathcal{D})(1-v^2)^{3/2}$ where $\mathcal{D}$ is the integration constant for the inner surface. From (6.11) it must be that

$$a(\tilde{v}_o) = b(\tilde{v}_o) \qquad a(\tilde{v}_i) = -b(\tilde{v}_i) \qquad |b(v)| < |a(v)| \; \forall v \in (\tilde{v}_i, \tilde{v}_o)$$

For these conditions to apply, $b(v)$ must start out negative at $v = \tilde{v}_i$, increase, turn positive, and cut the $a(v)$ curve from below at $v = \tilde{v}_o$. We have performed a rough numerical scan

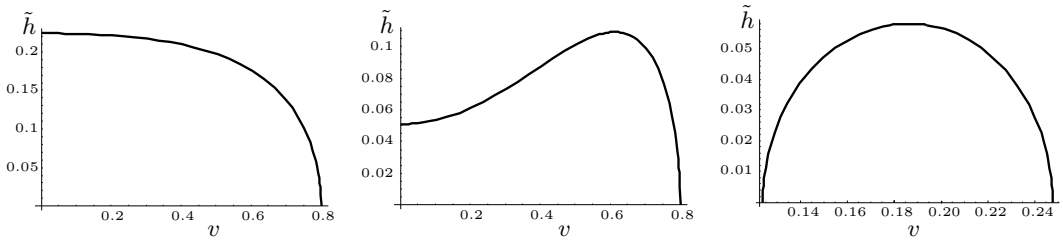

Figure 6.4: Profile of the surface of an ordinary ball, pinched ball and ring.

of allowed values of parameters $(\widetilde{T}^5, \widetilde{\Omega}, \mathcal{D})$; it appears that this behaviour never occurs (although we do not, however, have a rigourous proof for this claim). For all physically acceptable values of parameters, the curve $b(v)$ appears to either stay entirely below $a(v)$ or to cut it from above.

These considerations, which could presumably be converted into a proof with enough effort, lead us to believe that the existence of hollow balls is highly unlikely. We believe that similar reasoning is likely to rule out the existence of hollow rings, although this is more difficult to explicitly verify, as our understanding of the parameter ranges for acceptable ring solutions is incomplete. In fact, a thorough numerical scan was performed in [51] which did rule out the possibility of hollow rings and toroidally hollowed balls.

In order to understand intuitively why hollow rings and toroidally hollow balls are unlikely, note that the pressure at the inner and outermost parts of the hollowed out region is given by

$$\mathcal{P}(\tilde{v}_{\rm i}) = \rho_0 \widetilde{\Omega} \left(-|v''_{v=\tilde{v}_{\rm i}}| + \frac{1}{\tilde{v}_{\rm i}} \right), \qquad \mathcal{P}(\tilde{v}_{\rm o}) = \rho_0 \widetilde{\Omega} \left(-|v''_{v=\tilde{v}_{\rm o}}| - \frac{1}{\tilde{v}_{\rm o}} \right),$$

where $v''_{v=\tilde{v}_{\rm i}}$ is positive and $v''_{v=\tilde{v}_{\rm o}}$ is negative. Provided that $|v''_{v=\tilde{v}_{\rm i}}|$ and $|v''_{v=\tilde{v}_{\rm o}}|$ are not drastically different, we would require $\mathcal{P}(\tilde{v}_{\rm i}) > \mathcal{P}(\tilde{v}_{\rm o})$. However, the pressure increases monotonically with radius.

In conclusion, we strongly suspect, but have not yet fully proved, that the full set of rigidly rotating solutions to the equations of fluid dynamics in $d = 4$ is exhausted by ordinary balls, pinched balls and rings.

6.2 Five dimensional plasmarings

Up till now, we have presented an analysis of stationary fluid configurations of the three and four dimensional fluid flows. The analysis of analogous configurations in one higher dimension has an interesting new element. The rotation group in four spatial dimensions, $SO(4)$, has rank 2. Consequently a rotating lump of fluid in five dimensions will be characterised by three rather than two conserved charges (two angular momenta plus energy). When one of the two angular momenta is set to zero, it seems likely that the set of stationary solutions will be similar to those of the four dimensional fluid; in

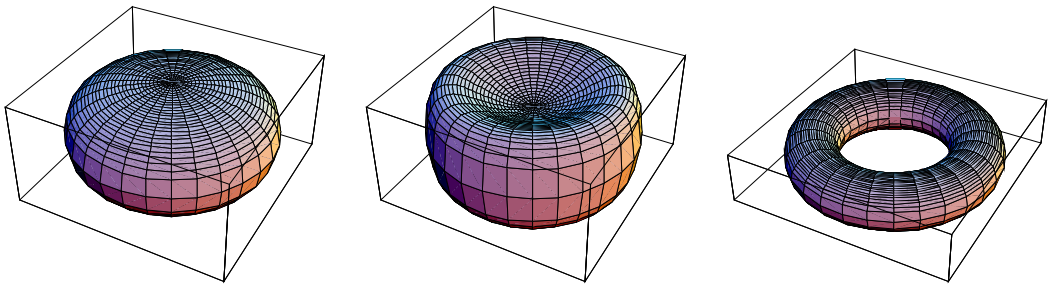

Figure 6.5: 3D plot of the surface of an ordinary ball, pinched ball and ring.

this limit we expect ball and ring configurations whose dual bulk horizon topologies are S^5 and $S^4 \times S^1$ respectively. However turning on the second angular momentum on the ring solution could centrifugally repel the fluid away from the second rotational axis, leading to a fluid configuration with dual bulk horizon topology $S^3 \times T^2$. Such configurations have not yet been discovered in gravity, and it would be exciting to either construct them in fluid mechanics, or to rule out their existence.

In this section we set up and partially solve the equations of stationary fluid flow in five dimensions. While the stationary equations of fluid dynamics are trivial to solve in the bulk in every dimension, boundary conditions are harder to impose in higher dimensions. In the particular case of 5 dimensions, the imposition of these boundary conditions requires the solution of a 2nd order ordinary differential equation, that we have not (yet?) been able to solve. It may be that a full study of this case would require careful numerical analysis, which we leave to future work. In the rest of this section we simply set up the relevant equations, and comment on the dual bulk interpretations of various possible solutions.

Consider a fluid propagating in flat five dimensional space

$$\mathrm{d}s^2 = -\mathrm{d}t^2 + \mathrm{d}r_1^2 + r_1^2 \mathrm{d}\phi_1^2 + \mathrm{d}r_2^2 + r_2^2 \mathrm{d}\phi_2^2 \,.$$

Consider a fluid flow with velocities given by $u^\mu = \gamma(1, 0, \Omega_1, 0, \Omega_2)$, where $\gamma = (1 - v_1^2 - v_2^2)^{-1/2}$, $v_1 = \Omega_1 r_1$ and $v_2 = \Omega_2 r_2$. Let the (upper/lower) fluid surface be given by $f(r_1, r_2) = \pm(h(r_1) - r_2) = 0$.

Following (2.30), once again, this leads to the temperature and pressure profile

$$\mathcal{T} = \frac{T}{\sqrt{1 - v_1^2 - v_2^2}} \,, \qquad \mathcal{P} = \frac{\alpha}{\mathcal{T}_{\rm c}} \left(\frac{T^6}{(1 - v_1^2 - v_2^2)^3} - \mathcal{T}_{\rm c}{}^6 \right) . \tag{6.16}$$

The extrinsic curvature of the surface is

$$\Theta = \mp \frac{r_1 h h'' + (1 + h'^2)(h h' - r_1)}{r_1 h (1 + h'^2)^{3/2}} \tag{6.17}$$

Substituting these into (2.31), we obtain the condition (the upper sign should be used for upper surfaces)

$$\frac{\widetilde{T}^6}{(1 - \Omega_1^2 r_1^2 - \Omega_2^2 h^2)^3} - 1 = \mp \xi' \frac{r_1 h h'' + (1 + h'^2)(h h' - r_1)}{r_1 h (1 + h'^2)^{3/2}} \tag{6.18}$$

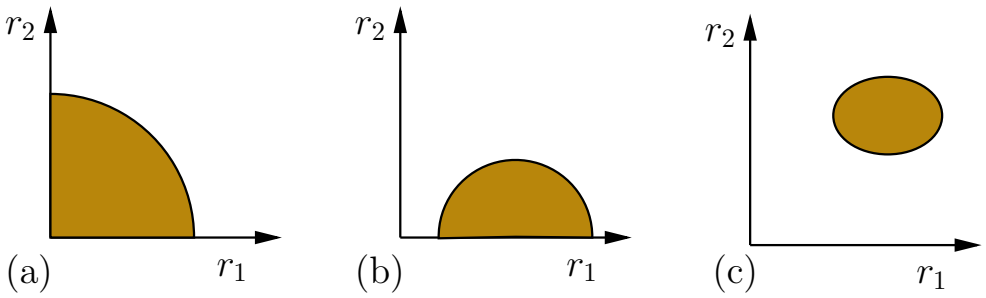

Figure 6.6: Topologies of five dimensional solutions.

Horizon topology	Plasma topology	Object
S^5	B^4	Ball
$S^4 \times S^1$	$B^3 \times S^1$	Ring
$S^3 \times T^2$	$B^2 \times T^2$	Torus
$S^3 \times S^2$	$B^1 \times S^3$	Hollow ball
$S^2 \times S^2 \times S^1$	$B^1 \times S^2 \times S^1$	Hollow ring
$S^2 \times T^3$	$B^1 \times T^3$	Hollow Torus
T^5	None	None

Table 6.2: Topologies of gravity and plasma solutions

Unfortunately we have not yet been able to solve this equation; we postpone further analysis of (6.18) to future work. In the rest of this section we qualitatively describe possible types of solutions to these equations, and their bulk dual horizon topologies.

In fig.6.6, we have sketched some possible topologies for these solutions. The first touches both the $r_1 = 0$ and $r_2 = 0$ axes and we refer to this as a ball. The second type only touches one of these axes and we refer to this as a ring. The third type touches neither of the axes, as the plasma has the topology of a solid three-torus we refer to this as a torus.

Each of these could be pinched near either axis, and there could be hollow versions (though the considerations of §6.1 make it seem unlikely that hollow configurations will actually be solutions).

The horizon topology of the dual black object can be found by fibering three circles over the shapes in fig.6.6. One of these circles degenerates at each axis (the angular coordinates ϕ_1 and ϕ_2), and the other degenerates on the fluid surface (the Scherk-Schwarz circle). The topologies generated are: listed in table 6.2.

6.3 Discussion

In this chapter we constructed solutions of fluid mechanics that are dual to black holes with horizon topologies S^4 and $S^3 \times S^1$. We have argued that fluid solutions dual

to horizon topologies $S^2 \times S^2$ and $S^2 \times T^2$ do not exist, although we were only able to conclusively rule out the former. Note that this does not tell us that such solutions cannot exist in gravity. Within the regime of our approximations we can only turn on one angular momentum, whereas black holes in six dimensions can have two independent angular momenta. We can only conclude that these two other topologies require both angular momenta to be non-zero.

Of particular interest are the pinched ball solutions. Emparan and Myers have suggested that ultra-spinning black holes in 6 dimensional flat space have Gregory-Laflamme type instabilities [36]. When such an instability appears, one expects a new branch of wavy solutions to appear, much like the wavy strings of [46]. As they were unable to provide more than a qualitative argument for their existence, the fact that we can construct wavy fluid mechanics solutions quantitatively is encouraging.

It should also be relatively straightforward, and rather interesting, to more fully analyse the thermodynamics of the 4 dimensional solutions presented in this chapter. This would shed light on which of the two proposed phase diagrams indicated in fig.1.2 is the correct one. Such an analysis has been carried out in [51], where they also ruled out the hollow ring solutions (dual to $S^2 \times T^2$ horizons). The phase diagram found there looks a lot closer to the second proposal in fig.1.2 than the first.

An extension of our work to obtain the moduli space of 5 and higher dimensional fluid configurations - and so 7 and higher dimensional gravitational black solutions should also be possible (though analytic solutions may be harder to obtain in higher dimensions). Such an extension would yield interesting information about horizon topologies in higher dimensional gravitational theories. An obvious conjecture based on intuition from fluid flows would be that the full set of stationary fluid solutions in 5 dimensions appear in three distinct topological classes; solutions whose bulk dual topologies would be S^5, $S^4 \times S^1$ and $S^3 \times T^2$. The reason one might expect the last solution is that in 5 (but no lower) dimensions, it is possible to have solutions that rotate about two independent axes; these two rotations should be able to create their own distinct centrifugal 'holes', resulting in the above topology. An approximate construction of the last two types of configuration has been presented in [3]. This construction relies on an expansion in powers of the ratio of the size of the various circles/spheres that appear in the topologies, much like the blackfold construction of [35]. This provides evidence that such horizon topologies do in fact exist in general raltivity.

Appendix A

Notation

We work in the $(-+++)$ signature. μ, ν denote space-time indices, $i, j = 1 \dots c$ label the c different R-charges and $a, b = 1 \dots n$ label the n different angular momenta. The dimensions of the bulk space-time (gravity side) is denoted by D whereas the spacetime dimensions of the space-time on the field theory side (excluding dimensions ignored in fluid mechanics) is denoted by d.

In chapter 3 we consider fluids on $S^{d-1} \times \mathbb{R}$ which are dual to gravity on AdS_D with $D = d + 1$.

In chapters 4–6 we consider fluids on $\mathbb{R}^{d-1,1} \times S^1$, truncated on the S^1. These are dual to gravity on Scherk-Schwarz compactified AdS_D with $D = d + 2$.

A summary of the variables used in this dissertation appears below. Numbers in parentheses refer to the equation where that variable is defined.

a^μ	acceleration (2.10)
$\mathcal{A}$	surface area of fluid
B^m	m-dimensional ball
c	no. of commuting R-charges
c_{s}	speed of sound (5.4)
C	confinement heat capacity
$\mathcal{C}, \mathcal{D}$	integration constants in §6.1
d	dimensionality of fluid
D	dimensionality of gravity dual
D_{ij}	diffusion coefficients
E	total energy of configuration
$\widetilde{E}$	see (4.26)
$f(x)$	surface at $f(x) = 0$
$g_\pm(v)$	boundary conditions (4.24)
G_D	Newton constant in (SS)AdS_D
$h(\nu)$	$\mathcal{P}/\mathcal{T}^d$, see (3.3)
h_i	$\partial h / \partial \nu_i$
$h(r)$	surface height $z = h(r)$ in Ch.6
$\tilde{h}(v)$	$\Omega h(v/\Omega)$
$h_{\mu\nu}$	induced metric of surface
H_i	black hole parameter in §3.5-3.6
j_i^μ	diffusion current
J_i^μ	R-charge current
J_S^μ	entropy current
K^μ	Killing vector for velocity
L	total angular momentum
$\widetilde{L}$	see (4.26)
l_{mfp}	thermalisation scale
l	periodicity of $y/2\pi$
l_a	rotational Killing vector
$\mathfrak{m}_i$	fluid chemical potential
m	black hole parameter in §3.5-3.6

n	no. of angular momenta *or* order of instability in Ch.5
n^μ	unit normal of surface
$\mathcal{P}$	proper fluid pressure
$P^{\mu\nu}$	projection tensor (2.4)
q^μ	heat flux
q	black hole parameter in §3.5-3.6
Q_X	conserved charge for current X
$\tilde{r}$	r/ξ'
$r_{\rm o}$	outer radius of plasma-ball/ring
$r_{\rm i}$	inner radius of plasmaring
$\tilde{r}_{\rm o}$	$r_{\rm o}/\xi'$
$\tilde{r}_{\rm i}$	$r_{\rm i}/\xi'$
$\mathfrak{r}_i$	proper R-charge density
R	radius of ball in §5.2.1
R_i	total R-charge
$\mathcal{R}_i$	fluid R-charge
r_+	horizon radius
$R_{\rm AdS}$	AdS radius
s	proper fluid entropy density
$s_{\rm c}$	confinement entropy density
s_i	black hole parameter in §3.5-3.6
S	total entropy of configuration
$\widetilde{S}$	see (4.26)
S^m	m-dimensional sphere
T	overall temperature
$\widetilde{T}$	$\mathcal{T}/\mathcal{T}_{\rm c}$
$\mathcal{T}$	proper fluid temperature
$\mathcal{T}_{\rm c}$	transition temperature
$T^{\mu\nu}$	stress tensor
u^μ	velocity vector
Δu	validity criterion (4.42)
v^2	$\sum_a g_{\phi_a\phi_a}\Omega_a^2$
$v_{\rm o}$	$\Omega r_{\rm o}$
$v_{\rm i}$	$\Omega r_{\rm i}$
V_d	volume of S^{d-1}, $\frac{2\pi^{d/2}}{\Gamma(d/2)}$
$\vec{w}$	vector field normal to deformed surface
w	W/l
W	width of string in §5.2
x, y	boundary scalings in §4.3.4
X_i	$1/(1+\kappa_i)$ (3.44)
$\mathcal{Z}_{\rm gc}$	grand partition function (2.38)
$\widetilde{\mathcal{Z}}_{\rm gc}$	see (4.26)
α	equation of state parameter (1.5)
β	$(\partial\widetilde{S}/\partial\widetilde{E})_{\widetilde{L}}$
γ	velocity normalisation $(1-v^2)^{-1/2}$
ϵ	ξ/l
ζ	bulk viscosity (2.13)
ζ^μ	arbitrary Killing vector
η	shear viscosity (2.13)
ϑ	expansion (2.10)
$\Theta^{\mu\nu}$	extrinsic curvature of surface (2.46)
Θ	trace of extrinsic curvature Θ^μ_μ (2.47)
κ	thermal conductivity (2.10)
κ_i	thermodynamic parameters (3.38)
μ_i	overall chemical potential
ν_i	$\mathfrak{m}_i/\mathcal{T}$
ν	unstable frequency $\omega = {\rm i}\nu/l$
ξ	surface thickness (2.27)
ξ'	$(d+1)\xi$, (4.14)
$\Pi^{\mu\nu}$	boundary stress tensor
ρ	proper fluid density
ρ_0	plasma vacuum energy
$\rho_{\rm c}$	confinement density
σ	surface tension
σ_E	surface energy density
σ_S	surface entropy density
σ_{R_i}	surface R-charge density
$\sigma^{\mu\nu}$	shear tensor (2.10)
ψ	$(\partial\widetilde{S}/\partial\widetilde{L})_{\widetilde{E}}$
ω	frequency of fluctuation
ϖ	$\omega - n\Omega$
$\widetilde{\omega}$	$\xi'\omega$
$\widetilde{\varpi}$	$\xi'\varpi$
Ω_a	angular velocity
$\widetilde{\Omega}_a$	$\xi'\Omega$

Bibliography

[1] S. Bhattacharyya, S. Lahiri, R. Loganayagam, and S. Minwalla, "Large rotating AdS black holes from fluid mechanics," *JHEP* **09** (2008) 054, arXiv:0708.1770 [hep-th].

[2] S. Lahiri and S. Minwalla, "Plasmarings as dual black rings," *JHEP* **05** (2008) 001, arXiv:0705.3404 [hep-th].

[3] J. Bhattacharya and S. Lahiri, "Lumps of plasma in arbitrary dimensions," arXiv:0903.4734 [hep-th].

[4] J. M. Maldacena, "The large N limit of superconformal field theories and supergravity," *Adv. Theor. Math. Phys.* **2** (1998) 231–252, arXiv:hep-th/9711200.

[5] S. S. Gubser, I. R. Klebanov, and A. M. Polyakov, "Gauge theory correlators from non-critical string theory," *Phys. Lett.* **B428** (1998) 105–114, arXiv:hep-th/9802109.

[6] E. Witten, "Anti-de Sitter space and holography," *Adv. Theor. Math. Phys.* **2** (1998) 253–291, arXiv:hep-th/9802150.

[7] O. Aharony, S. S. Gubser, J. M. Maldacena, H. Ooguri, and Y. Oz, "Large N field theories, string theory and gravity," *Phys. Rept.* **323** (2000) 183–386, arXiv:hep-th/9905111.

[8] A. Strominger, "The Inverse Dimensional Expansion In Quantum Gravity," *Phys. Rev.* **D24** (1981) 3082.

[9] N. E. J. Bjerrum-Bohr, "Quantum gravity at a large number of dimensions," *Nucl. Phys.* **B684** (2004) 209–234, arXiv:hep-th/0310263.

[10] H. W. Hamber and R. M. Williams, "Quantum gravity in large dimensions," *Phys. Rev.* **D73** (2006) 044031, arXiv:hep-th/0512003.

[11] V. Asnin *et al.*, "High and Low Dimensions in The Black Hole Negative Mode," *Class. Quant. Grav.* **24** (2007) 5527–5540, arXiv:0706.1555 [hep-th].

[12] T. Kaluza, "Zum Unitätsproblem in der Physik," *Sitzungsber. Preuss. Akad. Wiss.* **K1** (1921) 966–972.

[13] O. Klein, "Quantum theory and five-dimensional theory of relativity," *Z. Phys.* **37** (1926) 895–906.

[14] N. Arkani-Hamed, S. Dimopoulos, and G. R. Dvali, "The hierarchy problem and new dimensions at a millimeter," *Phys. Lett.* **B429** (1998) 263–272, arXiv:hep-ph/9803315.

[15] L. Randall and R. Sundrum, "A large mass hierarchy from a small extra dimension," *Phys. Rev. Lett.* **83** (1999) 3370–3373, arXiv:hep-ph/9905221.

[16] L. Randall and R. Sundrum, "An alternative to compactification," *Phys. Rev. Lett.* **83** (1999) 4690–4693, arXiv:hep-th/9906064.

[17] W. Israel, "Event horizons in static electrovac space-times," *Commun. Math. Phys.* **8** (1968) 245–260.

[18] S. W. Hawking, "Black holes in general relativity," *Commun. Math. Phys.* **25** (1972) 152–166.

[19] G. T. Horowitz and A. Strominger, "Black strings and P-branes," *Nucl. Phys.* **B360** (1991) 197–209.

[20] R. Emparan and H. S. Reall, "A rotating black ring in five dimensions," *Phys. Rev. Lett.* **88** (2002) 101101, arXiv:hep-th/0110260.

[21] R. Emparan and H. S. Reall, "Black rings," *Class. Quant. Grav.* **23** (2006) R169, arXiv:hep-th/0608012.

[22] R. Emparan, T. Harmark, V. Niarchos, N. A. Obers, and M. J. Rodriguez, "The Phase Structure of Higher-Dimensional Black Rings and Black Holes," *JHEP* **10** (2007) 110, arXiv:0708.2181 [hep-th].

[23] V. Niarchos, "Phases of Higher Dimensional Black Holes," *Mod. Phys. Lett.* **A23** (2008) 2625–2643, arXiv:0808.2776 [hep-th].

[24] G. Policastro, D. T. Son, and A. O. Starinets, "The shear viscosity of strongly coupled N = 4 supersymmetric Yang-Mills plasma," *Phys. Rev. Lett.* **87** (2001) 081601, arXiv:hep-th/0104066.

[25] D. T. Son and A. O. Starinets, "Viscosity, Black Holes, and Quantum Field Theory," *Ann. Rev. Nucl. Part. Sci.* **57** (2007) 95–118, arXiv:0704.0240 [hep-th].

[26] T. Damour and M. Lilley, "String theory, gravity and experiment," arXiv:0802.4169 [hep-th].

[27] K. S. Thorne, D. A. MacDonald, and R. H. Price, *Black Holes: The Membrane Paradigm*. Yale University Press, 1986.

[28] M. Parikh and F. Wilczek, "An action for black hole membranes," *Phys. Rev.* **D58** (1998) 064011, arXiv:gr-qc/9712077.

[29] V. Cardoso and O. J. C. Dias, "Gregory-Laflamme and Rayleigh-Plateau instabilities of black strings," *Phys. Rev. Lett.* **96** (2006) 181601, arXiv:hep-th/0602017.

[30] V. Cardoso and L. Gualtieri, "Equilibrium configurations of fluids and their stability in higher dimensions," *Class. Quant. Grav.* **23** (2006) 7151–7198, arXiv:hep-th/0610004.

[31] V. Cardoso, O. J. C. Dias, and L. Gualtieri, "The return of the membrane paradigm? Black holes and strings in the water tap," *Int. J. Mod. Phys.* **D17** (2008) 505–511, arXiv:0705.2777 [hep-th].

[32] C. Helfgott, Y. Oz, and Y. Yanay, "On the topology of black hole event horizons in higher dimensions," *JHEP* **02** (2006) 025, arXiv:hep-th/0509013.

[33] G. J. Galloway and R. Schoen, "A generalization of Hawking's black hole topology theorem to higher dimensions," *Commun. Math. Phys.* **266** (2006) 571–576, arXiv:gr-qc/0509107.

[34] R. C. Myers and M. J. Perry, "Black Holes in Higher Dimensional Space-Times," *Ann. Phys.* **172** (1986) 304.

[35] R. Emparan, T. Harmark, V. Niarchos, and N. A. Obers, "Blackfolds," arXiv:0902.0427 [hep-th].

[36] R. Emparan and R. C. Myers, "Instability of ultra-spinning black holes," *JHEP* **09** (2003) 025, arXiv:hep-th/0308056.

[37] R. Emparan *private communication*.

[38] R. Gregory and R. Laflamme, "Black strings and p-branes are unstable," *Phys. Rev. Lett.* **70** (1993) 2837–2840, arXiv:hep-th/9301052.

[39] R. Gregory and R. Laflamme, "The instability of charged black strings and p-branes," *Nucl. Phys.* **B428** (1994) 399–434, arXiv:hep-th/9404071.

[40] B. Kol, "The Phase Transition between Caged Black Holes and Black Strings - A Review," *Phys. Rept.* **422** (2006) 119–165, arXiv:hep-th/0411240.

[41] S. W. Hawking and G. F. R. Ellis, *The Large Scale Structure of Space-Time*. Cambridge University Press, 1973.

[42] G. T. Horowitz and K. Maeda, "Fate of the black string instability," *Phys. Rev. Lett.* **87** (2001) 131301, arXiv:hep-th/0105111.

[43] M. W. Choptuik *et al.*, "Towards the final fate of an unstable black string," *Phys. Rev.* **D68** (2003) 044001, arXiv:gr-qc/0304085.

[44] D. Garfinkle, L. Lehner, and F. Pretorius, "A numerical examination of an evolving black string horizon," *Phys. Rev.* **D71** (2005) 064009, arXiv:gr-qc/0412014.

[45] S. S. Gubser, "On non-uniform black branes," *Class. Quant. Grav.* **19** (2002) 4825–4844, arXiv:hep-th/0110193.

[46] T. Wiseman, "Static axisymmetric vacuum solutions and non-uniform black strings," *Class. Quant. Grav.* **20** (2003) 1137–1176, arXiv:hep-th/0209051.

[47] S. Bhattacharyya, V. E. Hubeny, S. Minwalla, and M. Rangamani, "Nonlinear Fluid Dynamics from Gravity," *JHEP* **02** (2008) 045, arXiv:0712.2456 [hep-th].

[48] Y. Brihaye, T. Delsate, and E. Radu, "On the stability of AdS black strings," *Phys. Lett.* **B662** (2008) 264–269, arXiv:0710.4034 [hep-th].

[49] E. Witten, "Anti-de Sitter space, thermal phase transition, and confinement in gauge theories," *Adv. Theor. Math. Phys.* **2** (1998) 505–532, arXiv:hep-th/9803131.

[50] O. Aharony, S. Minwalla, and T. Wiseman, "Plasma-balls in large N gauge theories and localized black holes," *Class. Quant. Grav.* **23** (2006) 2171–2210, arXiv:hep-th/0507219.

[51] S. Bhardwaj and J. Bhattacharya, "Thermodynamics of Plasmaballs and Plasmarings in 3+1 Dimensions," *JHEP* **03** (2009) 101, arXiv:0806.1897 [hep-th].

[52] N. Andersson and G. L. Comer, "Relativistic fluid dynamics: Physics for many different scales," arXiv:gr-qc/0605010.

[53] L. D. Landau and E. M. Lifshitz, *Fluid Mechanics*. Pergamon Press, London, 1959.

[54] C. Eckart, "The Thermodynamics of Irreversible Processes. III. Relativistic Theory of the Simple Fluid," *Phys. Rev.* **58** (Nov, 1940) 919–924.

[55] R. M. Wald, *General Relativity*. The University of Chicago Press, Chicago 60637, 1984.

[56] P. Kraus, F. Larsen, and R. Siebelink, "The gravitational action in asymptotically AdS and flat spacetimes," *Nucl. Phys.* **B563** (1999) 259–278, arXiv:hep-th/9906127.

[57] M. Henningson and K. Skenderis, "The holographic Weyl anomaly," *JHEP* **07** (1998) 023, arXiv:hep-th/9806087.

[58] S. de Haro, S. N. Solodukhin, and K. Skenderis, "Holographic reconstruction of spacetime and renormalization in the AdS/CFT correspondence," *Commun. Math. Phys.* **217** (2001) 595–622, arXiv:hep-th/0002230.

[59] K. Skenderis, "Asymptotically anti-de Sitter spacetimes and their stress energy tensor," *Int. J. Mod. Phys.* **A16** (2001) 740–749, arXiv:hep-th/0010138.

[60] I. Papadimitriou and K. Skenderis, "Thermodynamics of asymptotically locally AdS spacetimes," *JHEP* **08** (2005) 004, arXiv:hep-th/0505190.

[61] M. C. N. Cheng and K. Skenderis, "Positivity of energy for asymptotically locally AdS spacetimes," *JHEP* **08** (2005) 107, arXiv:hep-th/0506123.

[62] R. Olea, "Mass, angular momentum and thermodynamics in four- dimensional Kerr-AdS black holes," *JHEP* **06** (2005) 023, arXiv:hep-th/0504233.

[63] R. Olea, "Regularization of odd-dimensional AdS gravity: Kounterterms," *JHEP* **04** (2007) 073, arXiv:hep-th/0610230.

[64] S. W. Hawking, C. J. Hunter, and M. Taylor, "Rotation and the AdS/CFT correspondence," *Phys. Rev.* **D59** (1999) 064005, arXiv:hep-th/9811056.

[65] G. W. Gibbons, H. Lu, D. N. Page, and C. N. Pope, "The general Kerr-de Sitter metrics in all dimensions," *J. Geom. Phys.* **53** (2005) 49–73, arXiv:hep-th/0404008.

[66] G. W. Gibbons, M. J. Perry, and C. N. Pope, "The first law of thermodynamics for Kerr - anti-de Sitter black holes," *Class. Quant. Grav.* **22** (2005) 1503–1526, arXiv:hep-th/0408217.

[67] M. Cvetic, H. Lu, and C. N. Pope, "Charged rotating black holes in five dimensional U(1)**3 gauged N = 2 supergravity," *Phys. Rev.* **D70** (2004) 081502, arXiv:hep-th/0407058.

[68] Z. W. Chong, M. Cvetic, H. Lu, and C. N. Pope, "General non-extremal rotating black holes in minimal five- dimensional gauged supergravity," *Phys. Rev. Lett.* **95** (2005) 161301, arXiv:hep-th/0506029.

[69] Z. W. Chong, M. Cvetic, H. Lu, and C. N. Pope, "Five-dimensional gauged supergravity black holes with independent rotation parameters," *Phys. Rev.* **D72** (2005) 041901, arXiv:hep-th/0505112.

[70] Z. W. Chong, M. Cvetic, H. Lu, and C. N. Pope, "Non-extremal rotating black holes in five-dimensional gauged supergravity," *Phys. Lett.* **B644** (2007) 192–197, arXiv:hep-th/0606213.

[71] Z. W. Chong, M. Cvetic, H. Lu, and C. N. Pope, "Non-extremal charged rotating black holes in seven- dimensional gauged supergravity," *Phys. Lett.* **B626** (2005) 215–222, arXiv:hep-th/0412094.

[72] Z. W. Chong, M. Cvetic, H. Lu, and C. N. Pope, "Charged rotating black holes in four-dimensional gauged and ungauged supergravities," *Nucl. Phys.* **B717** (2005) 246–271, arXiv:hep-th/0411045.

[73] M. Cvetic, G. W. Gibbons, H. Lu, and C. N. Pope, "Rotating black holes in gauged supergravities: Thermodynamics, supersymmetric limits, topological solitons and time machines," arXiv:hep-th/0504080.

[74] N. Banerjee *et al.*, "Hydrodynamics from charged black branes," arXiv:0809.2596 [hep-th].

[75] J. Erdmenger, M. Haack, M. Kaminski, and A. Yarom, "Fluid dynamics of R-charged black holes," *JHEP* **01** (2009) 055, arXiv:0809.2488 [hep-th].

[76] D. T. Son and A. O. Starinets, "Hydrodynamics of R-charged black holes," *JHEP* **03** (2006) 052, arXiv:hep-th/0601157.

[77] S. S. Gubser and I. Mitra, "Instability of charged black holes in anti-de Sitter space," arXiv:hep-th/0009126.

[78] J. Kinney, J. M. Maldacena, S. Minwalla, and S. Raju, "An index for 4 dimensional super conformal theories," *Commun. Math. Phys.* **275** (2007) 209–254, arXiv:hep-th/0510251.

[79] T. Harmark and N. A. Obers, "Thermodynamics of spinning branes and their dual field theories," *JHEP* **01** (2000) 008, arXiv:hep-th/9910036.

[80] D. Astefanesei, K. Goldstein, R. P. Jena, A. Sen, and S. P. Trivedi, "Rotating attractors," *JHEP* **10** (2006) 058, arXiv:hep-th/0606244.

[81] W. Israel and J. M. Stewart, "Transient relativistic thermodynamics and kinetic theory," *Ann. Phys.* **118** (1979) 341–372.

[82] O. Aharony, J. Marsano, S. Minwalla, K. Papadodimas, and M. Van Raamsdonk, "The Hagedorn / deconfinement phase transition in weakly coupled large N gauge theories," *Adv. Theor. Math. Phys.* **8** (2004) 603–696, arXiv:hep-th/0310285.

[83] D. S. Berman and M. K. Parikh, "Holography and rotating AdS black holes," *Phys. Lett.* **B463** (1999) 168–173, arXiv:hep-th/9907003.

[84] H. Elvang, R. Emparan, and A. Virmani, "Dynamics and stability of black rings," *JHEP* **12** (2006) 074, arXiv:hep-th/0608076.

[85] R. Emparan, "Rotating circular strings, and infinite non-uniqueness of black rings," *JHEP* **03** (2004) 064, arXiv:hep-th/0402149.

[86] H. Poincare, "Sur l'equilibre d'une masse fluide animée d'un mouvement de rotation," *Acta Mathematica* **7** (1885) 259–380.

[87] G. Arcioni and E. Lozano-Tellechea, "Stability and critical phenomena of black holes and black rings," *Phys. Rev.* **D72** (2005) 104021, arXiv:hep-th/0412118.

[88] J. Katz, "On the number of unstable modes of an equilibrium," *Monthly Notices of the Royal Astronomical Society* **183** (June, 1978) 765–770.

[89] J. Katz, "On the Number of Unstable Modes of an Equilibrium - Part Two," *Monthly Notices of the Royal Astronomical Society* **189** (Dec., 1979) 817.

[90] R. Sorkin, "A Criterion for the onset of instability at a turning point," *Astrophys. J.* **249** (1981) 254–257.

[91] R. D. Sorkin, "A Stability criterion for many parameter equilibrium families," *Astrophys. J.* **257** (1982) 847–854.

[92] D. Astefanesei and E. Radu, "Quasilocal formalism and black ring thermodynamics," *Phys. Rev.* **D73** (2006) 044014, arXiv:hep-th/0509144.

[93] G. Arcioni and E. Lozano-Tellechea, "Stability and thermodynamics of black rings," arXiv:hep-th/0502121.

[94] H. Elvang and P. Figueras, "Black Saturn," *JHEP* **05** (2007) 050, arXiv:hep-th/0701035.

[95] J. P. Gauntlett and J. B. Gutowski, "Concentric black rings," *Phys. Rev.* **D71** (2005) 025013, arXiv:hep-th/0408010.

[96] J. P. Gauntlett and J. B. Gutowski, "General concentric black rings," *Phys. Rev.* **D71** (2005) 045002, arXiv:hep-th/0408122.

[97] H. Iguchi and T. Mishima, "Black di-ring and infinite nonuniqueness," *Phys. Rev.* **D75** (2007) 064018, arXiv:hep-th/0701043.

[98] J. Evslin and C. Krishnan, "The Black Di-Ring: An Inverse Scattering Construction," arXiv:0706.1231 [hep-th].

[99] H. Elvang, R. Emparan, and P. Figueras, "Phases of Five-Dimensional Black Holes," *JHEP* **05** (2007) 056, arXiv:hep-th/0702111.

[100] J. Evslin and C. Krishnan, "Metastable Black Saturns," *JHEP* **09** (2008) 003, arXiv:0804.4575 [hep-th].

[101] C.-S. Yih, *Fluid Mechanics*. West River Press, Ann Arbor, Michigan, 1977.

[102] V. Cardoso and O. J. C. Dias, "Bifurcation of Plasma Balls and Black Holes to Lobed Configurations," arXiv:0902.3560 [hep-th].

[103] S. S. Gubser and I. Mitra, "The evolution of unstable black holes in anti-de Sitter space," *JHEP* **08** (2001) 018, arXiv:hep-th/0011127.

[104] A. Buchel, "A holographic perspective on Gubser-Mitra conjecture," *Nucl. Phys.* **B731** (2005) 109–124, arXiv:hep-th/0507275.

[105] M. M. Caldarelli, O. J. C. Dias, R. Emparan, and D. Klemm, "Black Holes as Lumps of Fluid," arXiv:0811.2381 [hep-th].

[106] K. Copsey and G. T. Horowitz, "Gravity dual of gauge theory on S**2 x S**1 x R," *JHEP* **06** (2006) 021, arXiv:hep-th/0602003.

[107] R. B. Mann, E. Radu, and C. Stelea, "Black string solutions with negative cosmological constant," *JHEP* **09** (2006) 073, arXiv:hep-th/0604205.

[108] A. Bernamonti *et al.*, "Black strings in AdS_5," *JHEP* **01** (2008) 061, arXiv:0708.2402 [hep-th].